

AMERICAN UNIVERSITY OF BEIRUT

EFFECT OF CORTICAL BONE QUALITY AND QUANTITY
ON TWO ORTHODONTIC DISTALIZATION MODALITIES:
A FINITE ELEMENT ANALYSIS STUDY

by
MAKRAM JAMIL AMMOURY

A thesis
submitted in partial fulfillment of the requirements
for the degree of Master of Science in Orthodontics
to the Department of Otolaryngology- Head and Neck Surgery
of the Faculty of Medicine
at the American University of Beirut

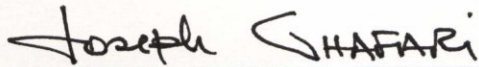
Beirut, Lebanon
January, 2017

EFFECT OF CORTICAL BONE QUALITY AND QUANTITY
ON TWO ORTHODONTIC DISTALIZATION MODALITIES:
A FINITE ELEMENT ANALYSIS STUDY

By

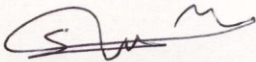
MAKRAM JAMIL AMMOURY

Approved by:



Dr. Joseph G. Ghafari, Professor and Head
Orthodontics and Dentofacial Orthopedics

Primary Advisor



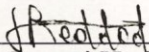
Dr. Samir Mustapha, Assistant Professor,
Department of Mechanical Engineering

Co-primary advisor



Dr. Elie Shamma, Assistant Professor
Department of Mechanical Engineering

Member of Committee



Dr. Ramzi Haddad, Assistant Professor
Orthodontics and Dentofacial Orthopedics

Member of Committee

Date of thesis defense: January 24, 2017

ACKNOWLEDGMENTS

**No one can whistle a symphony.
It takes a whole orchestra to play it.**
Halford Edward Luccock

This thesis is a reflection of an enormous amount of teamwork and cooperation. I would therefore like to take this opportunity to express my utmost appreciation to all the individuals who have contributed to this journey.

I am sincerely grateful to

Dr. Joseph Ghafari, for being a role model in teaching me the value of hard work and for giving me the opportunity to integrate the engineering discipline into orthodontic clinical research;

Dr. Samir Mustapha, for introducing me to the vast world of FEA and guiding me “as a non-engineer” throughout the different steps with all the accompanying hurdles;

Dr. Elie Shammam and Dr. Georges Ayyoub, for unconditionally sharing their intellectual and engineering knowledge since day one;

Dr. Ramzi Haddad, for his feedback and for bringing in clinical and practical insight to this work;

Dr. Maria Saadeh, for her assistance in the statistical computations;

Drs. Paul Dechow and Rola Hourani, for providing us with the material (individual data of cadavers and CT scan) necessary to perform this research;

Drs. Mutasem Shehadeh and Robert Habib, for providing the needed expert opinion in various aspects of this work;

Rawad Hayeck, Samah Mohtar and Rakan Ammoury, for their constant assistance from “behind-the-scenes” in different parts of this project;

Kinan Zeno for literally sharing “day and night” all phases of this journey and *Joe El Helou*, for making it enjoyable. The only thing better than a good team, is a team of good friends.

And last but not least, *my parents and family*, for all the love, prayers and support provided over the years which was the greatest gift anyone has ever given me.

AN ABSTRACT OF THE THESIS OF

Makram Jamil Ammourey for Master of Science
Major: Orthodontics

Title: Effect of cortical bone quality and quantity on two orthodontic distalization modalities: a finite element analysis study

Introduction:

Orthodontic mini-implants have been used to correct Class II malocclusions by distalizing the maxillary dentition via direct anchorage (direct pull from mini-implant to the teeth) and indirect anchorage (teeth pulled against other teeth anchored by the mini-implants).

Aims:

1. Develop a scheme for Finite Element Analysis (FEA) that would reflect true human individual variation. 2. Evaluate the effect of cortical bone stiffness and thickness on the rate of tooth movement in the two distalization modalities.

Our hypothesis was that cortical bone quality and quantity influence the rate of tooth movement in both conditions.

Methods:

A 3D model of the maxilla containing the different components (teeth, PDL, trabecular and cortical bones) was generated from a CT scan and material properties were assigned to each component. Cortical bone, the study variable, was divided into several masks, utilizing the data generated by Peterson et al. (2006), who measured stiffness and thickness of the maxilla in human cadavers. The data derived from 13 cadavers were incorporated into the 3D models to simulate individual variation of cortical bone at the different maxillary locations. Subsequently, a finite element analysis was used to simulate the direct and indirect distalization modalities. Outcome measures included stress distribution and displacement of the following permanent teeth: canine, first and second premolars, first and second molars. Statistical methods included t-tests and analyses of variance for group comparisons, and correlation tests for associations among variables.

Results:

In the direct anchorage modality, 55% of the total Von mises stress distribution was located at the canine and first premolar, while 68% of stress amounts were found at the molars in the indirect modality. Moreover, stress amounts decreased from the cervical to the apical parts of the PDL. High correlations were observed between PDL stress and crown displacement of the corresponding tooth in both modalities ($0.75 < r < 0.99$). In the stiffness variation experiments, stress amounts at the buccal, palatal, mesial and distal surfaces were significantly different from tooth to adjacent while in the thickness variation parts, tendency toward similar stress was noted between the same surfaces of adjacent teeth.

At the first molar, inverted significant correlations were found between buccal cortical bone stiffness and PDL stress amounts ($-0.68 < r < -0.82$) with higher

correlations found in the indirect modality ($-0.68 < r < -0.82$) compared to the direct modality ($-0.68 < r < -0.72$).

Correlations between bone stiffness and stress at the 3 vertical root levels (apical, middle, and cervical) of the mesial and distal surfaces were similar to total surface stress except for the disto-cervical area which did not correlate significantly with bone stiffness in both distalization modalities. At the canine, no significant correlations were observed between PDL stress amounts and the corresponding cortical bone stiffness ($r < -0.4$).

The use of isotropic rather than orthotropic material property of cortical bone resulted in lower PDL stress amounts in the indirect modality and at the canine in the direct modality, however the maximum difference found was equal to 51Pa.

Conclusions:

1. Using a novel approach that integrated human data on bone properties, we introduced a finite element analysis that accounted for individual variation.
2. Tooth movement is affected by the encounter of the moving tooth (molar, not canine) of the stiffer area of the buccal cortical bone, apparently regardless of the thickness of this bone. Accordingly, moving teeth away from the stiff outer cortex results in less resistance to tooth movement.
3. Planning distal movement of maxillary teeth against mini-implants should not follow a generic pattern, but rather take into account the anatomy of the jaw, including thickness of cortical bone around the involved teeth and posterior crowding. Therefore, treatment modalities would be chosen on the basis of individual anatomy, not only on force magnitude and vector, to generate the least amount of side effects.
4. Future research should elucidate time-dependent orthodontic movement, beyond the present initial static FEA conditions.

CONTENTS

ACKNOWLEDGEMENTS	v
ABSTRACT	vi
LIST OF ILLUSTRATIONS	xii
LIST OF TABLES	xv
LIST OF ABBREVIATIONS	xvii
1. INTRODUCTION	1
1.1. Interprofessional modes of research	1
1.2. Engineering influence in orthodontics: mechanics of tooth movement	1
1.3. Biology of tooth movement	3
2. LITERATURE REVIEW	6
2.1. Treatment of Class II malocclusion	6
2.1.1. Orthopedic treatment	6
2.1.2. Combined orthodontic-surgical treatment	7
2.1.3. Orthodontic treatment	7
2.1.3.1. Class II elastics	8
2.1.3.2. Extraction	8
2.1.3.3. Anchorage	9
2.1.3.4. Distalization / Non extraction treatment	10
2.2. Temporary anchorage devices (TADs)	21
2.2.1. Types	22
2.2.2. Indications	23
2.2.3. Failure risk	23
2.2.4. Distalization with TADs	24
2.3. Finite element analysis (FEA)	29
2.3.1. Definition	30
2.3.2. 3D imaging	31
2.3.2.1. Evolution toward 3D imaging	31
2.3.2.2. CBCT vs CT scans	32
2.3.3. Development of FEA in dentistry	34
2.3.4. Limitations	36

2.3.4.1. Inaccurate assumptions	36
2.3.4.2. Generalizability of results	37
2.3.4.3. Applicability of results	37
2.3.4.4. 3D modelling of human tissues	38
2.3.4.5. Tooth movement simulation over time	40
2.3.5. FEA in orthodontics	41
2.3.6. Human bones	49
2.3.6.1. Role of bone in the rate of tooth movement	50
2.3.6.2. Progress in bone modelling in orthopedic medicine	52
2.4. Significance	53
2.5. Specific aims	56
2.6. Hypothesis	56
3. MATERIALS AND METHODS	58
3.1. Material	58
3.1.1. Anatomical record	58
3.1.2. Individual data acquisition	59
3.2. Methods	63
3.2.1. 3D model	64
3.2.1.1. Model segmentation	64
3.2.1.2. Resampling	70
3.2.1.3. CAD processing	72
3.2.1.4. Individual variations	73
3.2.2. Finite Element Analysis (FEA)	79
3.2.2.1. Mesh size / Convergence testing	79
3.2.2.2. Material properties definition	82
3.2.2.3. Interactions	84
3.2.2.4. Loading scenario	87
3.2.2.5. Data collection and export	90
3.2.3. Statistical analysis	94
4. RESULTS	96
4.1. Stress comparison between the teeth	96
4.1.1. Part 1: Stiffness variation / Direct anchorage modality	96
4.1.2. Part 2: Stiffness variation / Indirect anchorage modality	98
4.1.3. Part 3: Thickness variation / Direct anchorage modality	100
4.1.4. Part 4: Thickness variation / Indirect anchorage modality	101
4.2. Comparison between direct and indirect anchorage modalities	103

4.3. Correlation between stress and displacement	106
4.4. Correlation between cortical bone properties and stress	107
4.4.1. Correlations with cortical bone thickness	107
4.4.2. Correlations with cortical bone stiffness	108
4.4.3. Correlation with vertical sections of the mesial and distal surfaces	109
4.4.3.1. Thickness	109
4.4.3.2. Stiffness	110
4.4.4. Correlation of stresses with the average stiffness	112
4.4.4.1. Canine	112
4.4.4.2. First molar	113
4.5. Multiple regression analysis	115
4.5.1. Canine	115
4.5.2. First molar	115
4.5.2.1. Stresses prediction from thickness values	115
4.5.2.2. Mesial stress prediction from stiffness values	115
4.5.2.3. Distal stress prediction from stiffness values	117
4.6. Stiffness variation stress vs Thickness variation stress	119
4.7. Effect of bone material property type on the PDL stress values	119
5. DISCUSSION	124
5.1. Strengths	124
5.1.1. Individual variation	124
5.1.2. Effect of bone characteristics on tooth movement	125
5.1.3. Orthotropic material properties	126
5.1.4. Complete 3D model	127
5.2. Comparison with FEA distalization studies	127
5.2.1. Distalization modalities	128
5.2.2. Model construction and set up	130
5.2.2.1. Bone	130
5.2.2.2. PDL	131
5.2.2.3. Interaction	132
5.2.3. Aims	133
5.2.4. Data collection	134
5.2.5. Results	135
5.2.5.1. Qualitative comparison	135
5.2.5.2. Quantitative assessment	137
5.3. Correlation between stress and displacement	140
5.4. Correlation between stress and bone properties (stiffness and	

thickness)	142
5.4.1. Theory 1: Composite material	142
5.4.2. Theory 2: Presence of direct contact between PDL and cortical bone	143
5.4.3. Synthesis on theories 1 and 2	147
5.5. Correlation between thickness and stiffness of cortical bone parts	150
5.6. Effect of material property type on results	150
5.7. Clinical implications	151
5.8. Limitations	153
5.9. Future research	154
6. CONCLUSION	156

ILLUSTRATIONS

Figure		Page
1.1	Moment to force ratio (M/F ratio)	2
2.1	Correction a complete Class II malocclusion treated with the extraction of the maxillary first premolars	9
2.2	Correction of complete Class II malocclusion with extraction of the 4 first premolars	9
2.3	The SAIF spring	11
2.4	Jasper jumper	12
2.5	Eureka spring	13
2.6	Superelastic NiTi for molar distalization	13
2.7	Jones Jig	14
2.8	Repelling magnets	15
2.9	Pendulum appliance	15
2.10	Distal Jet appliance	16
2.11	Keles-Sayinsu appliance	17
2.12	Correction of a complete Class II malocclusion treated with no extractions	18
2.13	Schematic of panoramic film indicating location and sites at which 3 mm of bone stock was consistently available	26
2.14	Schematic of panoramic film indicating location and sites at which 4 mm of bone stock was consistently available	26
2.15	Widths of the attached gingiva and alveolar mucosa in the maxillary anterior teeth	27
2.16	Different buccal and palatal TAD supported distalization	28
2.17	Dental movements with single and double miniscrews	29
2.18	3D model of the engineering structure to be constructed	31
2.19	FEA applied before the construction for design verification and detection of critical locations	31
2.20	Construction of the part after FEA	31
2.21	Axial images of the maxillary arch illustrating the image contrast in CBCT and MSCT images	33
2.22	Micro-computed tomography (CT) image and cone beam CT image to illustrate the resolution difference	34
2.23	Three dimensional finite element model of the lower first premolar	42
2.24	Complex FE model of the midface and the jaws	42
2.25	Tangential load (F_T) from the mandibular canine to the TAD and (F_A) Miniscrew tightening torque	44
2.26	Stress distribution for the tightening and tangential force	44
2.27	FE models and strain distribution results of FEA applied to molar protraction	45
2.28	Three distalization appliances used and eruption stages of second molars in the study by Kang et al. 2016	46
2.29	Displacement in the Y axis with three distalization appliances described by Kang et al. (2016)	47
2.30	Distalization modalities described by Yu et al. (2012)	47
2.31	Displacement in the Y axis of the study by Yu et al. (2012)	48
2.32	Various root morphologies (Kamble et al. 2012)	48

2.33	Bone resorption in adults and children	51
2.34	Bone density distribution in Hounsfield units (HU) in the FE model of human mandibular cortical bone segment	53
3.1	Cortical bone sites of the maxilla	61
3.2	3D patient specific model reconstruction and finite element simulation	63
3.3	Teeth mask captured using according to the grayscale value	65
3.4	Finalized teeth mask	65
3.5	Cortical bone layer mask	66
3.6	Roots mask	66
3.7	Mask 4	67
3.8	Gaps closed in mask 4	67
3.9	Trabecular bone mask	67
3.10	3D model of mask 7	68
3.11	Cortical bone (mask 8)	68
3.12	Inflated teeth mask	69
3.13	PDL mask	69
3.14	Smoothened masks	70
3.15	Geometry changes after resampling	70
3.16	PDL thickness change after resampling	71
3.17	CAD components (miniscrew and brackets)	73
3.18	Partition of cortical bone mask into different parts	74
3.19	Cortical bone parts constructed according to Peterson et al. (2006)	75
3.20	Areas of thickness measurements in the buccal cortical bone part at the premolar area	76
3.21	Technique applied to increase cortical bone thickness	77
3.22	Technique applied to decrease cortical bone thickness	78
3.23	TAD level axial cut of the original template and 12 models corresponding to 12 cadavers with modified cortical bone thickness ...	79
3.24	Scatter plot showing the results of the convergence testing	80
3.25	Color coded visualization result of the convergence testing	81
3.26	Meshed template model	81
3.27	Orthotropic material properties assigned to the buccal premolar area ..	84
3.28	Steps to define “surface to surface” interaction	85
3.29	Tolerance testing	86
3.30	Results of the interaction validation test	86
3.31	Direct anchorage modality	87
3.32	Datum axis system used to define the direct load direction	88
3.33	Indirect anchorage modality	88
3.34	Datum axes systems constructed parallel to the long axis	90
3.35	Loading scenario of the direct anchorage modality	91
3.36	Loading scenario of the indirect anchorage modality	91
3.37	Element sets	92
3.38	Representative example of labeling of various variables	93
3.39	Nodes sets	93
4.1	Graphic representation of the buccal teeth response to direct anchorage modality/stiffness variation	98
4.2	Graphic representation of the buccal teeth response to the indirect anchorage modality/stiffness variation	99

4.3	Graphic representation of the buccal teeth response to direct anchorage modality/thickness variation	101
4.4	Graphic representation of the buccal teeth response to indirect anchorage modality/thickness variation	102
4.5.	Color mapped representations showing stress and displacement distribution in the direct and indirect anchorage modalities	105
4.6	Graph showing the S1, S2 and S3 for every cadaver at every cortical bone area compared to the isotropic material property value used	121
4.7	Line graph showing the stresses recorded at the different buccal teeth in the direct anchorage modality with both material properties assumptions	121
4.8	Line graph showing very similar stresses recorded at the different buccal teeth in the indirect anchorage modality with both material properties assumptions	122
4.9	Bar chart showing the stresses obtained at the mesial surface for all the models evaluated) in the direct anchorage modality	122
4.10	Bar chart showing the stresses obtained at the mesial surface for all the models evaluated) in the indirect anchorage modality	123
5.1	Different views of the cortical bone around the maxillary teeth	131
5.2	Color mapped representations of the Von mises stress recorded at the PDL compared to the study by Sung et al. (2015)	136
5.3	Tension stresses (principal stress) at the PDL in the direct anchorage modality	140
5.4	Tension stresses (principal stress) at the PDL in the indirect anchorage modality	141
5.5	Composite material formed from multiple layers of materials with different physical and mechanical properties	143
5.6	Color mapped visualization of the Von mises stresses recorded at the trabecular bone	144
5.7	Proximity of the maxillary incisor root to the palatal cortex (<i>Ten Hoeve et al. 1977</i>)	144
5.8	Stress distribution at the trabecular bone and the buccal molar cortical part in the direct and indirect modalities	146
5.9	First molar displacement (magnified) seen on an axial cut mesial to the first molar and occlusal view	147
5.10	Horizontal cut showing the effect of a mesio-buccal rotation of the first molar on the contact with the cortical bone	148
5.11	3D model and 2D axial cut at the molar level showing a contact of the palatal root with the palatal cortical area	149
5.12	Anatomical differences between the canine and the molar	149
5.13	Anatomical factors that can affect molar displacement	155

TABLES

Table	Page
2.1 3D modelling softwares available	40
2.2 Stress values at the apical third for different root morphologies under different forces	49
3.1 Density (mg/cm ³), cortical thickness (mm) and ash weight	62
3.2 Elastic moduli in GPa	63
3.3 Material properties of various anatomical components commonly used in orthodontic Finite Element Analysis studies	82
3.4 Orthotropic material properties at the “Buccal cortical bone at incisors area (5)” for 15 cadavers	83
4.1 Descriptive statistics for the stress generated on the 4 surfaces of the buccal teeth, in the direct anchorage modality, with the stiffness variation (n=11)	95
4.2 Comparison of stress among the 5 teeth at each surface (stiffness/direct anchorage)	95
4.3 Pairwise comparisons for stress between the teeth at each surface in stiffness variation/direct anchorage (n=11)	95
4.4 Descriptive statistics for the stress generated on the 4 surfaces of the buccal teeth, in the indirect anchorage modality, with the stiffness variation (n=11)	98
4.5 Comparison of stress among the 5 teeth at each surface (stiffness/indirect anchorage)	99
4.6 Pairwise comparisons for stress between the teeth at each surface (stiffness/indirect anchorage)	99
4.7 Descriptive statistics for the stress generated on the 4 surfaces of the buccal teeth, in the direct anchorage modality, with the thickness variation (n=13).....	100
4.8 Comparison of stress among the 5 teeth at each surface (thickness/direct anchorage)	100
4.9 Pairwise comparisons for stress between the teeth at each surface (thickness/direct anchorage)	101
4.10 Descriptive statistics for the stress generated on the 4 surfaces of the buccal teeth, in the indirect anchorage modality, with the thickness variation (n=13)	101
4.11 Comparison of stress among the 5 teeth at each surface (thickness/indirect anchorage)	102
4.12 Pairwise comparisons for stress between the teeth at each surface (thickness/indirect anchorage)	102
4.13 Results of the paired t-tests to compare direct vs indirect anchorage modalities	103
4.14 Correlation between the stress amounts at the mesial surfaces of every tooth and the corresponding displacements in the direct modality.....	106
4.15 Correlation between the stress amounts at the mesial surfaces of every tooth and the corresponding displacements in the indirect modality	107

4.16	Correlations between stresses and thickness of the cortical bone at palatal and buccal incisors/canine areas.in both distalization modalities	107
4.17	Correlations between stresses and thickness of the cortical bone at palatal and buccal molar areas in both distalization modalities	107
4.18	Correlations between stresses and stiffness values of the cortical bone at palatal and buccal incisors and canine areas	108
4.19	Correlations between stresses and stiffness values of the cortical bone at palatal and buccal molar areas in both distalization modalities	109
4.20	Correlations of apical, middle and cervical canine stresses with thickness of the cortical bone at palatal and buccal incisors areas in both distalization modalities	110
4.21	Correlations of apical, middle and cervical molar stresses with thickness of the cortical bone at palatal and buccal molar areas in both distalization modalities	110
4.22	Correlations of apical, middle and cervical molar stresses with the stiffness values of the cortical bone at palatal and buccal incisors/canine areas in both distalization modalities	111
4.23	Correlations of apical, middle and cervical molar stresses with the stiffness values of the cortical bone at palatal and buccal incisors areas in both distalization modalities	112
4.24	Correlations between the canine stresses at the different surfaces and the average cortical bone stiffness	114
4.25	Correlations between the first molar stresses at the different surfaces and the average cortical bone stiffness	114
4.26	Bivariate and multivariate analyses for the prediction of the stresses at the mesial of the first molar in the direct anchorage modality	116
4.27	Bivariate and multivariate analyses for the prediction of the stresses at the mesial of the first molar in the indirect anchorage modality	117
4.28	Bivariate and multivariate analyses for the prediction of the stresses at the distal of the first molar in the direct anchorage modality	118
4.29	Bivariate and multivariate analyses for the prediction of the stresses at the distal of the first molar in the indirect anchorage modality	118
4.30	Correlation between stiffness and thickness of each cortical bone part	119
4.31	Averages of the S1, S2 and S3 at each site (n=11)	120
5.1	Magnitude of maximum and minimum sagittal displacements recorded in the different FEA distalization studies	138
5.2	Summary of the differences between the 4 different studies	139
5.3	Cortical bone impact on PDL stress and crown displacement based on the correlation results	146
5.4	Working guidelines in molar distalization against miniscrews	152

ABBREVIATIONS

STRESS AT THE CANINE

IN DIRECT DISTALIZATION		IN INDIRECT DISTALIZATION	
dTD3	Stress at distal of canine in the direct anchorage/thickness variation	iTD3	Stress at distal canine in the indirect anchorage/thickness variation
dTP3	Stress at palatal canine in the direct anchorage/thickness variation	iTP3	Stress at palatal canine in the indirect anchorage/thickness variation
dTM3	Stress at mesial canine in the direct anchorage/thickness variation	iTM3	Stress at mesial canine in the indirect anchorage/thickness variation
dtB3	Stress at buccal canine in the direct anchorage/thickness variation	iTB3	Stress at buccal of canine in the indirect anchorage/thickness variation
dTD3a	Stress at distal apical canine area in direct anchorage/thickness variation	iTD3a	Stress at apical distal canine area in indirect anchorage/thickness variation
dTD3m	Stress at middle distal canine area in direct anchorage/thickness variation	iTD3m	Stress at middle distal canine area in indirect anchorage/thickness variation
dTD3c	Stress at cervical distal canine area in direct anchorage/thickness variation	iTD3c	Stress at cervical distal canine area in indirect anchorage/thickness variation
dTM3a	Stress at apical mesial canine area in direct anchorage/thickness variation	iTM3a	Stress at apical mesial canine area in indirect anchorage/thickness variation
dTM3m	Stress at middle mesial canine area in direct anchorage/thickness variation	iTM3m	Stress at middle mesial canine area in indirect anchorage/thickness variation
dTM3c	Stress at cervical mesial canine area in direct anchorage/thickness variation	iTM3c	Stress at cervical mesial canine area in indirect anchorage/thickness variation
dSD3	Stress at distal of canine in direct anchorage/stiffness variation	iSD3	Stress at distal canine in indirect anchorage/stiffness variation
dSP3	Stress at palatal of canine in direct anchorage/stiffness variation	iSP3	Stress at palatal canine in indirect anchorage/stiffness variation
dSM3	Stress at mesial of canine in direct anchorage/stiffness variation	iSM3	Stress at mesial canine in indirect anchorage/stiffness variation
dSB3	Stress at buccal of canine in direct anchorage/stiffness variation	iSB3	Stress at buccal canine in indirect anchorage/stiffness variation
dSD3a	Stress at apical distal canine area in direct anchorage/stiffness variation	iSD3a	Stress at apical distal canine area in indirect anchorage/stiffness variation
dSD3m	Stress at middle distal canine area in direct anchorage/stiffness variation	iSD3m	Stress at middle distal canine area in indirect anchorage/stiffness variation
dSD3c	Stress at cervical distal canine area in direct anchorage/stiffness variation	iSD3c	Stress at cervical distal canine area in indirect anchorage/stiffness variation
dSM3a	Stress at apical mesial canine area in direct anchorage/stiffness variation	iSM3a	Stress at apical mesial canine area in indirect anchorage/stiffness variation
dSM3m	Stress at middle mesial canine area in direct anchorage/stiffness variation	iSM3m	Stress at middle mesial canine area in indirect anchorage/stiffness variation
dSM3c	Stress at cervical mesial canine area in direct anchorage/stiffness variation	iSM3c	Stress at cervical mesial canine area in indirect anchorage/stiffness variation

DISPLACEMENT AT THE CANINE

IN DIRECT DISTALIZATION		IN INDIRECT DISTALIZATION	
dSU3	Total displacement of the centroid of the canine	iSU3	Total displacement of the centroid of the canine
dSU3x	Canine displacement in the x axis	iSU3x	Canine displacement in the x axis
dSU3y	Canine displacement in the y axis	iSU3y	Canine displacement in the y axis
dSU3z	Canine displacement in the z axis	iSU3z	Canine displacement in the z axis

STRESS AT THE FIRST MOLAR

IN DIRECT DISTALIZATION		IN INDIRECT DISTALIZATION	
dTD6	Stress at distal of first molar in the direct anchorage/thickness variation	iTD6	Stress at distal of first molar in indirect anchorage/thickness variation
dTP6	Stress at palatal first molar in the direct anchorage/thickness variation	iTP6	Stress at palatal first molar in indirect anchorage/thickness variation
dTM6	Stress at mesial first molar in direct anchorage/thickness variation	iTM6	Stress at mesial first molar in indirect anchorage/thickness variation
dtB6	Stress at buccal first molar in direct anchorage/thickness variation	iTB6	Stress at buccal first molar in indirect anchorage/thickness variation
dTD6a	Stress at apical distal first molar area in direct anchorage/thickness variation	iTD6a	Stress at apical distal first molar area in indirect anchorage/thickness variation
dTD6m	Stress at middle distal first molar area in direct anchorage/thickness variation	iTD6m	Stress at middle distal first molar area in indirect anchorage/thickness variation
dTD6c	Stress at cervical distal first molar area in direct anchorage/thickness variation	iTD6c	Stress at cervical distal first molar area in indirect anchorage/thickness variation
dTM6a	Stress at apical mesial first molar area in direct anchorage/thickness variation	iTM6a	Stress at apical mesial first molar area in indirect anchorage/thickness variation
dTM6m	Stress at middle mesial first molar area in direct anchorage/thickness variation	iTM6m	Stress at middle mesial first molar area in indirect anchorage/thickness variation
dTM6c	Stress at cervical mesial first molar area in direct anchorage/thickness variation	iTM6c	Stress at cervical mesial first molar area in indirect anchorage/thickness variation
dSD6	Stress at distal first molar in direct anchorage/stiffness variation	iSD6	Stress at distal first molar in indirect anchorage/stiffness variation
dSP6	Stress at palatal first molar in direct anchorage/stiffness variation	iSP6	Stress at palatal first molar in indirect anchorage/stiffness variation
dSM6	Stress at mesial first molar in direct anchorage/stiffness variation	iSM6	Stress at mesial first molar in indirect anchorage/stiffness variation
dSB6	Stress at buccal first molar in direct anchorage/stiffness variation	iSB6	Stress at buccal first molar in indirect anchorage/stiffness variation
dSD6a	Stress at apical distal first molar area in direct anchorage/stiffness variation	iSD6a	Stress at apical distal first molar area in indirect anchorage/stiffness variation
dSD6m	Stress at middle distal first molar area in direct anchorage/stiffness variation	iSD6m	Stress at middle distal first molar area in indirect anchorage/stiffness variation
dSD6c	Stress at cervical distal first molar area in direct anchorage/stiffness variation	iSD6c	Stress at cervical distal first molar area in indirect anchorage/stiffness variation
dSM6a	Stress at apical mesial first molar area in direct anchorage/stiffness variation	iSM6a	Stress at apical mesial first molar area in indirect anchorage/stiffness variation
dSM6m	Stress at middle mesial first molar area in direct anchorage/stiffness variation	iSM6m	Stress at middle mesial first molar area in indirect anchorage/stiffness variation
dSM6c	Stress at cervical mesial first molar area in direct anchorage/stiffness variation	iSM6c	Stress at cervical mesial first molar area in indirect anchorage/stiffness variation

DISPLACEMENT AT THE FIRST MOLAR

IN DIRECT DISTALIZATION		IN INDIRECT DISTALIZATION	
dSU6	Total displacement of the centroid of first molar	iSU6	Total displacement of the centroid of first molar
dSU6x	First molar displacement in the x axis	iSU6x	First molar displacement in the x axis
dSU6y	First molar displacement in the y axis	iSU6y	First molar displacement in the y axis
dSU6z	First molar displacement in the z axis	iSU6z	First molar displacement in the z axis

STRESS AND DISPLACEMENT AT FIRST PREMOLAR

IN DIRECT DISTALIZATION		IN INDIRECT DISTALIZATION	
dSM4	Stress at the mesial of first premolar in direct anchorage/stiffness variation	iSM4	Stress at the mesial of first premolar in indirect anchorage/stiffness variation
dSU4	Total displacement of the centroid of the first premolar	iSU4	Total displacement of the centroid of the first premolar
dSU4x	First premolar displacement in the x axis	iSU4x	First premolar displacement in the x axis
dSU4y	First premolar displacement in the y axis	iSU4y	First premolar displacement in the y axis
dSU4z	First premolar displacement in the z axis	iSU4z	First premolar displacement in the z axis

STRESS AND DISPLACEMENT AT SECOND PREMOLAR

IN DIRECT DISTALIZATION		IN INDIRECT DISTALIZATION	
dSM5	Stress at the mesial of second premolar in direct anchorage/stiffness variation	iSM5	Stress at mesial of second premolar in indirect anchorage/stiffness variation
dSU5	Total displacement of the centroid of the second premolar	iSU5	Total displacement of the centroid of the second premolar
dSU5x	Second premolar displacement in x axis	iSU5x	Second premolar displacement in the x axis
dSU5y	Second premolar displacement in y axis	iSU5y	Second premolar displacement in the y axis
dSU5z	Second premolar displacement in y axis	iSU5z	Second premolar displacement in the z axis

STRESS AND DISPLACEMENT AT SECOND MOLAR

IN DIRECT DISTALIZATION		IN INDIRECT DISTALIZATION	
dSM7	Stress at the mesial of the second molar in direct anchorage/stiffness variation	iSM7	Stress at mesial of second molar in indirect anchorage/stiffness variation
dSU7	Total displacement of the centroid of the second molar	iSU7	Total displacement of the centroid of the second molar
dSU7x	Second molar displacement in the x axis	iSU7x	Second molar displacement in the x axis
dSU7y	Second molar displacement in the y axis	iSU7y	Second molar displacement in the y axis
dSU7z	Second molar displacement in the z axis	iSU7z	Second molar displacement in the z axis

dSD	Stress at distal surface in the direct anchorage in the stiffness variation part	iSD	Stress at distal surface in the indirect anchorage in the stiffness variation part
dSP	Stress at palatal surface in the direct anchorage in the stiffness variation part	iSP	Stress at palatal surface in the indirect anchorage in the stiffness variation part
dSM	Stress at mesial surface in the direct anchorage in the stiffness variation part	iSM	Stress at mesial surface in the indirect anchorage in the stiffness variation part
dSB	Stress at buccal surface in the direct anchorage in the stiffness variation part	iSB	Stress at buccal surface in the indirect anchorage in the stiffness variation part
dTD	Stress at distal surface in the direct anchorage in the thickness variation part	iTD	Stress at distal surface in the indirect anchorage in the thickness variation part
dTP	Stress at palatal surface in the direct anchorage in the thickness variation part	iTP	Stress at palatal surface in the indirect anchorage in the thickness variation part
dTM	Stress at mesial surface in the direct anchorage in the thickness variation part	iSM	Stress at mesial surface in the indirect anchorage in the thickness variation part
dTB	Stress at buccal surface in the direct anchorage in the thickness variation part	iTB	Stress at buccal surface in the indirect anchorage in the thickness variation part

FEM	Finite Element Method	FEA	Finite Element Analysis
FE	Finite Element	(OTM)	Orthodontic Tooth Movement
3D	Three Dimensional	2D	Two Dimensional
CCT	Controlled Clinical Trials	RCT	Randomized Controlled Trials
CT	Computed Tomography	CBCT	Cone beam computed tomography
DICOM	Digital Imaging and Communications in Medicine	CAD/CAM	Computer Aided Design/ Computer Aided Manufacturing
MSCT	Multi-Slice Spiral CT	HU	Hounsfield Unit
BMD	Bone Mineral Density	TAD	Temporary Anchorage Device
CEJ	Cemento Enamel Junction	TMJ	Temporo-Mandibular Joint
TP	Transpalatal Bar	NiTi	Nickel Titanium

Glossary

1. *Malocclusion*

Malocclusion is defined as any deviation from the normal or ideal relationship of the maxillary and mandibular teeth, as they are brought into functional contact. A major step in the development of orthodontics was Angle's classification of malocclusion (1899), in which he described 3 classes of malocclusion based on the occlusal relationship of the first molars (Angle, 1899)(Fig. a):

Class I: Normal relationship of the molars, but the line of occlusion is disturbed because of spaced, rotated or crowded teeth.

Class II or distocclusion: Mandibular molars distally positioned relative to the maxillary molars. It could be accompanied with disturbance of the line of occlusion.

Class III or mesiocclusion: Mandibular molars mesially positioned relative to the maxillary molars. It could be accompanied with disturbance of the line of occlusion.

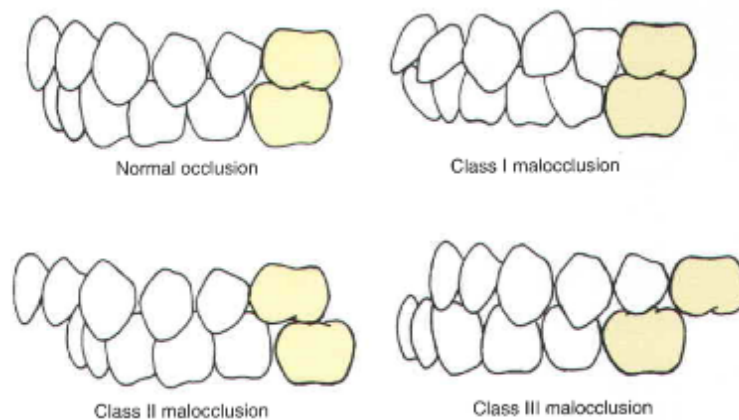


Fig. a Illustration of the various classes of malocclusion according to Angle (From (Proffit et al., 2012).

The Angle classification was criticized for its inability to accurately depict and differentiate between various malocclusions. (T. Graber, 1972; Rinchuse & Rinchuse, 1989), including many deficiencies:

1. Disregard of the relationship between teeth and face.
2. One dimensional (A-P) description of a three-dimensional malocclusion.
3. Based only on clinical examination, non-differentiating between dentoalveolar and skeletal discrepancies.
4. No account of arch length problems.
5. Non indicative of the severity of the problem.

Numerous attempts have followed to modify/improve on Angle's classification to replace it with a more sensitive indicator or develop methods founded on several indicators of malocclusion rather than relying solely on the molar relationship (Bjork & Solow, 1964; Ackerman & Proffit, 1969; Williams & Stephens, 1992). Because of its

simplicity, Angle's system withstood the test of time and remains the most commonly used.

2. Malocclusion measures

a. Sagittal occlusal measures

- Molar and canine occlusion: Angle classification is based on the molar occlusion only. The relationship between maxillary and mandibular canines can be evaluated similarly. Deviations of Class I halfway towards Class II or Class III are termed as "half cusp" Class II and Class III occlusions. Hence, 5 possible ordinal categorizations of molar and canine occlusion are possible on each side (right and left). A malocclusion is labeled subdivision when the deviation is unilateral.
- Overjet is the distance between the labial surface of the most labial mandibular incisor and the incisal edge of the most labial maxillary incisor when the teeth are in centric occlusion. Another index of the sagittal occlusion, the overjet equal 2 to 3 mm in normal occlusion. In the absence of dental compensation, a positive overjet accompanies Class II malocclusion; Class III malocclusion is accompanied by a null or negative overjet (or anterior crossbite).

b. Vertical occlusal measures

- Overbite is the vertical overlap between the maxillary and mandibular incisors. A percentage representing the amount of the coverage of the mandibular incisors by the maxillary incisors is given in the presence of a positive overlap of teeth or is labelled as zero in case teeth are edge to edge. The normal occlusion is characterized by an overbite of 20 to 30%.
- In the absence of overlap between the incisors, an anterior open bite is noted and is equal to the millimetric measurement between the incisal edges of the maxillary and mandibular incisors.

c. Transverse occlusal measures

- Posterior cross-bite is present when the mandibular posterior teeth are positioned more towards the cheek compared to upper posterior teeth which are occluding more towards the tongue. It can be uni or bilateral and involving 1 or many teeth.
- A midline discrepancy is the distance separating the maxillary and the mandibular midlines (contact surfaces between the right and left central incisors). It usually goes along a subdivision malocclusion but can have other causes.

d. Arch length discrepancy (ALD)

ALD defines the disparity in the relationship between sizes of teeth and jaw, expressed in crowding or spacing. Arch length excess exists when the arch perimeter (available space) exceeds the sum of teeth widths (required space), resulting in spacing among the teeth. Arch length deficiency refers to the arch perimeter being smaller than the sum of teeth widths, resulting in crowding of teeth, the most common type of malocclusion. Its treatment includes extractions of teeth, interproximal reduction and expansion (lateral, anterior and posterior).

Crowding and profile improvement are the main reason for extraction (often first premolars) in 83% of malocclusions (Baumrind et al., 1996). Post treatment stability and dental occlusion are other reasons for extraction. Premolar extraction does not guarantee stability of tooth alignment.

CHAPTER 1

INTRODUCTION

The present study is underlain by three bases: the progress in interprofessional research, the mechanics of orthodontic tooth movement, and the biological process involved in this therapeutic displacement.

1.1. Interprofessional modes of research

An essential facet of the scientific innovations in the medical field in the last decade is related to the exchange of information and utilization of technology across professional fields, mainly engineering. This development allowed the substitution of incidental discoveries based on trial and error approaches that were valuable in the past, with the more organized employment of knowledge acquired from other domains. Accordingly, the application of physical sciences in the medical and dental fields resulted in a more orderly experimental development best illustrated in the progress of 3D imaging, CAD/CAM technologies, material testing, appliance design and 3D modeling.

1.2. Engineering influence in orthodontics: mechanics of tooth movement

Many of the undesirable side effects that occur during orthodontic treatment can be attributed to the lack of understanding of the associated principles of physics, mathematics and engineering. In the past, clinicians tried to apply mathematical calculations to represent force systems, and applied static mechanical laws to explain

clinical responses. In this context, the type of tooth movement was predicted from the forces applied and moments generated.

Tanne et al. (1988) introduced the moment to force ratio for this determination, based on the fact that for most teeth the distance from the center of resistance of the tooth (nearly at 1/3 of the root occlusally) to the bracket is about 10 mm (Fig. 1.1). However, most orthodontic appliances deliver a complex set of forces and moments coupled with variation of biological parameters such as the bone height and stiffness, putting into question the reliability of the theoretical representation.

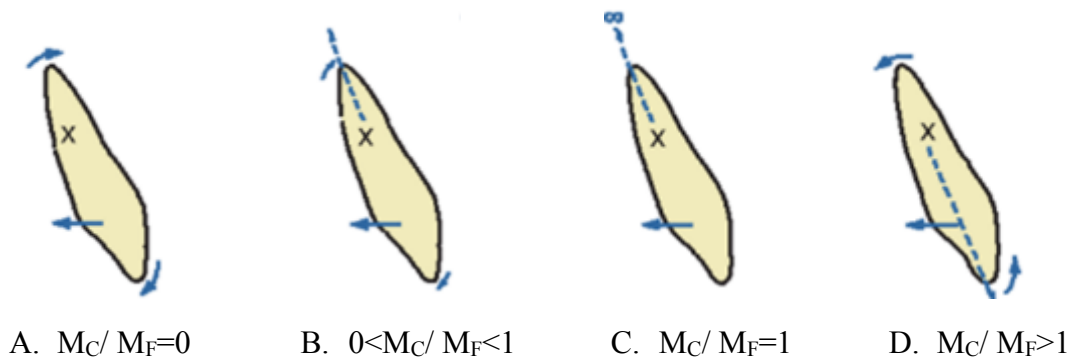


Fig. 1.1: Ratio between the moment produced by the force (M_F) and the counterbalancing moment generated by the bracket (M_C). **A-** $M_C / M_F = 0$ the tooth rotates around the center of resistance resulting in uncontrolled tipping movement; **B-** $0 < M_C / M_F < 1$ - the center of rotation moves apically resulting in controlled tipping movement; **C-** $M_C / M_F = 1$ - the center of rotation moves to the infinity resulting in translation movement; **D-** $M_C / M_F > 1$ - the center of rotation moves incisally resulting in root torque movement (Adapted from Tanne et al., 1988).

Critical to understanding the mechanics of tooth movement is the determination of the optimal force needed to achieve a specific displacement, while most compatible with harmless biologic reaction. Forces delivered by orthodontic appliances, as well as load-deflection rates of orthodontic springs and wires, can be measured by mechanical or electronic gauges. However, the problem resides in how the teeth respond to these measurable loads. Tissue response may be evaluated at three levels:

- Clinical, by assessing the rate of tooth movement, pain, root resorption, and tooth mobility.
- Cellular and biochemical, by measuring the biological markers present in response to force application, such as secondary messenger concentration and cellular activity (see section 1.3 below).
- Stress- strain level in the PDL. This domain is the least understood because it is impossible to measure clinically the stresses and strains in the PDL without altering the tissues, while results from animal studies may not be totally accurate in humans.

The ability to measure the stresses (load per unit area) in the PDL and correlate them with force magnitude would represent the ideal test of tissue reactions and project the optimal individual force for a specific movement. This objective has opened the door to the application of physical and numerical techniques, such as brittle coatings analysis, strain gauges, holography, two and three dimensional photoelasticity, and finite element analysis (FEA) to help understand and estimate tissue response to varying clinical scenarios of tooth movement.

Computer modeling techniques and FEA softwares have advanced remarkably, but most important to the future applications of these numerical techniques is the correct and constant association with the clinical environment and biologic systems.

1.3. Biology of tooth movement

Once explained mainly by the piezoelectric activity, which contributes to the maintenance of the skeleton, orthodontic tooth movement is better described by the pressure -tension theory that relies on chemical signals to stimulate cellular differentiation leading to tooth displacement. Thus, prolonged light pressure on the teeth

results in changes in blood flow and in mechanical changes (compression or tension) in the periodontal ligament (PDL.) Within hours, both phenomena lead to metabolic alterations in the form of release of cytokines, prostaglandins and other chemical agents along with enzymatic adjustments (Proffit et al., 2012).

Consequently, an inflammatory process is launched leading to a cascade of events encompassing cellular differentiation and secondary messenger cyclic adenosine phosphate (cAMP) level increase. In the next 48 hours, osteoclasts appear within the compressed PDL and engage in the “frontal resorption” of the adjacent bone indicating the beginning of tooth movement. Soon after, osteoblasts appear in the enlarged PDL at the tension side and initiate bone formation.

In the presence of heavy forces that block the blood vessels, blood supply is cut in the compression area, ensued by the propagation of a sterile necrosis in the PDL producing a hyalinized tissue. Several days later, osteoclasts appear within the adjacent bone marrow spaces and promote the “undermining resorption”, a process of resorption from within the bone that progresses to the surface, hence resulting in further delay of tooth movement. This mode of resorption is more painful than the frontal resorption.

The regional acceleratory phenomenon (RAP) is another example illustrating the biologic process of orthodontic tooth movement. RAP is a local response to a noxious stimulus by which various healing stages occur 2-10 times faster than normal physiologic healing leading to faster tissue formation (Frost, 1983). When bone is surgically irritated, a wound is created, which in turn initiates a localized inflammatory response catalyzing the recruitment of inflammatory markers (chemokines, prostaglandin E2, RANK/RANKL pathway) and cellular differentiation, and leading to

a substantial increase in osteoclasts migration and osteopenia (temporary decrease in bone mineral density), hence a faster tooth movement.

In conclusion, biologic principles affect the rate of tooth movement. The application of light continuous forces has proven to produce a more biologic response.

CHAPTER 2

LITERATURE REVIEW

2.1. Treatment of Class II malocclusion

Treatment of Class II malocclusion is challenging because much of its success relates not only to controlled mechanics, but also growth and patient compliance. Various treatment approaches can be adopted, ranging from orthopedic intervention to promote differential growth to orthodontic treatment, combined with orthognathic surgery when associated with a major skeletal dysplasia. Each approach has its own indications and advantages and yields different results.

2.1.1. Orthopedic treatment

Several randomized clinical trials and systematic reviews on the early treatment of Class II malocclusion have provided a substantial amount of evidence on orthopedic treatment (Harrison, O'Brien, & Worthington, 2007). Two major categories of appliances have been used: functional appliances and headgear.

A functional appliance (e.g. activator, bionator, Frankel and twin-block) modifies the posture of the mandible requiring the patient to position the jaw forward and downward. A backward and upward reaction is thus generated by the muscles and the soft tissues, transmitting the forces to the maxilla and leading to maxillary growth restraint ("headgear effect") while mandibular growth proceeds (Ghafari, Shoferb, Jacobsson-Hunta, Markowitzc, & Lasterb, 1998). This differential growth occurs along with dental movements, such as maxillary molar distal movement or mandibular incisor proclination.

A headgear is composed of 2 major components: the facebow used to apply the force to the teeth and the neckstrap or headcap responsible for the direction of the force. The aim is to restrain the forward and downward maxillary growth while mandibular growth proceeds normally in downward and forward growth.

While in theory the headgear targets the maxilla and a functional appliance the mandible, each appliance has an effect on the other non-directly targeted jaw, reinforcing the concept of differential growth as the main means of correction of the malocclusion in growing children (Ghafari et al., 1998).

2.1.2. Combined orthodontic-surgical treatment

Growth modification or orthodontic camouflage may not resolve Class II malocclusions with underlying severe skeletal dysplasia. Orthognathic surgery that repositions the jaws in the proper relationship becomes the ultimate treatment. Surgery is not a substitute for orthodontic treatment but complements it, requiring coordination between the orthodontist and the maxillofacial surgeon to achieve optimal results. In the past century, dramatic progress was made in this field resulting in better diagnosis, planning and results. Surgery is safer because of improved anesthetic procedures and advanced surgical techniques (Hegtvedt, Ollins, White, & Turvey, 1987).

2.1.3. Orthodontic treatment

As in any orthodontic treatment, Class II treatment may or may not involve extractions of teeth. The correction may result from the mesial movement of mandibular molars combined with proclination of mandibular incisors or from targeting the maxillary arch. Retracting protrusive maxillary incisors into extraction spaces is a

straightforward way to reduce the augmented overjet, notwithstanding its effect on profile esthetics. Another alternative is to move the maxillary buccal teeth posteriorly (or distally), thus providing space for retraction of the anterior teeth (distalization).

2.1.3.1. Class II elastics

Worn between the maxillary anterior teeth and mandibular posterior teeth, Class II elastics generate forces with opposite action on the maxillary buccal segments (distalization) and the mandibular teeth (protrusion). Protrusion of the mandibular teeth is more likely to occur because of the lesser resistance of mandibular teeth.

The elastics produce not only a transverse and anteroposterior effects but also a vertical force that tends to extrude the mandibular molars and the maxillary anterior teeth creating a clockwise rotation of the occlusal plane. These vertical effects are usually unwanted in adult patients causing a backward and downward rotation of the mandible and an increased gingival display. Hence, Class II elastics are rarely recommended as the major method of Class II correction. Their use for a short duration (3 to 4 months) to support anchorage or to complete the occlusal correction is often acceptable (Proffit et al., 2012).

2.1.3.2. Extraction

Crowding, biprotrusion and orthodontic camouflage treatment are the main indications for extractions in orthodontics. Extractions usually involve the premolar teeth but in some instances molars and canines are extracted, often decayed or periodontally compromised. Charles Tweed popularized extractions in the mid nineteenth century, extracting as many as 4 premolars and 2 molars to correct Class II

malocclusions (Ortial, 1987). Presently, numerous extraction patterns are reported in the literature. Extraction of all four premolars and only the maxillary premolars are illustrated in Figs. 2.1 - 2.2.

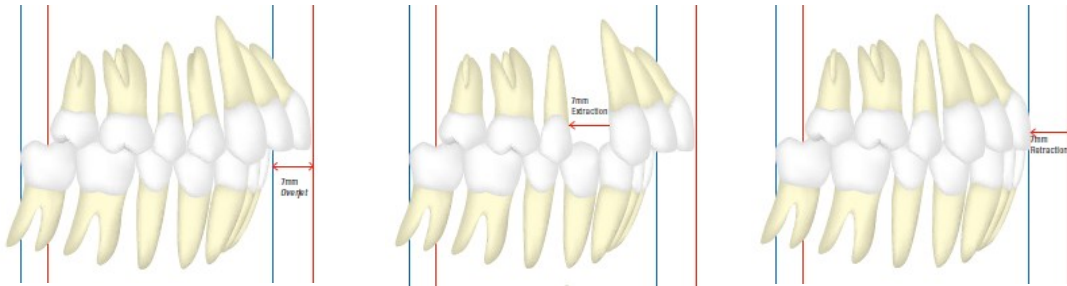


Fig. 2.1: Diagram showing the amount of movement required to correct a complete Class II malocclusion (7 mm overjet) treated with the extraction of the maxillary first premolars (Janson, Barros, Simão, & Freitas, 2009).

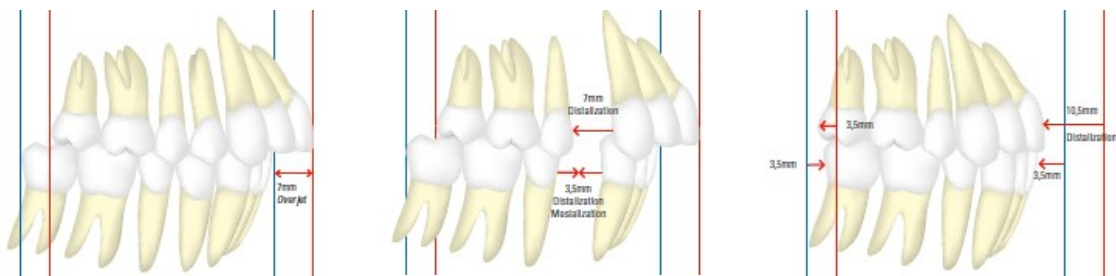


Fig. 2.2: Correction of complete Class II malocclusion (7 mm overjet) with a 3.5 mm lower incisors protrusion or crowding. Diagram illustrates treatment involving extraction of the 4 first premolars along with maxillary distalization.(Janson et al., 2009).

2.1.3.3. Anchorage

Anchorage is defined as the resistance to unwanted tooth movement. According to Newton's third law, for every desired action there is an equal and opposite reaction. This reaction force, usually undesirable, is transmitted to the other teeth. Anchorage reinforcements represent all the means the orthodontist uses to counteract these forces, and may be summarized in four types (Nanda, 2005)

- *Maximum anchorage*: Critical anchorage, whereby 75% of the space is closed by retraction of the anterior teeth.
- *Moderate anchorage*: 50% of the space is closed by retraction of anterior teeth, the posterior teeth moving forward equally.
- *Minimum anchorage*: Nearly 75% of the space is closed by mesial movement of the posterior unit. This type is difficult to achieve.
- *Absolute*: Such anchorage is needed when absolutely no mesial movement of posterior teeth is allowed; the space is closed entirely by distal movement of anterior teeth. Mini-implants or temporary anchorage devices usually provide this support.

Despite having more anchorage value compared to the anterior unit, reinforcement of the posterior unit is needed in the treatment of Class II malocclusions with extractions to achieve maximum to absolute anchorage (Nanda, 2005).

2.1.3.4. Distalization / Non extraction treatment

The concept of “distal driving” the maxillary buccal segment has a long orthodontic history. After realizing that Class II elastics treatment has minimal effect on maxillary molars, there was a shift toward appliances acting on the maxilla and the maxillary teeth to avoid unwanted side effects on the mandibular incisors. To address the demanding anchorage considerations, intraoral means based on palatal anchorage, interarch anchorage and extraoral forces have been used.

- Interarch methods

With an action similar to the Class II elastics, these appliances were mainly conceived for non-compliant patients. Despite decreasing the maxillary resistance (by

decreasing the number of maxillary teeth) flaring of the mandibular incisors remains a major component of to the Class II correction.

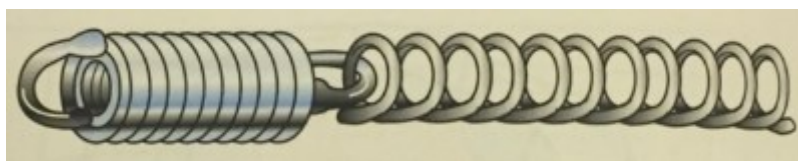


Fig. 2.3: The SAIF spring (T. M. Graber, Vanarsdall Jr, & Vig, 2006).

The Saif spring (Several adjustable intermaxillary force) developed by Armstrong in 1970s, was the first clinically useful interarch system (Fig. 2.3). Consisting of 2 springs (3mm diameter in 7 or 10mm lengths), one inside the other, the appliance was used to deliver Class II or Class III force. Problems were related to the high forces delivered (200 to 400 g/cm²) and the constant breakage that used to happen (Graber et al., 2006).

Introduced later (1990s), the Jasper Jumper is the most widely used interarch system. A curvilinear coil spring wrapped in a plastic cover with rotating attachments at both ends, the jumper allows for full range of mouth opening, unlike other appliances (Fig. 2.4). It employs “push” rather than the traditional “pull” forces of the Class II elastics and previous springs. Pull forces result in the extrusion of the maxillary anterior teeth and mandibular posterior teeth, increasing the lower face height and triggering a backward and downward mandibular rotation that accentuates the Class II condition. Alternatively, the push forces generated by the Jasper Jumper reduces these undesirable side effects because it causes an intrusion of the maxillary molars and mandibular incisors which opens the bite without any clockwise rotation of the mandible (Cope et al., 1994).

Due to its success, many companies tried to mimic the Jasper Jumper without a clear improvement over the original design. Some of its variations are called: Adjustable Bite Corrector, Bite fixer, Klapper Superspring II, Forsus Nitinol flat spring.

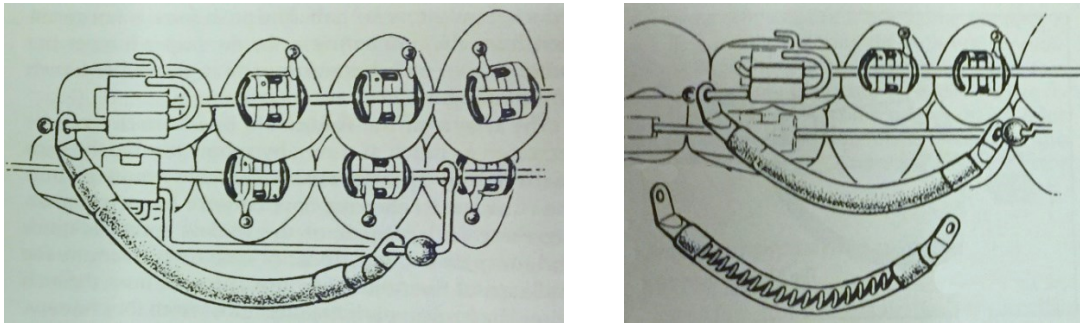


Fig. 2.4: Jasper jumper (Graber et al., 2006).

i

More recently the interarch compression springs became popular Class II treatment in non-compliant patients, offering inherent advantage over the curvilinear springs that include less spring fatigue, less breakage, and most importantly the ability to manipulate the force vector according to individual patient needs (Fig. 2.5).

Stromeyer et al. (2002) evaluated cephalometric changes after using the Eureka spring in 50 consecutively treated bilateral Class II patients. They found a sagittal correction at an average rate of 0.7 mm per month, and intrusion of the maxillary molars and mandibular incisors by 1 mm and 2 mm, respectively for every 3 mm of sagittal correction. Most importantly, half of the Class II correction was achieved by maxillary distalization, and indication that these springs are useful in malocclusions requiring minimum to moderate anchorage. However, DeVincenzo et al. (1997) reported a 25% relapse of 2 mm or more in a population of 115 patients treated with Eureka springs within the subsequent 4 months.

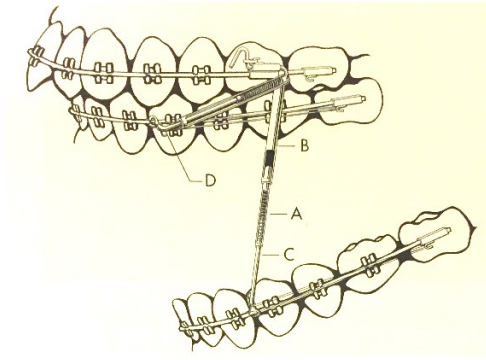


Fig. 2.5: Eureka spring (Graber et al., 2006).

- Palate- anchored distalization

Anchorage can be reinforced against the anterior palate, buttressed by the stiff cortical bone beneath the rugae. Removable appliances are not effective because of lack of stability (loose and ill fitted) and compliance issues (Proffit et al., 2012). Yet, the more successful fixed appliances usually include an acrylic “Nance”-type pad in contact with the rugae, frequently comprising wires extended to the premolars. Against the palatal anchorage several means are available to move the molars distally. The most common is the use of a NiTi open coil spring compressed against the molars, producing a light and continuous force, ideal for tooth movement.

Locatelli (1992) recommended the use of a superelastic NiTi wire with 2 stops (Fig. 2.6). The first stop is flush to the distal of the premolar bracket while the second stop is positioned mesial to the molar tube. As the wire tends to regain its original linear shape, its superelastic property engender forces moving the molar distally.

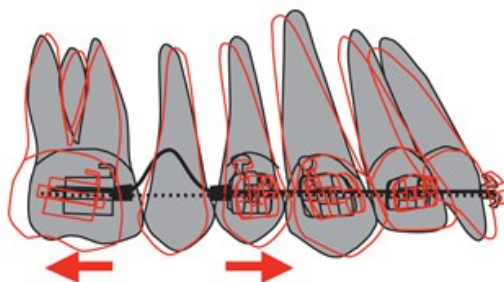


Fig. 2.6: Superelastic NiTi wire with 2 stops used to distalize the molar (Graber et al., 2006).

The use of Jigs in conjunction with a Nance arch was also described in a number of appliances such as the Jones Jig (Fig. 2.7), Lokar Molar Distalizer and the Keles Jig. The most popular is the Jones Jig, which generates a force of 70 to 75 g/cm² when its active open coil spring is compressed. This force is well below that generated by the pendulum appliance, which helps in controlling the side effects. Besides being bulky and causing distal crown tipping, these jig-containing appliances tend to break frequently (Haydar & Üner, 2000).



Fig. 2.7: Jones Jig, formed of 2 soldered wires, 1 heavy and 1 light that is engaged in the molar tube. A sliding sheath placed anteriorly is tied back to the premolar bracket to activate the open coil that slides on the heavy wire (Graber et al., 2006).

Repelling magnets of 3.5 mm diameter were also used. Although the force generated is less than the other techniques, manufactures claimed that bodily movement would occur due to the large magnetic field generated (Fig 2.8). The disadvantages include cost, toxicity, and most importantly the need for frequent activations because the force decreases when the teeth moves away from each other (Bondemark et al., 1994; Gianelly, 1998).

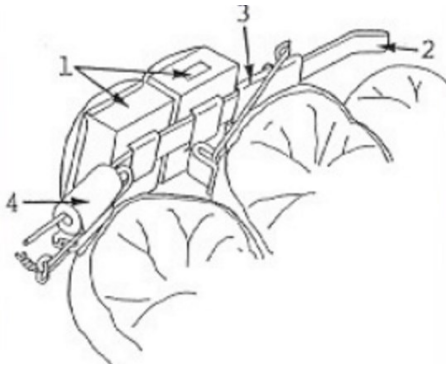


Fig. 2.8: Repelling magnets (Graber et al., 2006).

The pendulum appliance incorporates wires attached to the Nance button activated against the permanent first molars. When activated, the wire arms tend to move the molars in a distopalatal arc. To compensate for the lingual movement, the clinician can make modifications to the opening loops (Fig. 2.9).



Fig. 2.9: The pendulum appliance uses beta-titanium arms extended from the acrylic pad and attached to the palatal sheaths on the molar tube. The magnitude of the force delivered depends on the initial position of the arms. (Graber et al., 2006).

The following dentoalveolar movements have been reported following the use of the pendulum appliance: distalization of the maxillary molars with significant distal crown tipping and intrusion, mesial movement of the premolars, and proclination of the incisors; the last two effects represent loss of anchorage (Hilgers, 1992). When the pendulum was activated to deliver 200 to 250 gm, Byloff et al. (1997) reported that the

maxillary molars averaged 1mm/month of distal movement with a significant amount of distal tipping. The amount of anchorage loss is estimated to be one quarter to one third of the increase in arch length. When tip-back bends were incorporated into the appliance to minimize the tipping, greater loss of anchorage was recorded.

Many appliances used a design similar to the pendulum. The distal jet (Fig. 2.10) may induce decreased amount of tipping compared to the original pendulum design. The arms of the distal jet are characterized by the bayonet bend resulting in a line of force that is near the center of resistance of the molar. Light continuous forces are generated through an open coil present on the distal jet's arm and activated by a sliding sheath. Studies reported 1 degree of tipping per 1 millimeter of distal crown movement with the use of the distal jet (Carano & Testa, 2001).

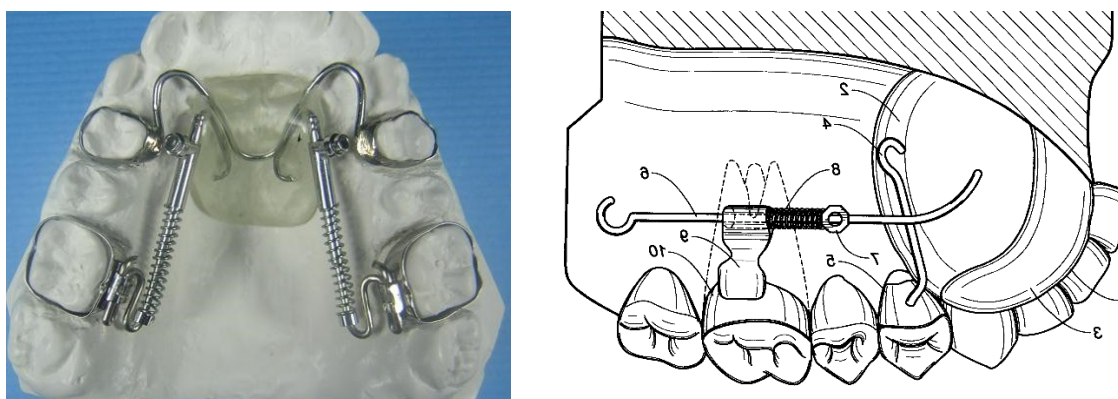


Fig. 2.10: Distal Jet appliance. It is difficult to fabricate the appliance at the level of the center of resistance in the presence of a shallow palatal vault (Graber et al., 2006).

The Keles-Sayinsu appliance consists of a distinctive arm with two helical loops distal to the first molar (one apical to the center of resistance of the molar and one at the level of the molar tube). The arm is inserted from the distal into the molar lingual tube (Fig. 2.11). As a result, two equal moments of opposite directions (therefore cancelling

each other) permits a bodily molar distalization with no rotation. However, anchorage loss was reported to be greater than in the other methods (Keles & Sayinsu, 2000).

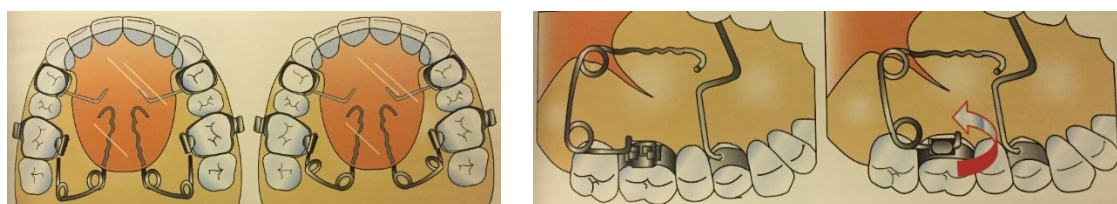


Fig. 2.11: Keles-Sayinsu appliance (Graber et al., 2006).

Distalization is often indicated in the correction of Class II malocclusion; it is also used in other malocclusions. The criteria of choice for this treatment modality are: straight to slightly convex subnasal profile; moderate lip protrusion; average to decreased lower facial height; Class II molar relationship (Fig. 2.12); deep overbite; mesially inclined maxillary first molars; loss of arch length due to premature loss of deciduous molars; mild to moderate arch perimeter discrepancy.

During distalization of maxillary molars, loss of anchorage may result in an overjet increase. Maxillary third or second molars are extracted to decrease resistance to distal displacement of the first molars. Once distalized, the molars become members of the anchorage set up to retract the more anterior teeth, thus risking at least partial relapse of the distal movement. Constructing a new Nance button, the addition of stopped archwires, and the use of interarch elastics may help increase the anchorage value of the posterior unit. Nevertheless, these traditional intraoral anchorage means may fall short of achieving maximal anchorage, thus making the correction of full Class II malocclusions with these mechanics unlikely. For this reason, overcorrection is sought in the distal displacement of the molars. Since the late 1990's, skeletal anchorage

has been used in treatments requiring maximum anchorage to reinforce the palatal anchorage, thus preventing unfavorable reactions.

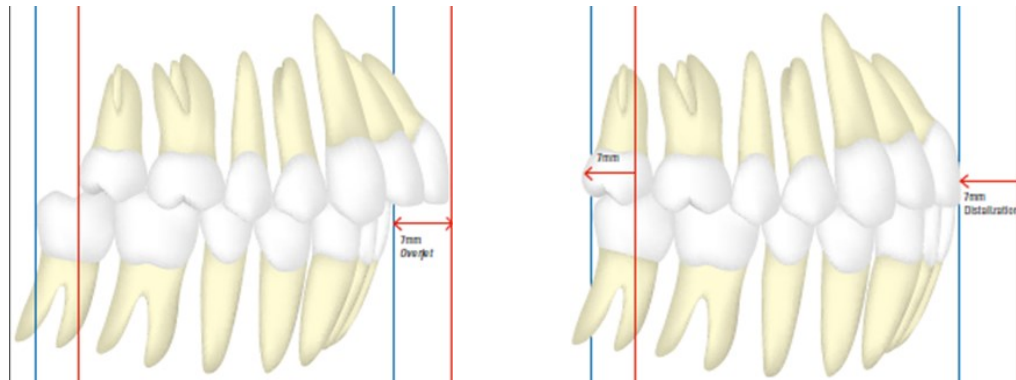


Fig. 2.12: Diagram showing the amount of movement required to correct a complete Class II malocclusion (7 mm overjet) treated with no extractions (Janson et al., 2009).

- Extraoral means

The use of extraoral means (headgear) to distalize and support the posterior unit, while efficient, requires patient acceptability and compliance, which can be problematic and hindering to the application of the better treatment option.

In the nonextraction approach, the extraoral force can generate the needed distalization. The force vector, dictated by the position of the extraoral anchor (neckstrap or headcap) and the length and angulation of the outer headgear bow, determine the nature of the vertical component (intrusion or extrusion) that accompanies the distal movement. Due to the bony resistance, molar intrusion is more difficult to achieve than extrusion, limiting the amount of distalization that occurs with the occipital force (high pull headgear).

The appliance can be adjusted to produce a force system that can move the molar bodily by directing the force vector through the level of the molar center of resistance, located in the midroot region. Upon superimposing pre and post-treatment

cephalographs on the maxillary base, Ghafari et al. (1998) showed that the straight pull headgear, applied for 2 years in growing children (n=63), moved the maxillary molars distally by nearly 2mm (1.8 ± 3.1 mm). Farret et al. (2008) showed also in a young population (n=22; ages 9-13 years) a comparable amount of molar distalization (2.5 mm) along with 10° of distal crown tipping and 0.3 mm of molar extrusion after treatment with cervical pull headgear for 6 months.

The headgear has also been used to retract the maxillary anterior teeth. Directly hooked to the archwire, whereby the name J-hook headgear, this appliance has two limitations: first, the force applied is of high and discontinuous nature, possibly unfavorable for tooth movement; second, significant friction and binding often reported on one side lead to asymmetric response (Proffit et al., 2012).

- Comparison of extraoral and intraoral appliances

The effectiveness of the headgear and other intraoral appliances has been compared in many studies. Lira et al. (2012) published a systematic review aiming to compare the maxillary dental effects of cervical headgear and pendulum appliance. Only randomized controlled trials (RCT) and controlled clinical trials (CCT) published between 1956 and 2008 were included. Of 48 articles, only 3 met the inclusion criteria, two of which had data before fixed appliance phase.

Tanner et al (2003) evaluated dental changes by superimposing on the palatal plane at ANS. The cervical pull headgear (CPHG) was worn by 13 patients (mean age 10.6 ± 1.42 years) for an average duration of 7.31 ± 4.09 months; the pendulum appliance (PA) was used in 13 patients (mean age 10.5 ± 0.82 years) for 11.38 ± 3.18 months. The mean amount of distalization was 3.15 ± 1.94 mm in the CPHG group and

3.81 ± 2.25 mm in the PA group. The CPHG created more distal tipping of the molar (11.77 ± 11.14°) compared with 6.96 ± 6.05° by the PA. However the main difference was in the mesial movement of the premolars with the Pendulum (-0.73 ± 3.53 mm) compared to a distal movement with the headgear (1.88 ± 1.12 mm) caused by the stretching of transeptal fibers.

Polat-Ozsoy et al. (2008) focused in their RCT on the incisors movement from pre and post- distalization cephalograms after treatment with the PA and CPHG. Unlike other studies, they found no clinically significant loss of anchorage at the incisor level with the PA. When measured on a coordinate system along a cranial horizontal, the maxillary incisor displaced 1.75 ± 2.89 mm with CPHG and 1.05 ± 3.09 mm with the PA. Against a vertical reference, the displacements were 2.51 ± 2.12 mm and 0.7 ± 2.47 mm, respectively.

However, the amount of distalization by both appliances is not stable, with some studies reporting total loss during the later stages of treatment. De Almeida- Pedrin et al (2009) showed maxillary molars mesialization after fixed appliance phase in 2 groups treated initially with the PA (n=22; mean age: 13.8) and headgear (n=30; mean age: 13.3). The anteroposterior changes of the maxillary molars, measured between the distal of the molar and the pterygomaxillary vertical (6-PTV) were more pronounced with the headgear (1.1 mm) compared to the pendulum (0.3 mm), showing the loss of a large part of the distal tipping generated by these appliances.

Angelieri et al (2008) observed similar outcomes for maxillary first molar movements in 2 groups of patients treated first with distalization, followed up by fixed appliances (CPHG group: n= 30; mean age=13.07 years; PA group: n= 22; mean age = 13.75 years). Greater tipping (6-PTV=1.65 mm) and extrusion (6-PP= 2.65 mm) of the

molars were observed with the CPHG than the PA (6-PTV=0.5 mm; 6-PP= 1.65 mm). During the retraction of the premolars, a CPHG was kept at night in both groups. However, lesser maxillary molars mesialization was observed in the PA group, possibly owing to the incorporated palatal anchorage provided by the Nance arc.

The greater extrusion of the molars with the CPHG group was likely due to the downward force vector compared to an intrusive component of the force delivered by the Pendulum. Still, the CPHG did not cause a greater mandibular clockwise rotation, as previously reported by Kim and Muhl (2001) and Phan et al. (2004), possibly because of the vertical growth at the level of the ramus noted in these growing patients. As expected, the PA caused greater loss of anchorage and less skeletal changes than the CPHG: the maxillary incisors proclined twice as much with the pendulum, albeit the difference was not statistically significant.

2.2. Temporary Anchorage Devices (TADs)

Anchorage control and patient compliance were practically resolved with the advent of temporary anchorage devices (TAD), also known as orthodontic miniscrews, microscrews, micro-implants, and mini-implants (Papadopoulos & Tarawneh, 2007). Creekmore and Eklund (1983) advocated the use of a metallic screw inserted in the alveolar bone that can withstand constant force of sufficient magnitude and duration to reposition an entire anterior maxillary dentition without becoming loose, painful, infected, or pathologic.

These implants are widely used because of the incomplete osseointegration, a distinct advantage in orthodontic applications, allowing for effective anchorage with relatively easy insertion and removal (Crismani et al., 2010).

2.2.1. Types

Before the introduction of TADs, osseointegrated dental implants were used as anchorage for tooth movement and secondarily as prosthetic abutments (Kokich, 1996; Roberts, Marshall, & Mozsary, 1990). Currently, there are two types of temporary anchorage devices (TADs) in orthodontics: screw implants and bone plates. Although bone plates are more stable and placed away from the teeth, they also have disadvantages such as limited placement locations and the need for surgical interventions to insert and remove them. Alternatively, screw implants are more frequently used in practice. As such, this review will concentrate on screw-type implants.

Stainless steel screws were marketed initially, but most miniscrews presently used are made from pure titanium or from an alloy of titanium with aluminum or vanadium, which are known for their biocompatibility. Mini-implants are not totally osseointegrated (<25%) and rely on mechanical retention for anchorage. They vary in diameters (between 1.2 and 2.3 mm), lengths (5 to 14 mm), pitch of screw threads, taper (conical or cylindrical), surface characteristics (sand blasted, acid etched), and heads (hook head, bracket head) (Papadopoulos & Tarawneh, 2007).

Depending on the tip form, two ways are used to insert the miniscrews. Self-tapping miniscrews with a rounded tip require a pre-drilled hole with a diameter similar to the screw per se. Self-drilling miniscrews could be inserted without preparation of the pilot hole due to the pointed screw tip and cutting threads. A metanalysis by Yi et al. (2016) showed similar success rates between the two methods.

2.2.2. Indications

Miniscrews provide practitioners superior control of various aspects of orthodontic treatment such as increasing orthodontic anchorage; reducing overall treatment duration; eliminating patient compliance with wearing appliances (e.g. headgear); and occasionally permitting orthodontic treatments previously thought to be impossible without surgery (Heymann & Tulloch, 2006; T. C.-K. Lee, Leung, Wong, & Rabie, 2008).

Miniscrews also facilitate various biomechanical movements, including: retraction of anterior teeth (H.-S. Park, Kwon, & Sung, 2005); protraction of maxillary and mandibular molars (Tseng et al., 2006); intrusion of incisors and molars (Y.-C. Park, Lee, Kim, & Jee, 2003); extraction space closure/canine retraction (H.-S. Park, Bae, Kyung, & Sung, 2001; Y.-C. Park, Chu, Choi, & Choi, 2005); midline correction (Carano, Velo, Leone, & Siciliani, 2005); molar uprighting (H.-S. Park, Kwon, & Sung, 2004b); leveling gingival contour (Roth, Yildirim, & Diedrich, 2004); correction of canted occlusal planes (Carano et al., 2005); en masse distalization of the maxillary arch (H.-S. Park, Bae, Kyung, & Sung, 2004); extrusion (Roth et al., 2004); de-impaction of canines and molars (Giancotti, Arcuri, & Barlattani, 2004; H.-S. Park, Kwon, & Sung, 2004a); maxillary expansion (Lagravère, Carey, Heo, Toogood, & Major, 2010); and support for temporary crowns in patients with missing teeth.

2.2.3. Failure risk

With the increased clinical use of TADs, the orthodontist's tolerance of miniscrew failure is likely to be very slim. Contrasted with the high success rate (95-97 %) of the osseointegrated endosseous dental implants (Fischer, Stenberg, Hedin, &

Sennerby, 2008; Jung et al., 2008), the success rates of TADs are lower and variable with reports ranging from 70.7% to 91.6% (Chen et al., 2008; Kuroda, Sugawara, Deguchi, Kyung, & Takano-Yamamoto, 2007; H.-S. Park, Jeong, & Kwon, 2006; Wiechmann, Meyer, & Büchter, 2007). Failure of TADs has been studied comprehensively. Reported explanations include:

- Host factors: Peri-implant inflammation (Chen et al., 2008; Miyawaki et al., 2003);(H.-S. Park et al., 2006); root proximity (Kuroda et al., 2007); placement in nonkeratinized tissues (Cheng, Tseng, Lee, & Kok, 2004); decreased bone density (Chen et al., 2008); thin cortical bone; placement in the mandible (Cheng et al., 2004; H.-S. Park et al., 2006); hyperdivergent skeletal pattern (Miyawaki et al., 2003).
- Design factors: Small diameter (Miyawaki et al., 2003).
- Operator factors: Placement in the right side of the mouth (H.-S. Park et al., 2006); tightness of implant insertion (Motoyoshi, Hirabayashi, Uemura, & Shimizu, 2006); over insertion (Kravitz & Kusnoto, 2007); unstable insertion angle and loading within two or three weeks (Ohashi, Pecho, Moron, & Lagravere, 2006); uprighting movement (Chen et al., 2008).

Many reports disagree with some of the factors mentioned above such as side of mouth placement, placement location, and mandibular divergence.

2.2.4. Distalization with TADs

TADs were introduced in an era when non-extraction treatments are favored. Distalization using TADs increased the chance of success for these treatments. Not only did they provide the ability to distalize the maxillary molars without risking anterior anchorage loss, they also made it possible to distalize en masse the maxillary buccal

segments or even the whole maxillary dentition. These benefits come with reduced side effects and less dependence on patient cooperation (Bechtold, Kim, Choi, Park, & Lee, 2012).

Palatal miniscrews used for distalization are gaining popularity, but interradicular TADs remain the most frequently used because (a) they are comparatively easier to place and remove (Arcuri, Muzzi, Santini, Barlattani, & Giancotti, 2007) and (b) they cause fewer irritation to soft tissues as they are placed in the attached gingiva. Yet, root proximity remains a major factor for interradicular TAD failure, and the risk persists of damaging anatomic structures and obstructing tooth movement when adjacent teeth are moved in the antero-posterior direction (Deguchi et al., 2006; Schnelle, Beck, Jaynes, & Huja, 2004).

Among various locations tested clinically and through research, the recommended placement of TADs that emerged from many anatomic studies was between first molar and second premolar at an angulation of 30°, for the following reasons:

- Safety: The distance between the roots of the maxillary 2nd premolar and 1st molar is on average 3.18mm at 5 to 7mm from the alveolar crest and increases to 4mm after alignment (*3-4mm is considered the minimum amount of bone required to place a miniscrew*) (H. S. Park, 2002). Similarly, based on 30 panoramic x-rays Schnelle et al. (2004) reported 3mm of bone stock present mesial to maxillary first molars and 4 mm mesial and distal to mandibular first molars (Fig. 2.13 and 2.14).

The average most coronal site for placement of a screw mesial to the maxillary first molar was at 6mm from the level of the CEJ. Correcting axial inclinations enables more adequate and coronal interradicular areas to become available.

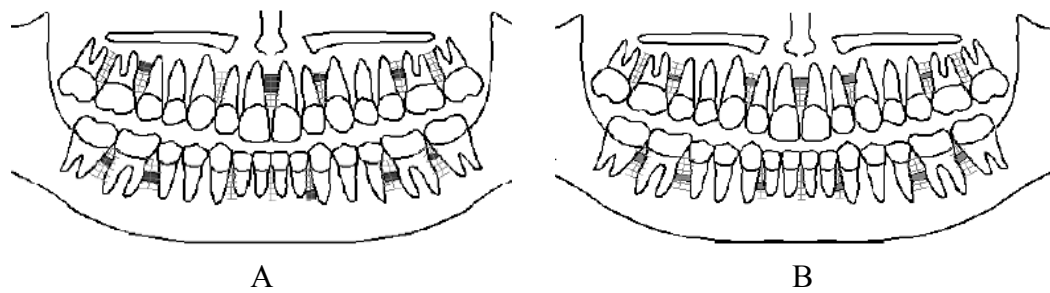


Fig. 2.13: Schematic of panoramic film indicating location and sites at which 3 mm of bone stock was consistently available ($\geq 90\%$). (a) Pretreatment (b) post alignment (Schnelle et al., 2004).

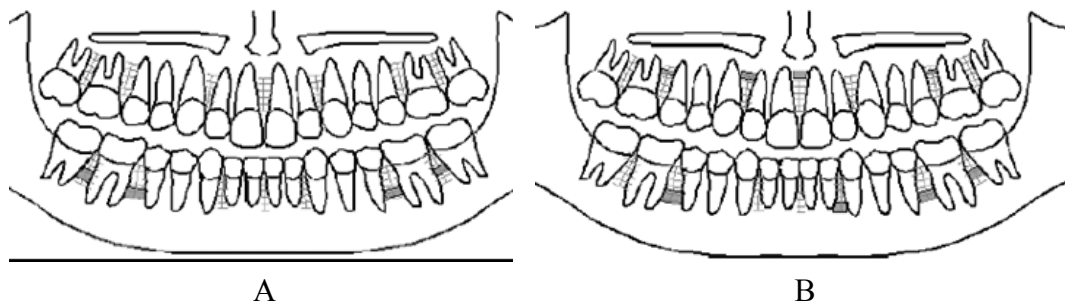


Fig. 2.14: Schematic of panoramic film indicating location and sites at which 4 mm of bone stock was consistently available ($\geq 90\%$). (a) Pretreatment (b) post alignment (Schnelle et al., 2004).

However, the mean width of attached gingiva ranges from 1 mm to 4 mm with the widest zone of attached gingiva at the level of the maxillary incisors and the narrowest in the premolar region irrespective of the method used in the assessment (Fig. 2.15) (Bowers, 1963). Therefore, it is likely that the adequate area for TADs placement in the maxillary premolars region is located in the alveolar mucosa. Thus, it is recommended to angulate the miniscrew toward the apex to reach better anatomical areas while keeping the head in the attached gingiva (H. S. Park, 2002). Conversely, Laursen et al. (2012) noted that changing the insertion angle from 90 to 45 degrees increases the risk of sinus perforation in the maxillary molar region.



Fig. 2.15: Widths of the attached gingiva and alveolar mucosa in the maxillary anterior teeth.

- Stability: More cortical bone exists mesial to the maxillary first molars (1.8 ± 0.6 mm). It has been postulated that an insertion angle from 20 to 60 degrees allow optimal cortical bone engagement. Deguchi et al. (2006) noted that contact between the miniscrew and cortical bone increased by 1.5 times when angulated by 30 degrees. Laursen et al (2012) showed an increase in cortical bone-to-implant contact by an average of 47% when angulating the TAD by 45 degrees.

Miniscrews can aid segmental distalization through a wide range of mechanics such as elastomeric chains, coils (NiTi and stainless-steel) and jigs. Inserted in the buccal or palatal bone, TADs may be used for indirect anchorage to support dental units to which clinical forces are applied, or direct anchorage when forces are applied directly from the TAD (Fig. 2.16). The use of direct anchorage mechanics to distalize the entire maxillary arch often creates undesirable effects such as a clockwise rotation of the occlusal plane, potentially leading to an increase in the gingival display. Bechtold et al. (2012) recommended using two buccal miniscrews to counteract the occlusal plane rotation. They showed significantly greater molar distalization and incisor retraction accompanied by intrusion compared to extrusion with the use of single miniscrew (Fig. 2.17).

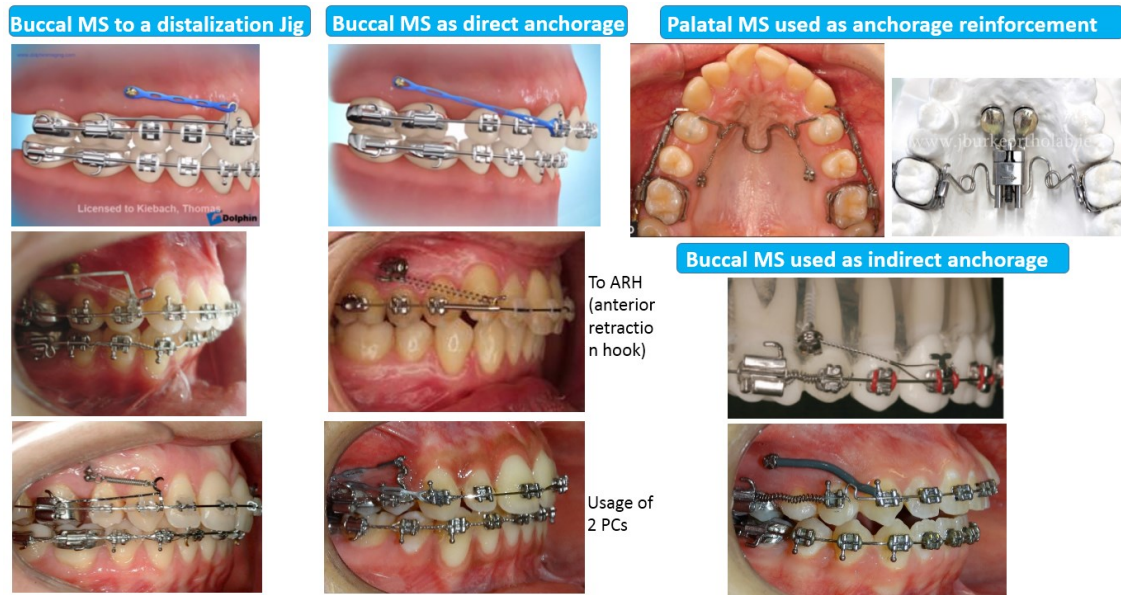


Fig. 2.16: Different buccal and palatal TAD supported distalization (Mizrahi & Mizrahi, 2007).

TADs were shown to limit loss of anchorage during distalization. In a metaanalysis, da Costa Grec et al. (2013) aimed to quantify and compare on cephalograms the amounts of distalization (molar distal movement) and anchorage loss (premolar mesial movement) of conventional (CA) and skeletal (SA) anchorage methods in the correction of Class II malocclusion with intraoral distalizers. In most of the 40 studies included (2 high, 27 medium, and 11 low quality), the pendulum and its variations (employing the Nance button as anchorage) were mainly used in the CA group and palatal miniscrews were used in the SA group. Six studies qualified for the metaanalysis that showed more distalization with SA (5.10 mm vs 3.34 mm) with no anchorage loss when direct anchorage was used. Small anchorage loss was reported from the study on indirect anchorage. After using direct anchorage to distalize maxillary posterior segments, Yamada et al. (2009) reported molar distalization by 3mm, but also intrusion by 0.6 mm, thus avoiding clockwise rotation of the mandible. The results were achieved without patient compliance, incisor proclination or significant root resorption at the level of the molars.

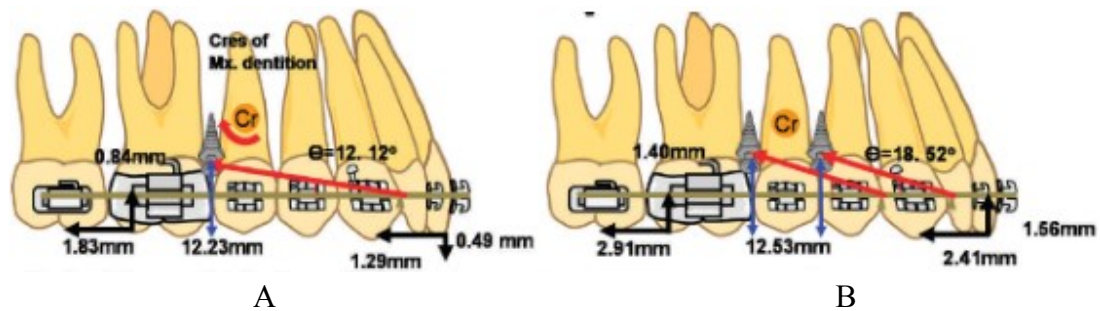


Fig. 2.17: Dental movements with (A) Single miniscrew: Distalization and clockwise rotation and with (B) Dual miniscrews: Distalization and intrusion (Bechtold et al., 2012).

While asserting the established need for TADs in orthodontics, these studies disclose a lack of knowledge of the mechanical underpinning of direct and indirect anchorage, particularly the influence of individual variation related to anatomy of the maxillary arch, particularly its bony characteristics that play a major role in resistance to orthodontic movement.

2.3. Finite Element Analysis (FEA)

The lack of precise information about the reactions following the application of orthodontic forces motivated orthodontists to use mathematical calculations, by means of force vectors and moments, to estimate the resultant tooth movements. Despite its accuracy, this theoretical approach does not take into consideration the biological environment in which these forces and moments are applied, leading to clinical results different than predicted.

The emergence of 3D imaging allowed for precise visualization of the individual anatomy. Dental clinical applications emerged from this advancement to provide safer and more accurate procedures, especially in implant dentistry. Dental researchers used precise 3D images of real anatomy to produce detailed 3D models using 3D

reconstruction softwares. These models helped better exploit the “Finite Element Analysis” (FEA), an engineering tool previously used with 2D models, to manipulate force systems in vitro. The aim was to elucidate and understand the causes of frequent undesirable reactions that lead to increased orthodontic treatment duration.

However, FEA application has been limited owing to the difficulty of generating complete accurate models of the jaws and teeth, and has been restricted in most studies to a single model, disregarding the individual variations encountered clinically. Despite these limitations, FEA remains a unique and presently only instrument that could help reach in the future a point where a “virtual patient “, created from the true individual 3D representation, is subjected to planned clinical scenarios before applying them in vivo with anticipated outcome.

2.3.1. Definition

First developed in 1943 by R. Courant who utilized the Ritz method, FEA is a modern tool for numerical stress analysis that approximates physical models into numerical mathematical equations (Tanne, Sakuda, & Burstone, 1987). The analysis involves, first discretization of the structure into its components called “finite elements” connected to each other by nodes with well-defined physical properties (e.g. stiffness, elasticity). Then, a quantitative analysis is conducted to approximate the reactions and interactions within each element (Vasudeva, 2009). Equations from all the elements need to be solved simultaneously, a task that can only be performed by computers. Engineering phenomena such as deflection, stress, strains, vibration, energy storage and many other can be calculated.

FEA is capable of solving complex mechanical problems. Originally used to verify design integrity and identify critical locations in components without having to build the part or assembly, the method was later recognized as a technique to approximate physiologic and biologic problems that can be modelled by mathematical equations (Figs. 2.18, 2.19, 2.20). Dentistry took advantage of the FEA approaches with emphasis on mechanotherapy.

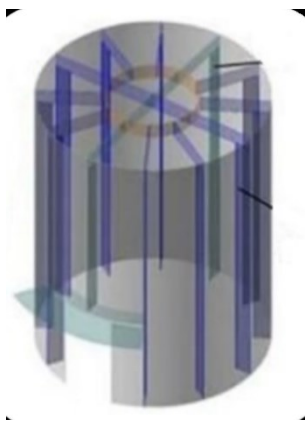


Fig. 2.18: 3D model of the engineering structure to be constructed.

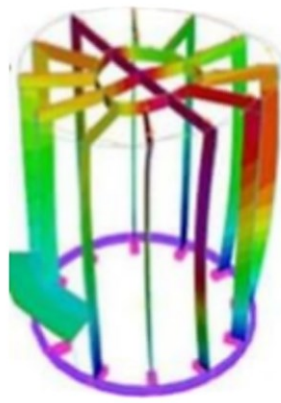


Fig. 2.19: FEA applied before the construction to verify the design and detect any critical locations.

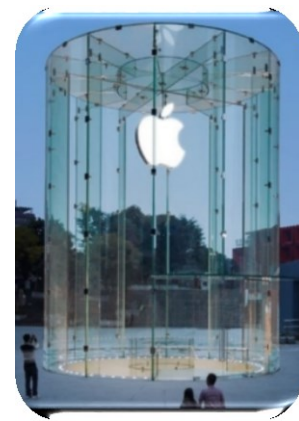


Fig. 2.20: Construction of the part after FEA. (<http://www.mulpix.com> - accessed January 24, 2017)

2.3.2. 3D imaging

2.3.2.1. Evolution toward 3D imaging

Traditional 2D diagnostic imaging records have for long been the standard in orthodontics despite many limitations that affected their accuracy and prevented their adoption to generate 3D models for experimental and clinical analysis. Object magnification, distortion, projective displacement as well as superimposition of structures are some of these limitations. Over the past decade, medicine and later dentistry adopted 3D technology to assist diagnosis and treatment planning.

Controversy emerged regarding the routine use of cone beam computed tomography [CBCT] (in dentistry) and CT scans (in medicine).

In orthodontics, some opinions went as far as questioning the added benefits of 3D imaging in diagnosis and regular clinical practice. The debate was tempered with the release of guidelines by the American Association of Orthodontists (AAO) and the American Academy of Oral and Maxillofacial Radiology (AAOMR) that did not support the routine use of ionizing radiation in standard orthodontic diagnosis and treatment planning, while acknowledging the value of 3D imaging in the following clinical situations: retained/impacted permanent teeth; facial asymmetries; craniofacial anomalies; severe skeletal discrepancies with indication of orthodontic-surgical treatment; bone irregularities; TMJ malformation and airway assessment.

2.3.2.2. CBCT vs CT scans

Both equipments belong to computed tomography, but differ significantly in irradiation doses, image capturing, quality and interpretation. Medical CT scans use a fan-shaped x-ray beam to record data that are captured by image detectors organized in an arc around the patient, generating a single slice per rotation. Image resolution depends on the distance separating the captured slices, which reconstitute the object. On the other hand, CBCT captures the image in a single-turn motion to create the whole volume of the object. This type of imaging is faster than the CT scan's spiral motion resulting in less radiation to the patient.

Loubele et al. (2007) compared jaw dimensions and bone quality assessment between images obtained from a CBCT and multi-slice spiral CT scan (MSCT). Jaw measurements were performed with digital calipers on 25 human mandibles and bone

quality assessment was carried out on one formalized maxilla. They served as controls to compare with x-ray measurements. Despite underestimating the bone widths, CBCT (on average 0.23 mm narrower) and MSCT (on average 0.49 mm narrower) measurements were reliable. As for subjective image quality, CBCT was better in delineating the lamina dura and PDL, but the MSCT offered better visualization of the cortical bone and gingiva. The latter conclusion was also confirmed by Scarfe et al. (2012) who concluded that MSCT has a better contrast (Fig. 2.21). High contrast resolution means more discrimination between different tissue types (i.e. bone, teeth and soft tissue).

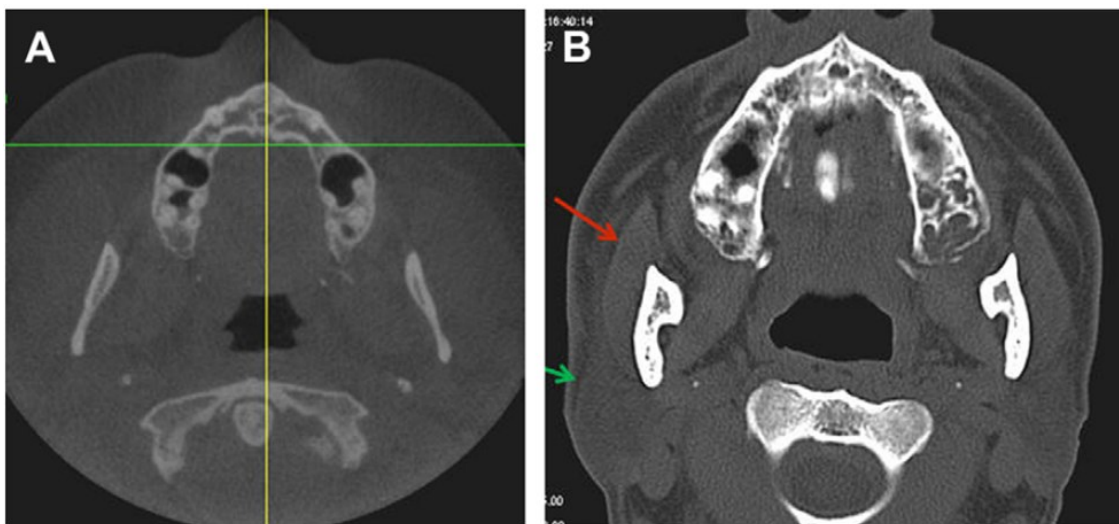


Fig. 2.21: Axial images at the level of the maxillary arch illustrating the image contrast in CBCT (A) and MSCT (B) images. Notice the considerably higher soft tissue and bone contrast in the MSCT image (Scarfe, 2012).

The gap in image resolution between CBCT and CT scans, which was less significant with the old CT scan machines, augmented with the newer multi-slice CT technologies. The disparity is magnified in reference to the high resolution Micro CT, which depicts detailed bone morphology and tissue mineral density (including BMD:

bone mineral density) better than any other CT scan (D.-G. Kim, 2014). These properties elevate the Micro CT to the ideal source for accurate tissue modeling, albeit at the expense of higher radiation doses (Fig. 2.22).

The Hounsfield Unit scale (HU) used in MSCT to measure radiodensity provide reliable measurements of the tissue represented. In CBCT, the degree of x-ray attenuation is shown by gray scale (voxel value). CBCT manufacturers and software providers present gray scales as HUs; however, these measurements are not true HUs (Armstrong, 2006). The CBCT image value of a voxel of an organ depends on its position. Thus, areas possessing identical densities might appear with different greyscale values in the CBCT scan depending on their relative positions in the organ being scanned (De Vos, Casselman, & Swennen, 2009).

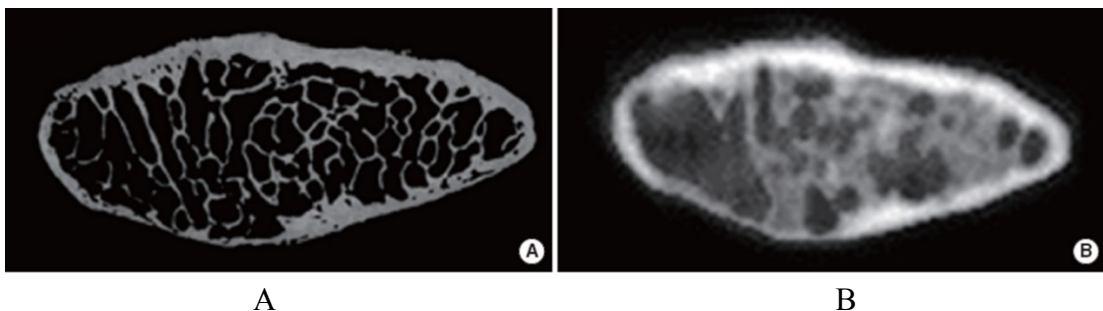


Fig. 2.22: **A-** Micro-computed tomography (CT) image ($27 \times 27 \times 27 \mu\text{m}^3$ voxel size); **B-** cone beam CT image ($200 \times 200 \times 200 \mu\text{m}^3$ voxel size) of the same human condyle (D.-G. Kim, 2014).

2.3.3. Development of FEA in dentistry

Ledley and Huang (1968) first used FEA in dentistry when they developed a linear model of a tooth based on experimental data and on linear displacement force analysis. Stress analysis studies of inlays, crowns, bases supporting restorations, fixed bridges, complete dentures, partial dentures and endodontic posts have been reported, as well as studies of teeth, bone, and oral tissues. FEA has also been employed to model

and predict the biomechanical performance of various implant designs used in dentistry and medicine (Gačnik, Ren, & Hren, 2014).

The FE method has improved significantly since its introduction to dental research. In the first era (1970-1990), dental models were two dimensional based on simplified representation of geometry. Analyses were not computerized and often limited by the high number of calculations necessary to provide useful analysis. In the early FEA studies, assumptions and constraints were added to overcome the geometric discontinuity in the models, leading to potential mathematical errors putting the validity of the FE models of this era in doubt (Ko, Rocha, & Larson, 2012).

3D models from true human anatomical records were introduced during the second era (1990-2000). Manual and semiautomatic meshing gradually evolved during this time. In addition to the more detailed 3D reconstruction, specific solvers (e.g. poroelasticity, homogenization theory, dynamic response) were adapted from the engineering field to study dental problems. In general, the element size was relatively large because of the then immature meshing techniques, which yielded inaccurate models and time consuming to build (Ko et al., 2012).

In fact, constructing accurate and suitable FE meshes of the studied geometry is essential since FE simulations results are highly sensitive to geometric modelling assumptions (Hohmann et al., 2011) This construction became possible with advancements made in computer and software capabilities, and the use of initial anatomical records with better resolution (μ CT images). During this era, more complex 3D structures (e.g. occlusal surfaces, pulp, dentin, enamel) were simulated in greater details and meshing capability of FE solvers significantly improved (Ko et al., 2012).

2.3.4. Limitations

2.3.4.1. Inaccurate assumptions

In FEA, the results obtained are only “as good as the initial data used to set the parameters of tissue response” (Middleton et al. 1996). Unlike engineering structures, there is no complete knowledge of the mechanical behavior of biologic tissues. This shortcoming is mainly related to the complex anatomy, lack of experimental studies, and absence of modern technologies to measure the properties of the oral tissues. As a result, certain assumptions are accepted in the FEA studies applied in orthodontics (Qian, Chen, & Katona, 2001).

Tooth movement is a periodontally-driven mechanism, thus the importance of the material property definition of the periodontal ligament. The results of a systematic review about the mechanical assumptions of PDL in FEA studies indicated the use of a myriad of modelling approaches encompassing linear-elastic, viscoelastic, hyperelastic and multiphase approaches (Fill et al., 2012). Moreover, an affinity for using simplified approaches/assumptions (linear-elastic) may have inadequately represented the PDL because it prevents full characterization of its time-dependent behavior.

Furthermore, wrong assumptions are not only limited to the PDL. Bone material properties have been judged to be linear elastic in the utmost majority of the studies. Schwartz-Dabney et al. (2003) showed variations in material anisotropy (material properties differ by direction) and direction of maximum stiffness in the different areas of 10 dentate mandibles. Local anisotropy and regional variations in skeletal material properties can have drastic effects on the relationship between stress and strain (Cowin & Hart, 1990).

As a consequence of using different material properties assumptions in studies involving tooth movement, various ranges of results are obtained preventing comprehensive comparisons even between two papers. The resulting quantitative data have hypothetical value and not any major clinical relevance.

2.3.4.2. Generalizability of results

By definition, generalizability is the extent to which findings from a study can be generalized (or extended) to the natural settings (i.e., outside the lab). FEA allows inferences and readings to be made from a single mathematical solution for one single set up or scenario.

In the engineering field a single problem with predetermined initial settings and properties allows for a single solution or result. However, in the medical and dental fields' individual variations lead to different results for a similar clinical problem. Thus, clinical trials are needed that include samples representing the variations present in the population, following well-defined research protocols with proper statistical analyses to test the validity and significance of the results.

Unfortunately, most of the dental FEA studies followed the “single-model” engineering method, leading to question the clinical significance of their results. Future studies must account for variations existing between real patients, thereby creating a closer link between the virtual finite element models and actual clinical situations.

2.3.4.3. Applicability of results

The majority of FEA studies measure stresses (Von Misses and principal), findings that do not have a known direct clinical implication. Does increased stress

values reflect increase of tooth movement, more pain, more hyalinization (therefore slower tooth movement), or more root resorption? Thus, the need for studies that link stress values to clinical measures (ex: pain, resorption, speed of tooth movement). This type of research would be revolutionary because it would translate FEA studies into strong contributions to dental knowledge by answering questions that experimental studies cannot answer because of ethical or logistical limitations.

To date, increased stress units (Von Mises) at the PDL was correlated with increased tooth movement (displacement) in most studies using FEA (Cai et al., 2015; Kang et al., 2016; Vasudeva, 2009). This interpretation can be explained by the fact that

Stress (σ) = stiffness (E) \times strain (ϵ) where:

- Strain is the relative increase in length of a sample

$$\text{strain } (\epsilon) = (\text{final length} - \text{initial length}) / (\text{initial length})$$

- Stiffness is defined by the Young's Modulus of elasticity (E), which is always a positive value.

2.3.4.4. 3D Modelling of Human Tissues

One inherent shortcoming in utilizing FEA simulation is the difficulty to model the actual anatomy of human hard and soft-tissues. The considerable time and effort required to generate a realistic model is a significant problem. Despite the enormous progress made in the 3D modeling softwares, manual segmentation still dominates the segmentation process. Creating an accurate maxillary or mandibular arch, complete with enamel, dentin, pulp and PDL for each tooth, as well as lamina dura and distinct cortical and trabecular bones may take hundreds of hours (Pollei, 2009).

Owing to the small space they occupy, the PDL tissue and the trabeculae of the spongy bone are difficult to visualize using normal resolution CT and CBCT scans, posing a critical issue during FE model construction. Several protocols are used to create a layer between the teeth and the bone representing the PDL. However, the layer thickness depends on the highest resolution the 3D modeling software can read. This interaction led to the adoption of various PDL thicknesses in different investigations (Fill et al., 2012).

In a study comparing different digital reconstruction softwares, González Carcedo et al. (2010) found only 4 software packages (Mimics, Simpleware/ScanIP, Amira, 3D Slicer) capable of analyzing medical images (Table 2.1).

Except for the 3D Slicer software, all others were rated as easy to moderately easy to use, and contain the tools to perform the following:

- Prepare the data (import the data, improve image quality, crop, resize, resample)
- Preprocessing: Image noise reduction with filters: Gaussian, smoothing, cavity fill
- Manual and semiautomatic segmentation (threshold based and flood fill)
- Angular and linear measurements on the 2D slices and on the 3D model
- Mesh generation, adjustment, editing and refinement
- Creation of a 3D preview model
- Exporting the meshed model in the following formats: Patran, Ansys, Abaqus, Fluent, Nastran, and Comsol

We adopted Simpleware/ScanIP for the 3D modelling in this study because it has the capability of model segmentation, 3D modelling and FE model generation in conjunction with easier user interface, availability of good tutorials (with examples and problems) and fast online support.

Table 2.1: 3D modelling softwares available (González Carcedo, 2010).

Name Program	Evaluation	Description
Mimics	✓	} For a more extensible evaluation
Simpleware ScanIP / ScanFE	✓	
Amira	✓	
3D-Slicer (IA-mesh/Free Surfer)	✓	
Slicer Dicer	✗	It creates orthogonal and oblique slices, and projected it in a plane.
Microdicom	✗	It is for manipulation of DICOM images 2D. Not3D
Gemident	✗	It is for identification regions and colours in images and photographs.
ITK - VTK	✗	It uses language C++, is complex.
ImageJ - FIJI	✗	Images processing is in 2D and 3D but it only process, does not create models.

2.3.4.5. Tooth movement simulation over time

The difficulty to model the mechanical behavior of human tissues and their response to mechanical forces over time reflects another shortcoming of FEA simulations. Most FEA studies provide a “snap-shot” view of the initial conditions (stresses, displacement...) within the model; they do not depict changes that occur over time, such as bone remodeling, healing, and friction.

To date, simulation of long-term orthodontic tooth movement (OTM) quantitatively and accurately has not been possible with FEA because the physiologic and biomechanical processes of OTM are not fully understood and represented mathematically (Ammar et al. 2011).

Middleton et al. (1996) were the first to introduce a time-dependent (continuous/ dynamic) finite element model for tooth movement. Aiming to validate that

OTM is a “periodontally mediated phenomenon”, all tissues were assigned with linear elastic material properties (therefore do not exhibit time dependent behavior), except for the PDL where a viscoelastic material property was incorporated using an overlay model. They found that only the periodontal ligament experienced a strain above the threshold ($= 0.02$) necessary to initiate a bone remodeling process, a finding that confirmed their hypothesis.

Cheng et al. (2004) proposed a soft-tissue driven bone remodeling model for simulating OTM in a time-dependent manner. To determine the remodeling parameters, the FEA simulation used clinical data from an in vivo study conducted for this purpose.

The addition of a time dependent feature would be a novel approach allowing for all treatment mechanics to be simulated in silico (on computer softwares) and observe the results before applying them clinically, thus avoiding side effects and complications.

2.3.5. FEA in Orthodontics

Despite all the limitations, FEA remains a promising tool especially in orthodontic research where it represents a significant percentage of dental applications. The method is non-invasive, accurate and provides quantitative detailed data regarding physiological responses in internal structures, such as the periodontal ligament and the alveolar bone. Moreover, it allows for the possibility to study a homogenous sample while controlling all study variables and to anticipate the tissue responses to the orthodontic mechanics applied.

Tanne et al. (1987) were the first to introduce FEA into orthodontics (Fig. 2.23). Earlier studies indicated stress levels following the application of a force in a single

tooth system that was constructed on the basis of average anatomic morphology (Cobo et al. 1993).

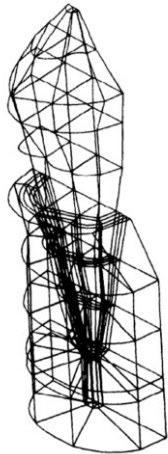


Fig. 2.23: Three dimensional finite element model of the lower first premolar. The model consists of 240 isoparametric elements and comprises the tooth, PDL and alveolar bone (Tanne et al., 1987).

With advances in softwares and the introduction of 3D radiography in dentistry, more sophisticated models were generated to study stresses in a group of teeth (Liu, Zhu, & Zhang, 2015) (Fig. 2.24).

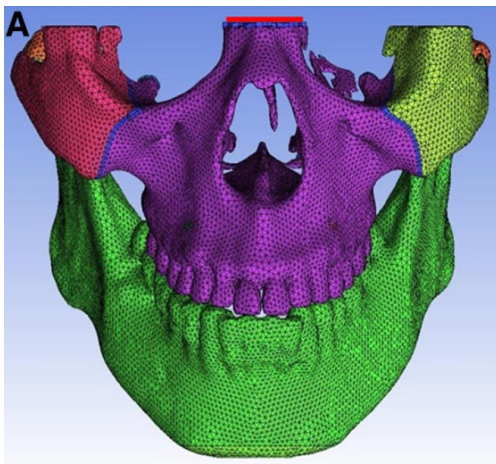


Fig. 2.24: Complex FE model of the midface and the jaws (Liu et al., 2015).

In the last decade FEM was extensively used in orthodontic research, highlighting several variables involved in orthodontic mechanics, such as:

1. Stress distribution areas in the periodontal ligament (PDL) and alveolar bone during different types of tooth movements: canine and incisors retraction (Lombardo et al.,

2014; S.-J. Sung, Jang, Chun, & Moon, 2010) ; molar and incisors intrusion (Çifter & Saraç, 2011); torque expression (Liang, Rong, Lin, & Xu, 2009); distalization (E.-H. Sung et al., 2015); molar protraction (Kojima & Fukui, 2008); maxillary expansion (Han, Kim, & Park, 2009; H. K. Lee et al., 2012); alignment of impacted canines (Wang et al., 2014); maxillary protraction (K. Y. Kim et al., 2015; Yan et al., 2013) and during aligner therapy (Gomez, Peña, Martínez, Giraldo, & Cardona, 2014).

2. Stress distribution on different orthodontic components such as archwires and TADs (Ammar et al., 2011; C. Holberg, Winterhalder, Rudzki-Janson, & Wichelhaus, 2014; Suzuki et al., 2011; Techalertpaisarn & Versluis, 2013)

3. Direction and amount of tooth displacement during different types of tooth movements: Molar protraction (Kojima & Fukui, 2008; Liang et al., 2009; Nihara et al., 2015); distalization (E.-H. Sung et al., 2015; Yu et al., 2014); molar intrusion (Çifter & Saraç, 2011); torque expression (Liang et al., 2009); maxillary expansion (Han et al., 2009; H. K. Lee et al., 2012); aligner treatment (Gomez et al., 2014); maxillary protraction (K. Y. Kim et al., 2015; Yan et al., 2013) and incisors retraction (Lombardo et al., 2014; S.-J. Sung et al., 2010).

4. Strain distribution in the bone and PDL (P. D. D. C. Holberg, Winterhalder, Holberg, Wichelhaus, & Rudzki-Janson, 2014)

5. Ideal position of orthodontic appliances during specific mechanics; (Kojima, Kawamura, & Fukui, 2012; Nihara et al., 2015)

6. Areas most likely to present root resorption. (Kamble, Lohkare, Hararey, & Mundada, 2012)

Ammar et al (2011) evaluated the stress profile on the miniscrew implant and periimplant bone caused by both a tangential orthodontic force and tightening loads.

They also assessed the effects of orthodontic bracket hook length and force angulation on resulting stress response of the canine PDL (Fig. 2.25).

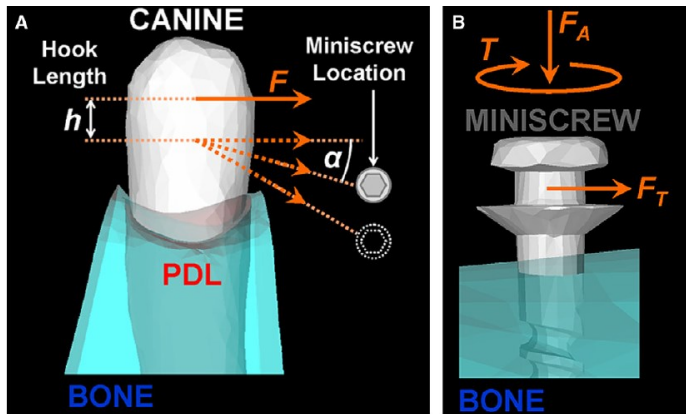


Fig. 2.25: Loading scenarios
A- different directions of a tangential load (F_T) from the mandibular canine to the TAD
B- Miniscrew subjected to placement load composed of a tightening torque (T) and compressive axial force (F_A) (Ammar et al., 2011).

Critical areas of stress in the loaded miniscrew were located at the top 2 threads and were higher during placement load compared with orthodontic load (Fig. 2.26). Moreover, stresses at the TADs seemed to decrease with larger implant diameter. However, this model used a miniscrew to retract a single-rooted mandibular canine without considering the inclusion of the other teeth as is usually the clinical situation.

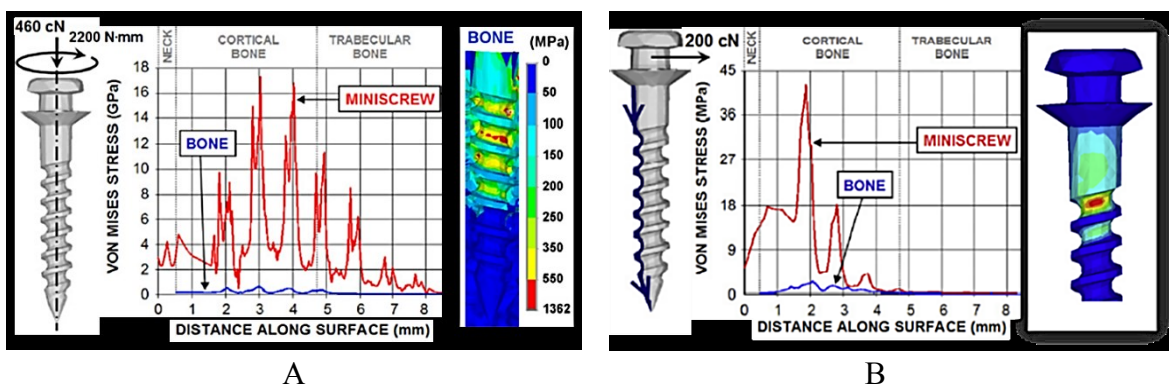


Fig. 2.26: Stress distribution for: **A-** Tightening; **B-** tangential force (Ammar et al., 2011).

Using FEA, Holberg et al. (2014) demonstrated higher risk of anchorage loss during mandibular molar protraction with indirect anchorage compared with direct

anchorage. Anchorage loss with the indirect method was slightly lower than with full dental anchorage, but much higher than with direct miniscrew anchorage (Fig. 2.27).

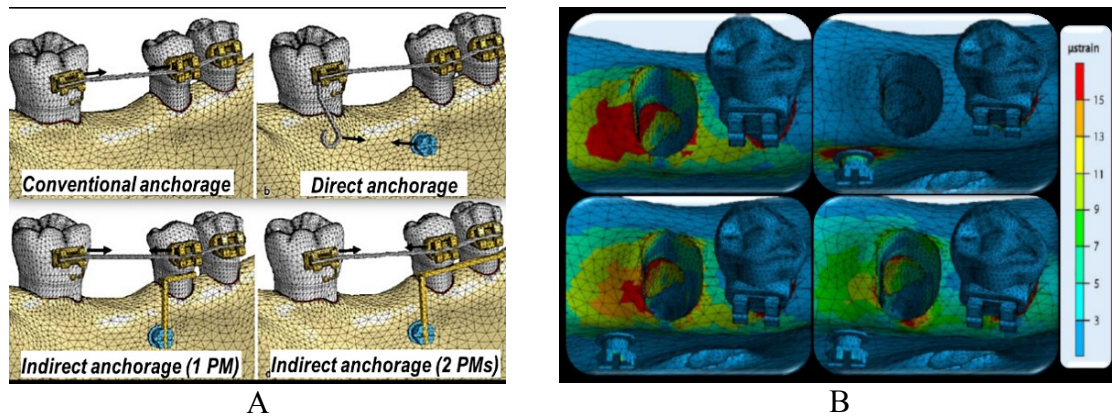


Fig. 2.27: A- FE models of the different anchorage situations; B- Strain distribution results of the FEA showing the least amount of anchorage loss in the direct anchorage modality (Ammar et al., 2011).

The authors concluded that at most, indirect miniscrew anchorage had a slightly protective effect. Unlike other FEA studies where stresses or displacement were analyzed at the PDL or the tooth itself, this study gauged strain values at the alveolar bone, under the stipulation that dental movement is accompanied by enhanced strain on the alveolus, leading to functional adaptation. Therefore, high strain values on the alveolar bone around the anchor tooth reveal a strong tendency for anchorage loss, low values the opposite.

Kang et al. (2016) evaluated the effects of maxillary second and third molar eruption status on the distalization of first molars using a force of 150 gm delivered by a modified palatal anchorage plate (MPAP), bone anchored pendulum and headgear. The eruption stages were divided into 3 groups (Fig. 2.28): (1) second molar at the cervical third of the first molar root; (2) fully erupted second molar; (3) erupting third molar at the cervical third of the second molar root.

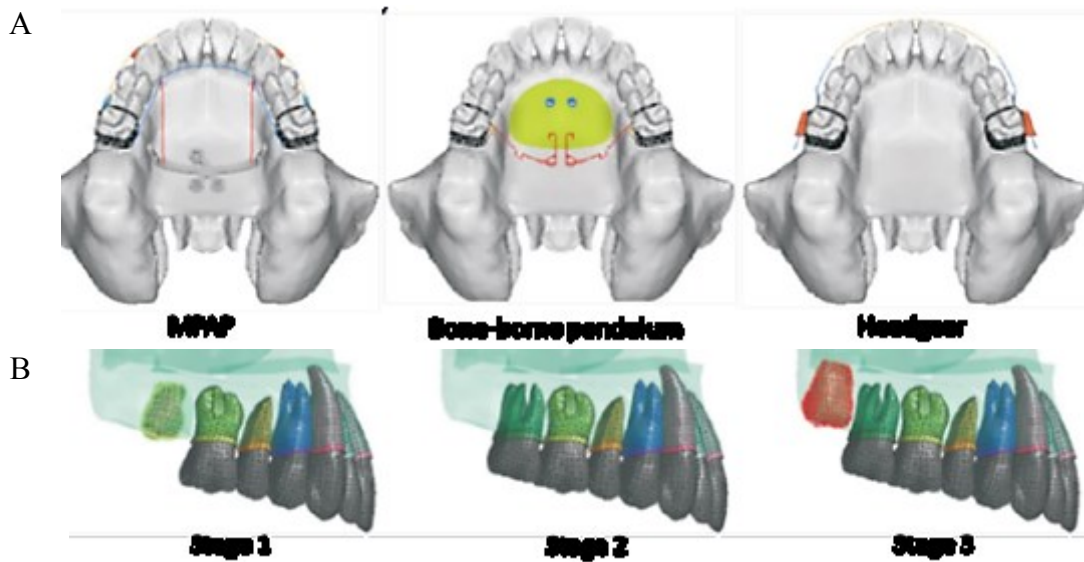


Fig. 2.28: A- The 3 appliances used; B- Eruption stages (Kang et al., 2016).

i

No significant difference in displacement was noted among all appliances between stages 2 and 3, indicating that the presence of third molars did not affect distalization. In stages 1 and 2 MPAP caused more distalization at the root than the crown of the first molar with less mesial-in rotation after eruption of the second molar (2). The bone-anchored pendulum resulted in distalization, distal-buccal tipping, and intrusion. Yet more buccal tipping and extrusion instead of intrusion resulted when the second molars were present. For all eruption stages, the headgear caused the largest amount of distal tipping of the first molar accompanied by extrusion and distal-in rotation (Fig. 2.29).

Yu et al. (2014) found that distalization with a palatal plate rather than mini-implants on the buccal side provided bodily molar movement without tipping or extrusion, and with no significant displacement of incisor (Fig. 2.30; Fig. 2.31).

However, this study has 2 limitations:

- First the model was constructed based on a dentoform, without differentiating between the stiff cortical bone and the trabecular bone; therefore the model does not represent the real anatomy.

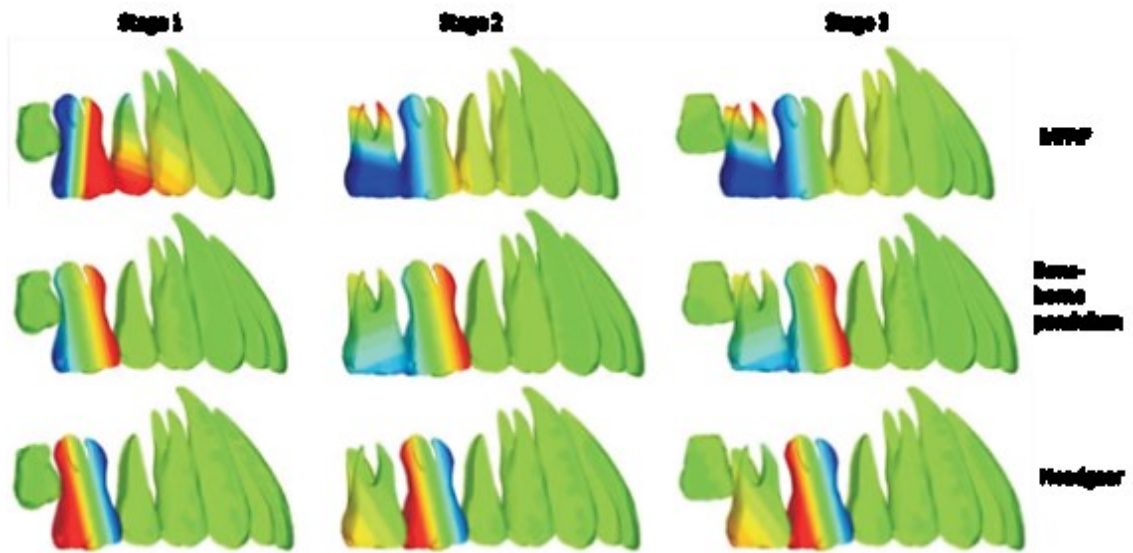


Fig. 2.29: Displacement in the Y axis. **A-** More root movement with MPAP; **B-** Similar distal tipping for all stages with the Bone- anchored pendulum and **C-** higher distal tipping with the headgear.

- Second, interactions between teeth were defined via contact at an individual element located at the contact point area (E.-H. Sung et al., 2015). In this method, all teeth are considered as one object.

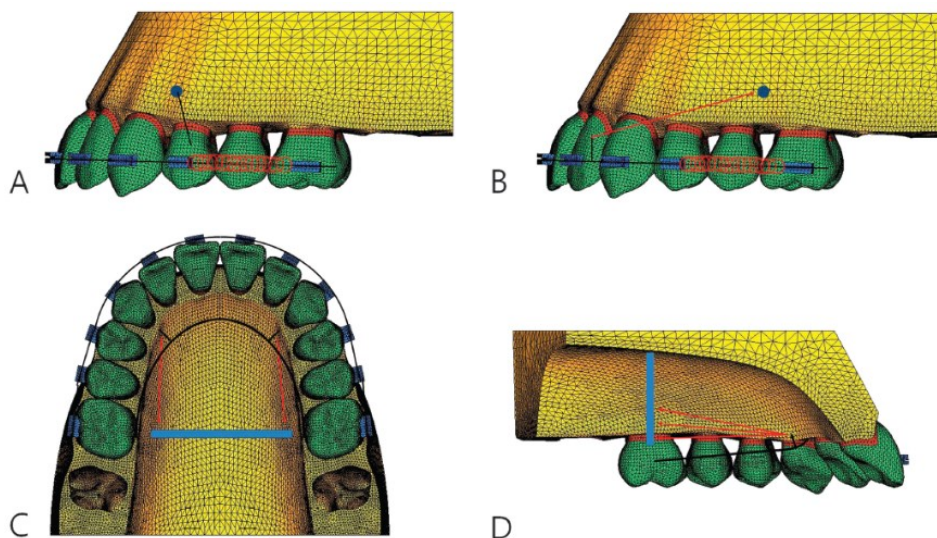


Fig. 2.30: **A-** Indirect anchorage; **B-** Direct anchorage modality modified with a coil spring between the second premolar and first molar; **C -D** Palatal plate at the level of the first molars. Three indentations on the lever arms of the palatal plate were used to apply force at 4, 7 and 10 mm apical to archwire (Yu et al., 2014).

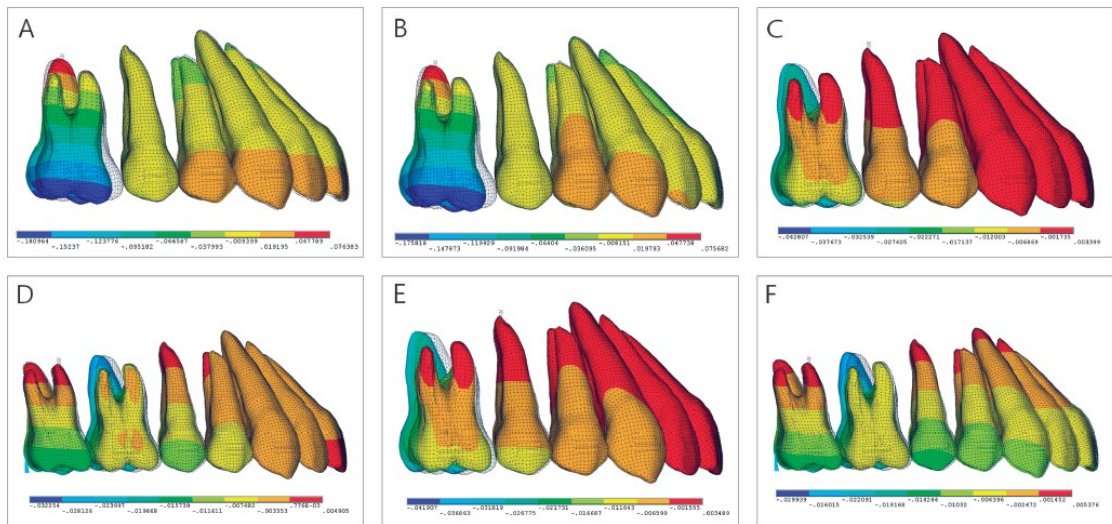


Fig. 2.31: Displacements in the Y axis of the maxillary dentition. **A-** Indirect anchorage; **B-** Modified direct anchorage modality; **C-** Distalization with the palatal plate with the lever arm at 10 mm; **D-** Similar to C with the second molar erupted; **E-** Similar to C with a cinch back bend applied to imply en masse distalization; **F-** Similar to E with the second molars erupted (Yu et al., 2014).

Kamble et al. (2012) evaluated root resorption with various orthodontic tooth movements (intrusion, extrusion, rotation and tipping) in reference to maxillary incisor root morphology (Fig. 2.32). Stress distribution varied with root shape (normal, short, blunt, dilacerated, and pipette), indicating that teeth with deviated root morphology were at higher risk of root resorption (Table 2.2). However, this study did not compare the effect of force magnitude on the stresses that occurred.

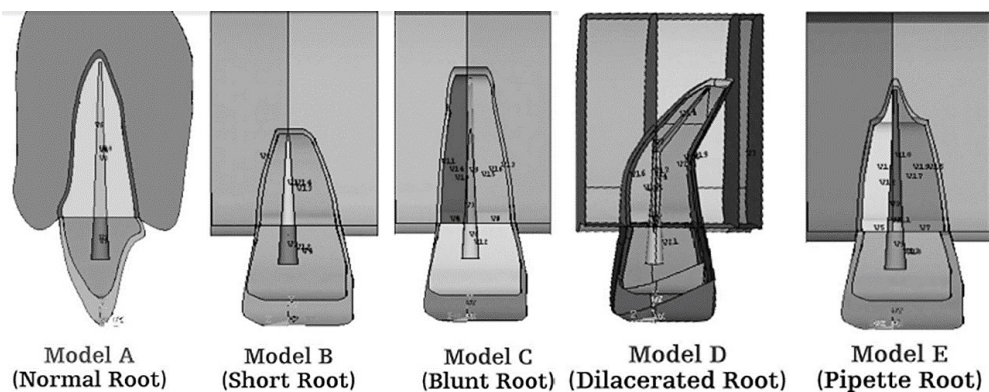


Fig. 2.32: Various root morphologies (Kamble et al., 2012).

Table 2.2: Stress values at the apical third for different root morphologies under different forces (Kamble et al., 2012).

Stress Produced in Different Areas of the Root					
Type of Force Applied	Normal Root A	Short Root A	Blunt Root A	Dilacerated Root A	Pipette Root A
Intrusion	0.000007	0.0000466	0.0000245	0.000141	0.0000627
Extrusion	0.0000267	0.000119	0.00016	0.000622	0.000247
Tipping	0.0000837	0.0000693	0.0000886	0.000309	0.0000945
Rotation	0.0000423	0.000206	0.000511	0.000805	0.000206

* All the values are in N/mm². C indicates cervical area; M, middle one-third areas; and A, apical area.

2.3.6. Human bones

Human bones are typical anisotropic and heterogeneous material characterized by wide variations in their physical and mechanical properties (An & Draughn, 1999). Bone properties are dependent on the age, gender, and health status of the subject, and on the skeletal site (Rho, Hobatho, & Ashman, 1995).

In a CT scan, a Hounsfield Unit (HU) is proportional to the degree of x-ray attenuation. HUs are allocated to each pixel to show an image that represents the density of the tissue. In dentistry, CT scans HU values were used to measure bone density prior to implant placement (Norton & Gamble, 2001). Many investigators evaluated the structures of jaw bones using CT scans and found extreme variations in the density of the trabecular bone tissue of the edentulous maxilla (Lindh, Obrant, & Petersson, 2004). Variations are also present in the density of cortical bone in the interradicular areas of dentate maxilla (Chugh, Ganeshkar, Revankar, & Jain, 2013; Peterson, Wang, & Dechow, 2006).

2.3.6.1. Role of bone in the rate of tooth movement

Notable differences in tooth movement rate between subjects have been attributed to numerous factors including anatomical and physiological variances between

individual patients (Rees & Jacobsen, 1997). The influence of alveolar bone properties on the rate of orthodontic tooth movement is well established in the orthodontic literature. Ricketts (1979) defined “cortical anchorage” because the compact bone offers resistance to tooth movement and can be used to the orthodontist’s advantage to fortify the anchor unit. He advocated torquing the roots of the mandibular molars buccally against the thick buccal cortical plate in this area to inhibit their mesial movement in extraction treatments where maximum anchorage is needed or when Class II elastics are used.

Clinical studies on endosseous implants were used to compare the rate of tooth movement in the dense bone present in the posterior mandible with the maxillary posterior area characterized by less bone density. Roberts et al. (1990) noted that the same teeth move twice as fast in growing children compared to adults. A maximal rate approaching 2 mm/month in the maxilla is possible with space closure mechanics or with a full time wear of headgear in a growing child compared with 1 mm/month for similar movements in an adult.

Similarly, mandibular molars can be mesially translated at a rate of 0.7 mm/month in children compared to 0.33 mm/month in adults. However, decreased bone density present in growing individuals was not the only reason for the related differences. Other histological factors such as the more cellular PDL and the growth related extrusion contribute to the faster tooth movement. The molar extrusion movement result in a considerably smaller volume of bone resorbed during space closure in growing child (Roberts, Arbuckle, & Analoui, 1996; Roberts et al., 1990) (Fig. 2.33).

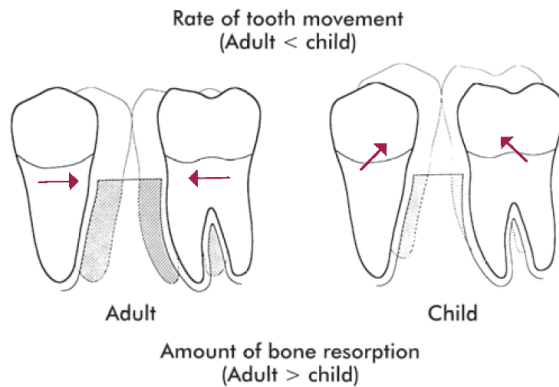


Fig. 2.33: Bone resorption in adults and children (L. W. Graber, Vanarsdall Jr, & Vig, 2011).

Moreover, cortical thickness can delay tooth movement. A thick cortical plate is equivalent to an old extraction site where the loss of a tooth lead to the resorption of the spongy bone and the interposition of a dense layer of cortical bone within the alveolar process. Closing such an extraction space is extremely difficult because tooth movement is slowed down as the roots encounter the compact bone along the alveolar ridge (T. M. Graber et al., 2006).

Even if bone remodeling is slow in these situations, penetration of the cortical bone may still occur but with an increased risk of root resorption. A composite analysis of four similar conditions of mandibular molar protraction in adult patients showed that the second molars moved at a rate of about 0.6 mm/month during the first 8 months and decreased to 0.33 mm/month thereafter. The total duration of mandibular molar space closure was about 2 years (Roberts et al., 1996). On the other hand, molar protraction in the maxilla could be achieved at a rate of 1 mm/month in adults because of thinner buccal and palatal cortical plates (Sicher & DuBrul, 1970).

These findings suggest that the rate of tooth movement is affected by growth, type of tooth movement, and bone characteristics (density and volume). Before Peterson et al's studies on maxillary bone characteristics (2006) [see Methods section], no

systematic quantitative biomechanical analysis of the human maxilla existed except for some qualitative attempts (Peterson et al., 2006; Sicher & DuBrul, 1970). As a result, previous clinical research has failed to correlate, for similar occlusal and metabolic conditions, the rate of tooth movement with bone stiffness and thickness. FEA incorporates the means to control for these variables and thus help in testing the effect of bone properties on the rate of tooth movement under similar initial conditions.

2.3.6.2.. Progress in bone modelling in orthopedic medicine

In orthopedic medicine, bone mineral density values calculated on CT scans have been used as a tool for osteoporosis management including fracture risk assessment, preoperative planning, and assessment of fracture healing (Schreiber et al., 2011). Patient-specific bone analysis protocols, introduced in the field of orthopedics (Viceconti et al., 2004), highlighted the differences with respect to shape, morphology, genetics and overall physiology of each individual in a more extensive manner (Trabelsi et al., 2011).

Information pertaining to individual patients is incorporated in the FEA to personalize the biomechanical models of bone. This approach, called “Bone Mapping”, implies that the mechanical properties of bone significantly correlate with bone mineral density and HU values obtained from CT scans (Wachter et al., 2002). Specific preprocessing softwares superimpose the 3D model and the actual scan, then automatically assign for each element a material property that correlates to the HU value of the same voxel in the scan (Gačnik et al., 2014) (Fig. 2.34).

This promising protocol was described as the state of the art in bone finite element modeling, whereby FEA would one day become a valuable diagnostic and

therapeutic tool in orthopedic medicine through improving the sensitivity and specificity of the obtained analytical results, and helping to provide the patients with personalized healthcare (Taddei et al., 2006; Viceconti et al., 2004).

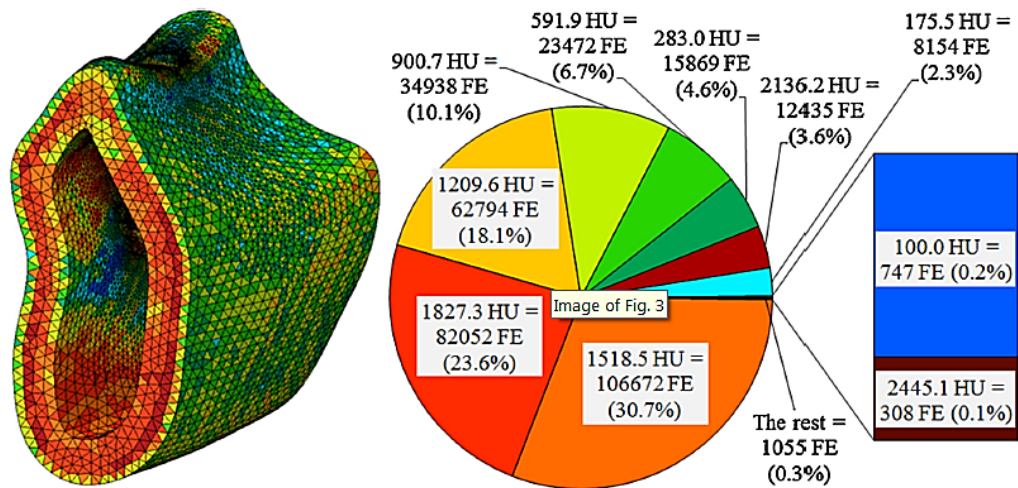


Fig. 2.34: Bone density distribution in Hounsfield units (HU) in the FE model of human mandibular cortical bone segment (Gačnik et al., 2014)

2.4. Significance

Static finite element analysis assessment may not simulate the reality of tooth movement but by discretizing the geometry into its elements and validating the assumptions given to these elements from clinical data, the results should come closer to real clinical settings. This important benefit will constitute one of our contributions in this research. However, at a different scale, the introduction of individual variation drawn from actual human material shall elevate the method to closer adherence to clinical reality. Indeed, no FEA study to date has approached the context of variability of response.

The outcome of the results is expected to widen the scope of FEA simulation, the only non-invasive procedure that can produce both qualitative and quantitative data

on biomechanical responses of teeth and bone during orthodontic movement. This landmark attempt shall be followed by much research to explore not only stresses but also real time displacement, all toward the eventual development of the science to a point when mechanotherapy may be planned with controlled personalized tooth movements that also would minimize side effects.

Defining the properties of bone is critical when FE analysis of a bony structure is contemplated. In previous FEA studies, bone variation was not accounted for as an element affecting the results. This study accounts for variations in cortical bone stiffness of real patients, thereby creating a closer link between the virtual finite element models and actual clinical situations. While previous studies evaluated the stress resulting from different distalization modalities, they did not factor in the effect of cortical bone thickness on the stresses.

In this context, the importance of deciphering the material properties of specifically the compact bone involved in specific tooth movements must be noted. The reason for this focus is the fact that trabecular bone usually does not hamper tooth movement. The role of cortical bone in hindering (Ten Hove and Mulie, 1977) or actually aiding (Rickets, 1980) tooth movement has been shown as a general determining factor, however not in the context of common tooth movements such as the distalization of molars or premolars. We aim to determine how cortical bone affects tooth movement by analyzing the effect of stiffness (related to bone density) and thickness of the cortex.

Accordingly, we investigate actual variations in stiffness, taking at the same time account of density and geometry. Accordingly, the results should underline which of the variables, stiffness, thickness, or both impact the initial stress and displacement

following the application of two modalities of tooth movement. The fact that this displacement will be anchored against mini-implants eliminates the confounding effect of the movement of an anchoring unit.

Finally, this study should shed light on the application of the FEA method itself in orthodontics, sorting out the validity of the various assumptions about the tissues surrounding teeth (PDL, bone) that are necessary to perform the method. Until further tools are developed to simulate human anatomy, FEA offers a valuable opportunity, albeit somewhat cumbersome and demanding, to explore body response in a totally non-invasive way, based on records taken for regular diagnostic and therapeutic reasons, and not exclusively for research purposes. The ultimate achievement would require coupling the mechanical study with the biologic response (such as amount of tooth movement, crevicular fluid markers and pain) to tooth movement in future investigations. We expect and hope that the present study shall lay additional foundations toward that objective.

2.5. Specific aims

Aims related to orthodontic distalization of maxillary molars:

1. Compare the stress levels on the teeth in different scenarios of distalization using miniscrews (direct vs indirect anchorage).
2. Test the influence of the cortical bone geometry (*through thickness and stiffness*) on the stress and displacement in of tooth movement.

Aims related to FEA application in orthodontics:

3. Develop a complete model for tooth movement taking into account individual variation in the anatomy of the maxilla and biomechanical characteristics of the bone.
4. Introduce new interaction properties between the teeth.
5. Assess the response to forces according to the orthotropic properties of the bone (evaluate the response in relation to variations in stiffness as per defined characteristics of maxillary bone biomechanics).

2.6. Hypothesis

In relation to orthodontic distalization of maxillary molars:

- Direct and indirect anchorage modalities have differential effects on teeth: more anterior with the direct, more posterior with the indirect mode.
- Direct anchorage provides more distalization stresses distributed on more teeth of the buccal segment.
- Initial tooth displacement is related to the stress generated by the distalizing force: more displacement with higher stresses.
- Cortical bone stiffness and thickness influence the rate of tooth movement

independently (thickness has a greater influence on displacement).

In relation to FEA application in orthodontics:

- Individual variation in the anatomy of the maxilla influences stress generation.
- Interaction properties between the teeth can mimic clinical situation.
- The orthotropic properties of the bone can influence stress generation in differential contributions.

CHAPTER 3

MATERIAL AND METHODS

3.1 Material

This research was approved by the institutional review board (IRB) of the American University of Beirut (date of approval: October 5, 2015).

3.1.1. *Anatomical record*

The pre-treatment cranial CT scan (in DICOM format) of an adult patient seeking radiologic assessment of the head at the Department of Radiology at the American University of Beirut Medical Center was used for the 3D model generation of the maxillary arch of an adult patient with all permanent teeth present except the third molars.

The following characteristics were the basis for exclusion:

- CT scan of patients undergoing orthodontic treatment
- Malaligned teeth
- Presence of deciduous teeth
- Missing or extracted teeth
- Presence of any craniofacial anomaly (e.g. cleft lip/palate)
- Absence of any medical condition affecting the maxilla or bones in general

We opted for CT scan imaging because we needed high contrast quality to help differentiate the trabecular from the cortical bone. CT scans provide better resolution and more importantly better contrast compared to the regular CBCT usually requested

in clinical settings. In addition, the CT scan is a powerful non-destructive tool that allows for longitudinal diagnoses of bone properties (e.g. density).

Ideally, the scans should be obtained with a cross-section of at least 0.25 mm distance to achieve adequate resolution necessary for model construction. Micro CT images are considered the gold standard for 3D Model construction because they possess the best resolution compared to other computer tomography images. Because of no added diagnostic value and most importantly to minimize radiation on patients, CT scans are not taken with full resolution in the radiology department at AUBMC. Therefore, the CT scan library at the hospital contains X-rays with a resolution between 0.4 and 0.6 mm.

The CT scan chosen was taken with a full head field of view for the diagnosis of sinusitis and has a resolution of $0.3 \times 0.3 \times 0.4$ mm with high contrast and was provided on a CD without any details on the patient's identity. The scan disclosed a well aligned complete dentition, parallel roots and a perfect Class I occlusion with the midlines on, suggesting that the patient possibly had a previous orthodontic treatment.

3.1.2. Individual Data Acquisition

Because of the integration of the data from Peterson et al. (2006) into the methods of this study, it is described in this section rather than in the Literature Review.

Thickness and stiffness of interradicular maxillary cortical bone from 15 cadavers served as the study variables that were input into the finite element analysis. These measurements resulted from a study by Peterson et al (2006), which was supported by The National Institutes of Health (NIH), National Institute of Dental and

Craniofacial Research (NIDCR); Grant number K08 DE00403. Human tissue use conformed to the NIH, state, and federal standards (Peterson et al., 2006).

This study entitled “Material Properties of the Dentate Maxilla” aimed to explore the variability in the characteristics of the cortical bone of the dentate maxilla. The hypothesis was that important regional differences existed within the maxilla that would correspond to variations in function and development. Specimens were removed from the crania of 15 dentate human cadavers: 7 females (48–95 years of age) and 8 males (50–89 years of age) with a median age of 58.9 years. All crania were frozen at -10°C shortly after death and were maintained in a fresh (unembalmed) condition. The freezing process has been found to have a minimal effect on the elastic properties of the bone (Evans, 1973; Dechow and Huynh, 1996; Zioupos and Currey, 1998).

Cylindrical cortical bone specimens (4 mm in diameter) were harvested from 15 maxillary sites located in three distinct regions: the palate (four sites), alveolar bone (four sites), and the body of the maxilla (seven sites) (Fig. 3.1). Trabecular bone was removed from the inner aspect of the cortical plate with a fine grinding wheel. The samples were later stored in a solution of 95% ethanol and isotonic saline in equal proportions. These media maintains the elastic properties of cortical bone over time with minimal change (Ashman et al., 1984; Dechow and Huynh, 1996).

Each prepared bone specimen was measured using a digital caliper to determine the *thickness* of the bone cylinder. *Apparent density* was calculated based on Archimedes’ principle of buoyancy (using sample weight and differential volume in water). *Material property* testing was performed using the pulse transmission technique. Using the linear elastic wave theory (Ashman et al., 1984), the specimen material properties were derived from various velocities with the following directions:

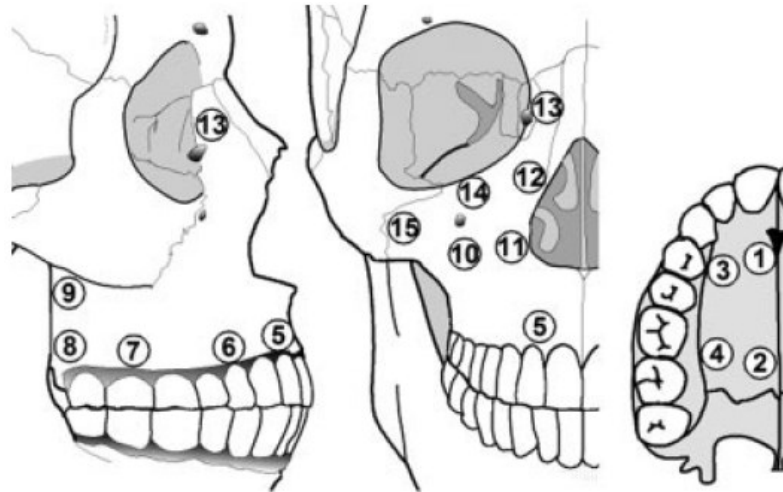


Fig. 3.1: Cortical bone sites in the maxilla (numbered for reference) (Peterson et al., 2006).

- Maximum stiffness or d_3 corresponded with the direction of peak ultrasonic velocity and is parallel to the long axis of the three-pillars of the maxilla [zygomaticomaxillary, pterygomaxillary, and frontomaxillary] (Sicher and DuBrul, 1970).
- Minimum stiffness or d_2 : Perpendicular to the axis of maximum stiffness within the plane of the cortical plate.
- d_1 : Through the thickness of the cortical plate.

Elastic modulus (E), a measure of the ability of a structure to resist deformation in a given direction, was defined by E_1 , E_2 , or E_3 according to the axis direction.

Shear modulus (G), a measure of the stiffness in shear or angular deformation relative to applied shearing loads in a plane formed by the two axes was indicated by the subscripts (G_{12} , G_{31} , or G_{32}).

Poisson's ratio (ν), a measure of the ability of a structure to resist deformation perpendicular to that of the applied load, as defined in the subscripts indicate orientation for Poisson's ratios in the same manner as in describing the shear moduli (ν_{12} , ν_{21} , ν_{13} , ν_{31} , ν_{23} , ν_{32}).

The results showed significant differences between sites in thickness and density that discretely outlined regions of the maxilla. Overall, where cortical bone was thin, its density was high. Cortical bone near the incisors and canines (sites 3, 5, and 6) had greater thickness than at other maxillary alveolar sites, but its density and stiffness were intermediate.

The values for elastic moduli demonstrated differences by direction, in that E3 was larger than E2, which was larger than E1. There were significant differences between sites for E2 and E3. The majority of sites within the dentate maxilla were moderately anisotropic with ratios ranging from 0.69 to 0.85. Site 7 above the second molar and under the root of the zygomatic process had the densest and stiffest cortical bone in the buccal alveolar area. Palatal cortical bone areas had relatively higher stiffness than buccal areas (Table 3.1; Table 3.2).

Table 3.1: Density (mg/cm³), cortical thickness (mm) and ash weight (Peterson et al., 2006).

Site	N	Density		Thickness		Ash weight	
		Mean	SD	Mean	Mean	%	Mean
1	12	1.65	0.17	1.7	0.5	56	5
2	10	1.75	0.14	1.8	0.9	55	9
3	11	1.75	0.18	2.3	1.1	57	5
4	10	1.70	0.16	2.0	1.0	53	7
5	14	1.65	0.15	2.2	1.3	57	5
6	8	1.64	0.19	2.4	1.6	58	9
7	11	1.72	0.20	2.1	0.9	54	11
8	6	1.61	0.14	1.2	0.6	54	15
9	6	1.77	0.16	1.0	0.3	53	15
10	10	1.75	0.16	1.2	0.5	56	8
11	9	1.69	0.15	1.7	0.7	54	11
12	11	1.82	0.12	1.5	0.4	53	12
13	11	1.83	0.17	1.4	0.3	50	13
14	11	1.81	0.11	1.5	0.6	55	7
15	7	1.90	0.12	1.1	0.3	61	5
Grand mean		1.75	0.16	1.9	0.9	56	9
ANOVA		F	F	P	F	P	F
Sites		4.7	0.001	5.4	0.001	NS	NS

Table 3.2: Elastic moduli in GPa (Peterson et al., 2006).

Site	E_1		E_2		E_3	
	Mean	SD	Mean	SD	Mean	SD
1	8.3	1.9	11.3	2.7	14.1	2.9
2	8.9	1.9	11.9	2.3	16.5	4.0
3	10.3	2.0	13.6	2.1	17.3	3.4
4	8.9	2.9	10.9	2.7	15.6	3.7
5	10.0	3.3	11.0	2.7	14.3	3.8
6	7.2	1.5	8.7	2.3	12.2	1.9
7	9.8	2.4	11.3	3.0	16.0	4.3
8	6.9	1.1	8.8	1.0	10.5	1.3
9	9.8	2.3	11.7	1.4	15.6	2.8
10	7.6	2.3	10.7	3.3	14.2	4.2
11	9.0	1.9	11.2	2.2	16.4	3.6
12	10.0	1.7	13.5	1.6	17.6	3.4
13	9.9	3.0	12.8	2.8	17.0	3.3
14	9.4	1.6	13.3	2.1	17.8	2.3
15	9.2	1.5	14.0	1.7	18.7	3.4
Grand mean	9.1	2.3	11.7	2.7	15.6	3.7
ANOVA	F	P	F	P	F	P
Sites	1.51	NS	3.02	0.001	3.87	0.001

3.2 Methods

The sequential methodology from image capture to finite element analysis is represented in a flow chart of 7 steps, developed in a FEA study of miniscrews (Ammar et al., 2011; Fig.3.2).

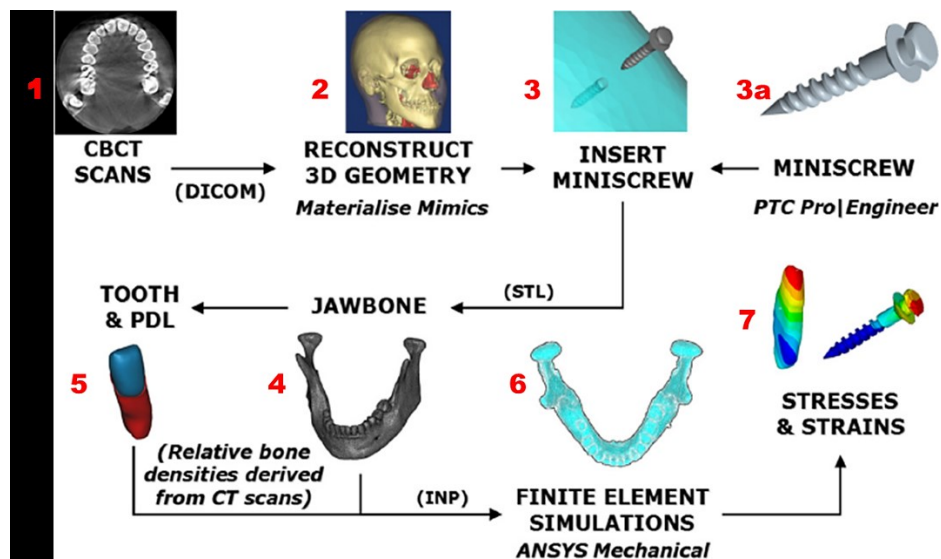


Fig. 3.2: The approach for 3D patient-specific model reconstruction and dental finite element simulations (after Ammar et al, 2011).

Different softwares are used from the computer tomography image reconstruction (1) to the finite element simulations (6). Steps 1 to 5 correspond to the development of the 3D model; steps 6 and 7 relate to the FE analysis.

3.2.1. 3D Model

3.2.1.1 Model segmentation

The CT image was imported and segmented using the image processing and digital reconstruction software ScanIP™ 7.0 (Simpleware Ltd., Exeter UK). The region of interest included the maxillary bone and teeth (using the *crop tool* in ScanIP™).

Masks of every tooth, periodontal ligament as well as cortical and trabecular bone were created using manual and automated tools (see below). Manual segmentation was minimized, as much as possible in order to save time and obtain reproducible and consistent outcomes.

- Teeth mask

In CT scans, a Hounsfield Unit (HU) is proportional to the degree of x-ray attenuation and is allocated to each pixel to show the image that represents the density of the tissue. All teeth cause similar attenuation of the x-rays thus have similar Hounsfield unit.

For this reason, it is appropriate to first use the ‘*Segmentation with Threshold*’ tool that identifies voxels with Hounsfield units in a specific range to capture the voxels associated to the teeth. A HU range between 945 and 3071 was used to detect all teeth voxels, but some others represented remnant parts of the dense cortical bone (Fig. 3.3).

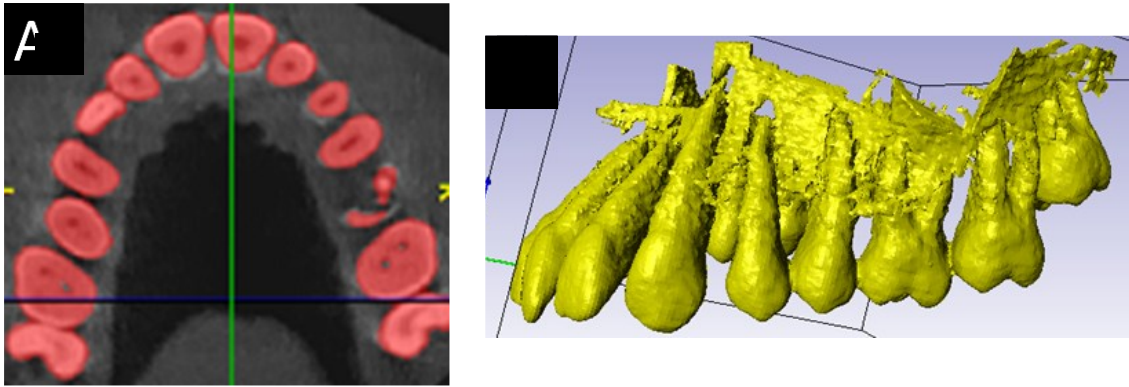


Fig. 3.3: Teeth mask captured according to the grayscale value using the *Segmentation with Threshold* tool: **A-** 2D axial cut; **B-** 3D view.

Editing of the masks to remove these excesses was performed initially using automated filters to remove unconnected fragments (*'flood fill'* command), to breakdown large fragments (*'morphological filters: Open and Erode'*), and to delete small fragments (*'Island remover'*). Afterwards, manual segmentation was used to finalize the teeth mask on the 2D sections to add or remove pixels (*'paint/unpaint tool'* or *'paint/unpaint with threshold tool'*) or directly on the 3D model (using *'3D editing tool: Delete - Erode Open'*) to apply the morphological filters: Open, Erode or delete on a part of the 3D model (Fig. 3.4).

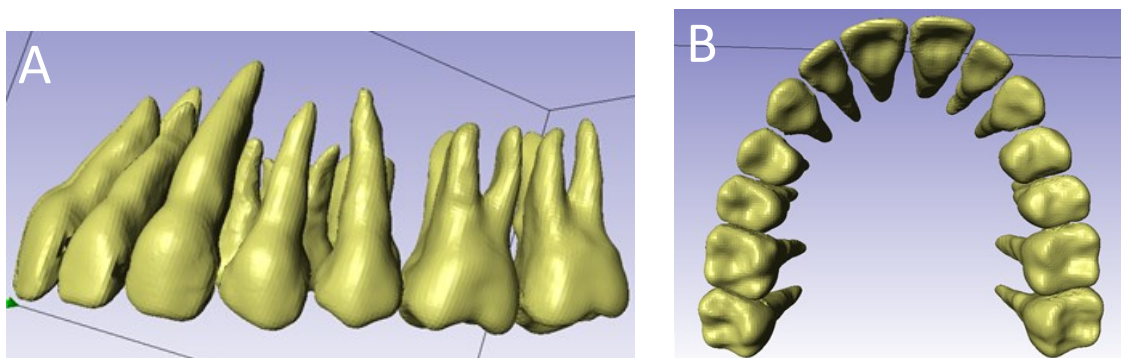


Fig. 3.4: Finalized teeth mask: **A-** Lateral view; **B-** Axial view.

- Bone masks

Bone density may differ among various regions of the same jaw and areas of differing densities may only be separated by millimeters (Gultekin, & Yalcin, 2012). As a result, bone segmentation is more arduous and demands more manual work.

In a first step, we created a mask called “cortical layer” (mask 2) using the ‘*Segmentation with Threshold tool*’ and manual segmentation with ‘*paint/unpaint tool*’. This mask does not represent the cortical bone because it does not include all the voxels related to it and is perforated in the areas opposing the teeth (which will increase after smoothing). It is only a tool to generate both cortical and trabecular masks (Fig. 3.5).

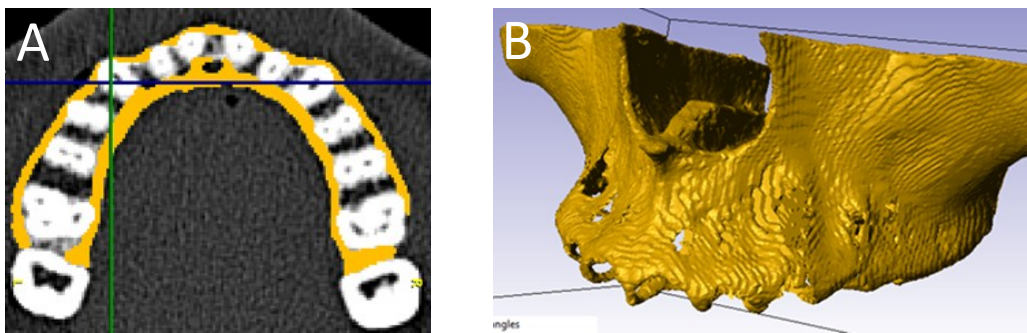


Fig. 3.5: Cortical bone layer mask: **A-** 2D axial cut; **B-** 3D view.

A mask of the roots (mask 3) was created by duplicating the teeth mask, then by removing the crowns (with the *3D edit tool-delete*; Fig. 3.6). Mask (mask 4) was generated by uniting the roots mask (mask 3) and cortical layer (mask 2), (Fig. 3.7).

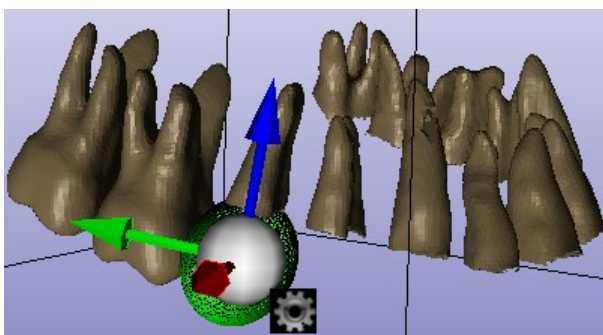


Fig. 3.6: Roots mask (mask 3).

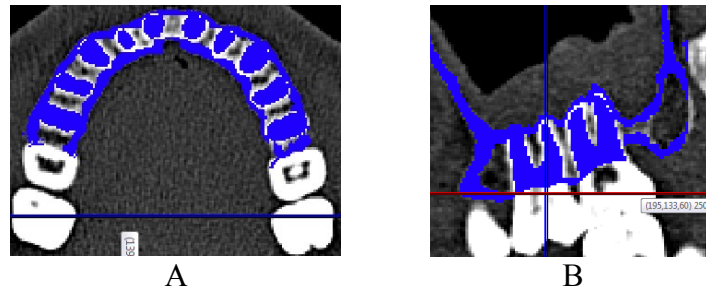


Fig. 3.7: Mask 4: **A-** 2D axial cut; **B-** 2D Sagittal cut.

The gaps (mask 4) were closed (using the ‘*morphological close*’, ‘*cavity fill*’ and ‘*paint tool*’; Fig 3.8). These gaps represent the future location of the trabecular bone (mask 5). Subsequently, the roots (mask 3) and the cortical layer (mask 2) were subtracted to obtain the trabecular bone (mask 5), (Fig 3.9).



Fig. 3.8: Gaps closed in mask 4: **A-**2D axial cut; **B-** 2D frontal cut.

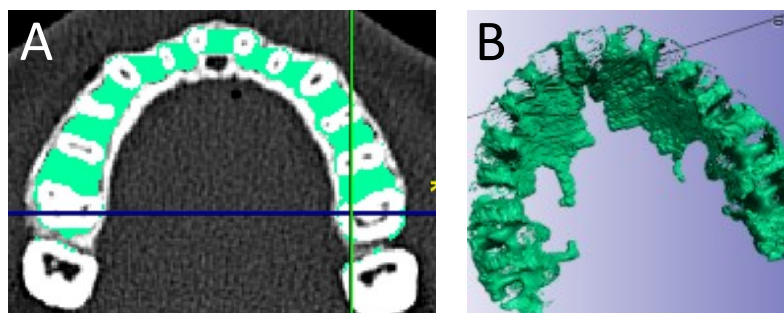


Fig. 3.9: Trabecular bone (mask 5): **A-** Axial cut; **B-** 3D view.

To avoid any perforation of the cortical bone mask facing the roots of the teeth, the roots (mask 3) were thickened by 3 pixels in the X and Y direction using the

'*morphological dilate tool*'. The resulting dilated root (mask 6) was then united with the cortical layer (mask 2) to form mask 7 (Fig. 3.10). The cortical bone (mask 8) was obtained by subtracting the roots (mask 3) and the trabecular bone (mask 5) from the mask 7 (Fig. 3.11).

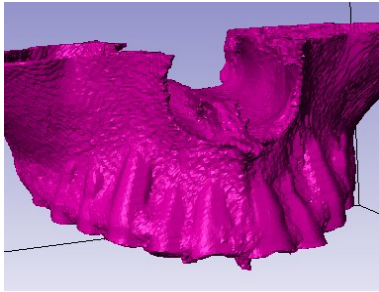


Fig. 3.10: 3D view of mask 7.

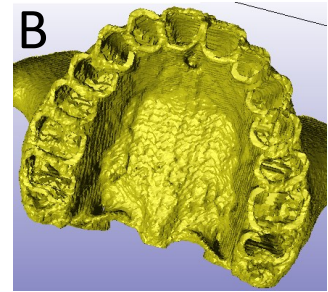
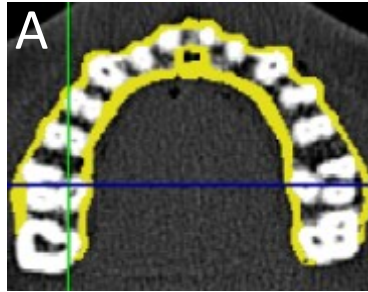


Fig. 3.11: Cortical bone (mask 8): A- 2D axial cut; B- 3D view.

- Periodontal ligaments mask

The periodontal ligament (PDL) cannot be captured on the CT scan.

Consequently, the PDL mask was created with a thickness assumption of 0.3 mm (Bowers, 1963). The construction included 5 steps:

- *Duplication* of the teeth mask
- Expansion of the new teeth mask (mask 9) by 1 voxel (0.3 to 0.4 mm) away from the surface of the tooth using the *morphological dilate tool* (Fig. 3.12).
- Uniting the trabecular bone (mask 5) and the cortical bone (mask 8) to form the bone mask (mask 10).
- Selecting the common area between the bone (mask 10) and the expanded teeth (mask 9), which will eventually represent the PDL (mask 11), using the '*Intersection Boolean operation tool*'.

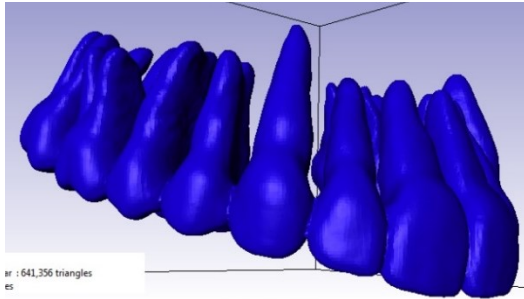


Fig. 3.12: Inflated teeth mask (by 1 pixel).

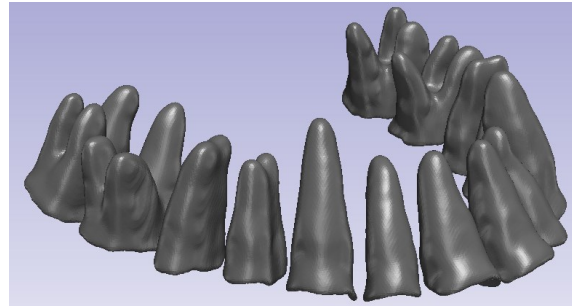


Fig. 3.13: PDL mask (mask11).

- Smoothing

In ScanIP, only one mask can occupy a voxel (3D pixel) at any one time, therefore masks listed higher in the dataset browser take priority over those lower. Accordingly, smoothing should start from the internal masks first (teeth mask) before reaching the outer masks (cortical bone mask).

The *Recursive Gaussian* filter (Intensity 2) was used to smoothen all masks.

Smoothing with this filter implies :

- “Shaving” of the masks, thus removing pixels from the outer surfaces leading to their shrinkage (1 pixel of shrinkage for a Recursive Gaussian intensity 2).
- Formation of unassigned pixels at the interface between the masks.

To counteract the shrinkage, all masks were enlarged by 1 pixel using the ‘*morphological dilate*’ tool. As for the formation of unassigned pixels, the same editing workflow that was used to correct geometric changes caused by resampling (check section 3.2.1.2) was performed for every mask after smoothing.

Further smoothing was done prior to the generation of the FE Model. In the model configuration, ‘*Smart mask smoothening option*’ employs the underlying greyscale information to improve a model’s smoothness and accuracy while preserving volume algorithm (Fig. 3.14).

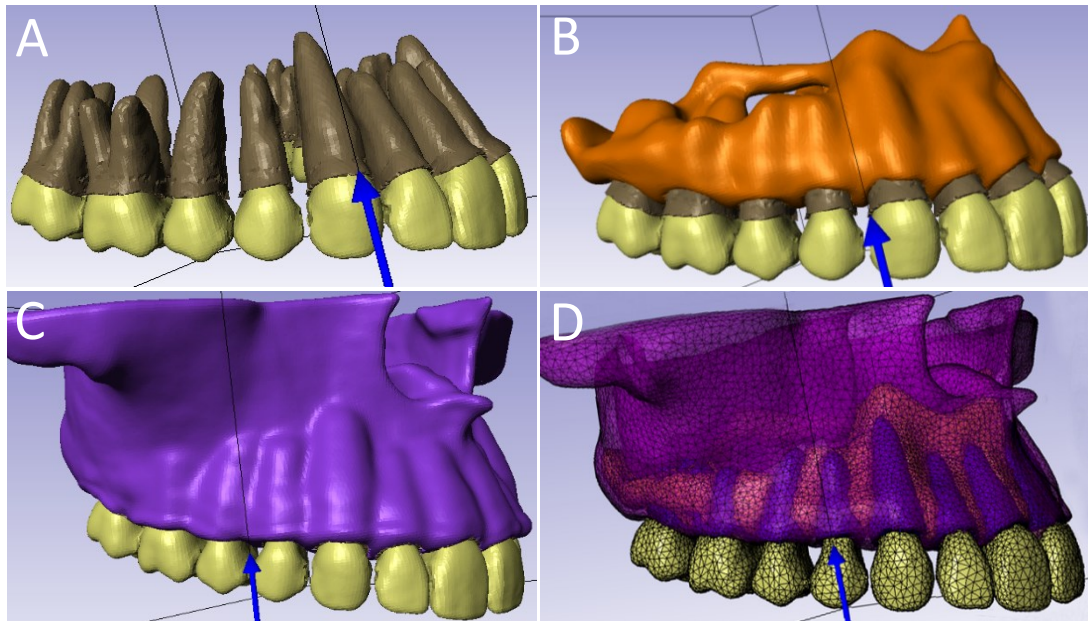


Fig. 3.14: A- Smoothed teeth and PDL masks; B- Smoothed trabecular bone mask; C- Smoothed cortical bone mask; D- Further smoothing of the FE model.

3.2.1.2. Resampling

Resampling is a tool that changes the resolution of the 3D model by changing the size and shape of the pixels. The drawback of this tool is the increase of the size of the background data and the RAM used by the computer hence resampling must not be exaggerated. Moreover, resampling causes changes in the geometry of the model, producing a mix between the masks and the formation of pixels that are not assigned to any mask (usually at the interface between the masks; Fig. 3.15).

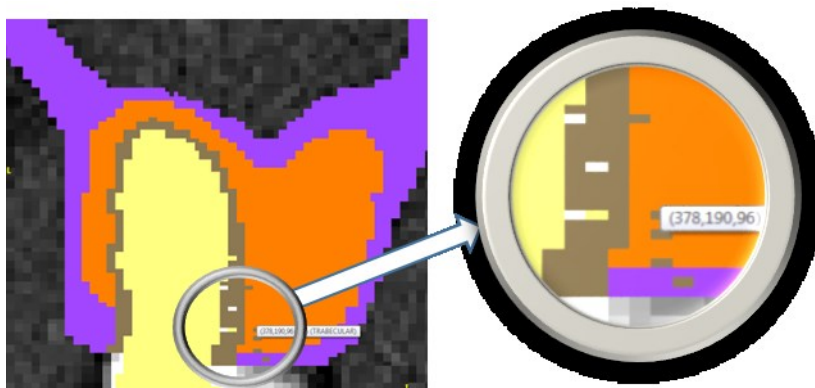


Fig. 3.15: Unassigned pixels (white color) between the teeth mask (in yellow) and the PDL mask (brown) - Mixing between the trabecular (orange), cortical (blue) and the PDL masks.

We resampled the model to decrease the pixel size from 0.4 mm to 0.2 mm for the following reasons:

- The PDL layer thickness at the curvatures of the teeth was more than 0.5 mm, making it *thicker* than what was measured experimentally (Bowers, 1963), (Fig. 3.16).
- Having decided to adopt “Surface to Surface” interaction settings between the teeth, the distance between the teeth should be minimized for the FEA solver (Abaqus) to detect adjacent surfaces (see section 3.2.2.3).
- The cuboid original voxel shape of the CT scan (0.41*0.41*0.34 mm) makes it harder to implement geometric variations such as cortical bone thickness increase/decrease (see section 3.2.1.4).

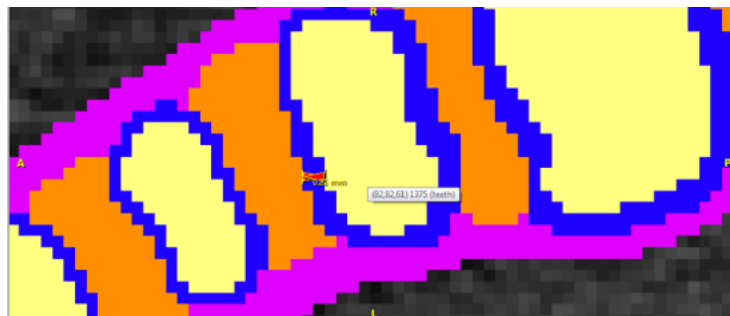


Fig. 3.16: PDL thickness of 0.8 mm at the level of the second premolar.

To minimize the increase of the file size, we tried to obtain the smallest image extent prior to the resampling by further cropping the model to just include the needed areas. The ‘*Shrink wrap*’ tool was used for this purpose to reduce the image background to the smallest cuboid fitting the masks. The image extent was reduced from 265 x 223 x 172 pixels (135.71MB) to 265 x 141 x 137 pixels (68.35 MB).

To correct the geometric changes (unassigned pixels and mixing between masks) between the PDL and bone masks, these steps were followed: 1. Duplicate the

PDL mask; 2. Unite it with the surrounding masks (trabecular and cortical bones); 3. Fill the unassigned pixels (using the *cavity fill* and the *morphological close* tools); 4. Subtract the new PDL layer to have conforming mask interfaces.

The same workflow was used for the trabecular and cortical bone masks.

3.2.1.3. CAD processing

The miniscrew and brackets were sketched in Autodesk® 3ds Max® Design software reproducing commercially available brackets (Mini-Twin bracket Orthos, SDS Ormco) and miniscrew (OSAS - DEWIMED - Tuttlingen, Baden-Württemberg, Germany). The miniscrew dimensions followed the ideal dimensions: 6 mm length, 1.5 mm diameter, reported as the ideal dimensions by Deguchi et al. (2006).

The .max files were converted into .stl files and imported into +CAD add-on module (Simpleware Ltd., Exter, UK) to position the CAD geometry. The miniscrew was placed 5 mm apical to the cemento-enamel junction (CEJ) between the right second premolar and first molar, where enough interradicular space is commonly available.

To simplify the analysis, the bracket was placed only in the middle of the maxillary right canine crown and following its long axis with the purpose of defining the point of application and direction of the load. To simulate the other brackets and the movement of teeth along the archwire, an axis system following the long axis of every tooth was created in Abaqus. Subsequently, specific boundary conditions allowing for accurate tooth movement were assigned to 10 to 15 nodes located at the level of the bracket position (see Section 3.2.2.4).

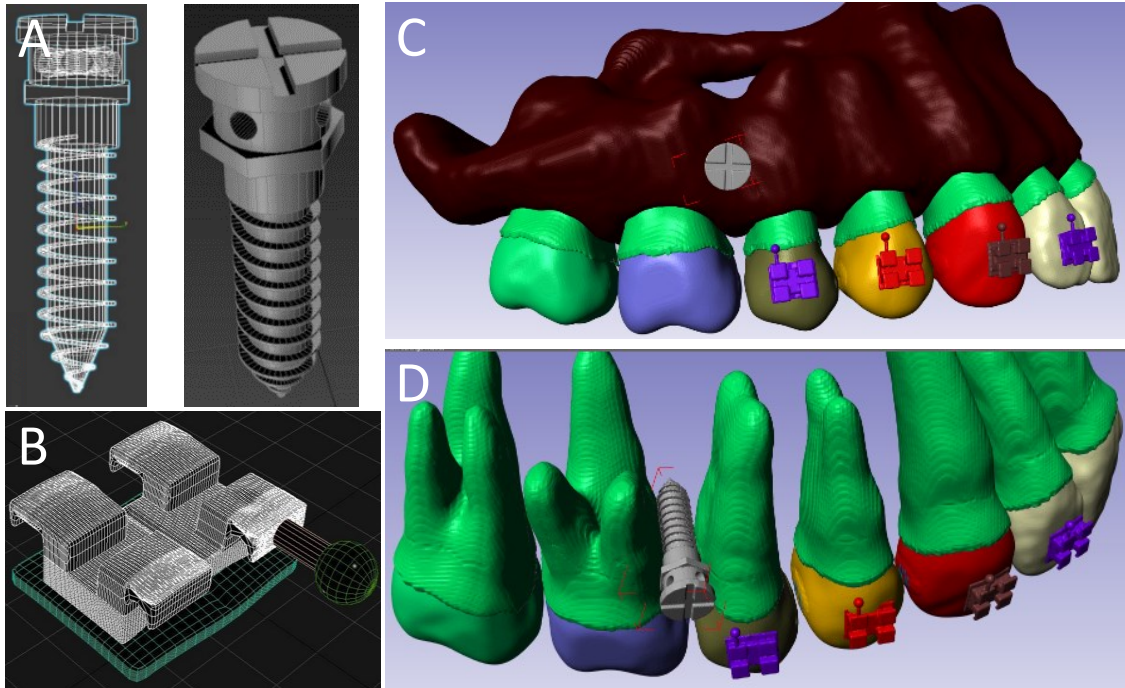


Fig. 3.17: CAD sketched in Autodesk® 3ds Max® Design software: **A-** TAD; **B-** Bracket; **C- D** Placement of the CAD objects in the model using the +CAD add-on module (Simpleware Ltd).

3.2.1.4. Individual variations

Anatomical variations of cortical bone stiffness and thickness were produced from the initial model to simulate clinical situations. Unpublished individual data from 15 cadavers obtained as discussed previously in section 3.1.2. from Peterson et al. 2006 were used to replicate different bone characteristics found in real patients.

- Stiffness variation

To be able to modify the thickness and assign an individual material property to each region of the cortical bone, the right side of its mask was divided into 7 areas of interest directly related to our mechanical model (4 buccal and 3 palatal areas) matching the classification by Peterson et al (2006) (Fig. 3.18).

In ScanIP™, a new mask was created for each part. For the areas 3,4,6,7, and 8, the 3D editing tool was used to create cuboid shape objects that extended from the

cervical contour of the original cortical bone mask to 4 to 6 mm above the root apices. These masks reached to the middle of the alveolar ridge and cut the corresponding interdental areas in their middle. As for the area 5, two cuboid shape objects were used to select the cortical bone area spreading from the right to the left canines with the same cervical and apical borders as the previous objects; then they were combined using the ‘Union Boolean operation’ (Fig 3.18). The following steps were then taken:

- Fill option was used for each mask leading to the formation of 6 filled cuboid shaped masks.
- Intersection Boolean operation was used between each one of these “filled boxes” masks and the cortical bone mask (9) to select the common voxels, which correspond to the cortical bone present in each box.
- The adjacent “cortical bone parts” masks were subtracted from each other to identify and correct pixels shared by more than 1 mask .
- Manual segmentation (using the paint/unpaint tool) was used to join disconnected pixels (Fig.3.18).

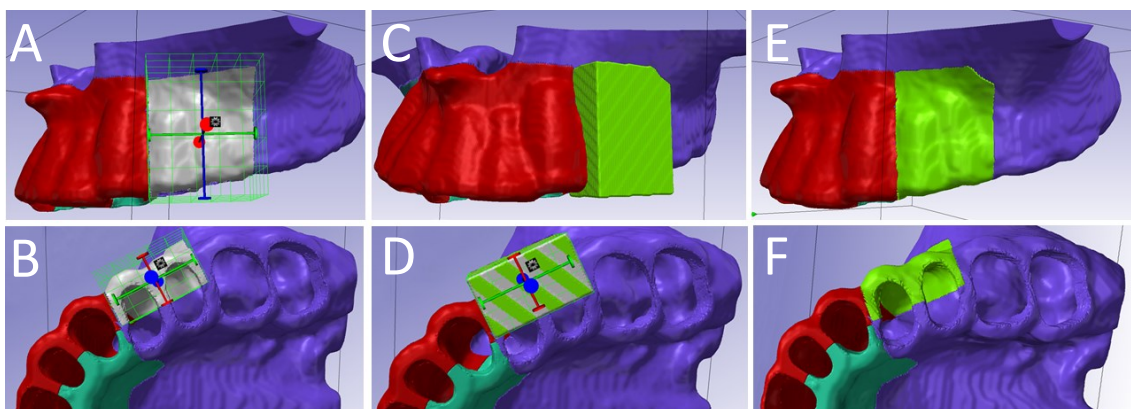


Fig. 3.18: Creation of the buccal premolar cortical bone part. **A-B** 3D editing tool used to create cuboid shape objects; **C-D** fill option used to form filled cuboid shaped mask; **E-F** Intersection Boolean operation used with the original cortical bone mask to form the cortical bone part.

Similarly, area 1 (palatal incisors/canine) was created by using a cylinder object and selecting the palatal area extending to the middle of the alveolar ridge of the area 5. This object was filled and the ‘Intersection Boolean operation’ was used to select the palatal cortical bone between the right and left canines (Fig. 3.19).

Finally, each cortical bone part was assigned a material property from the individual values provided at the maxillary sites 1, 3, 4,5,6,7 and 8 (Section 3.2.2.2.).

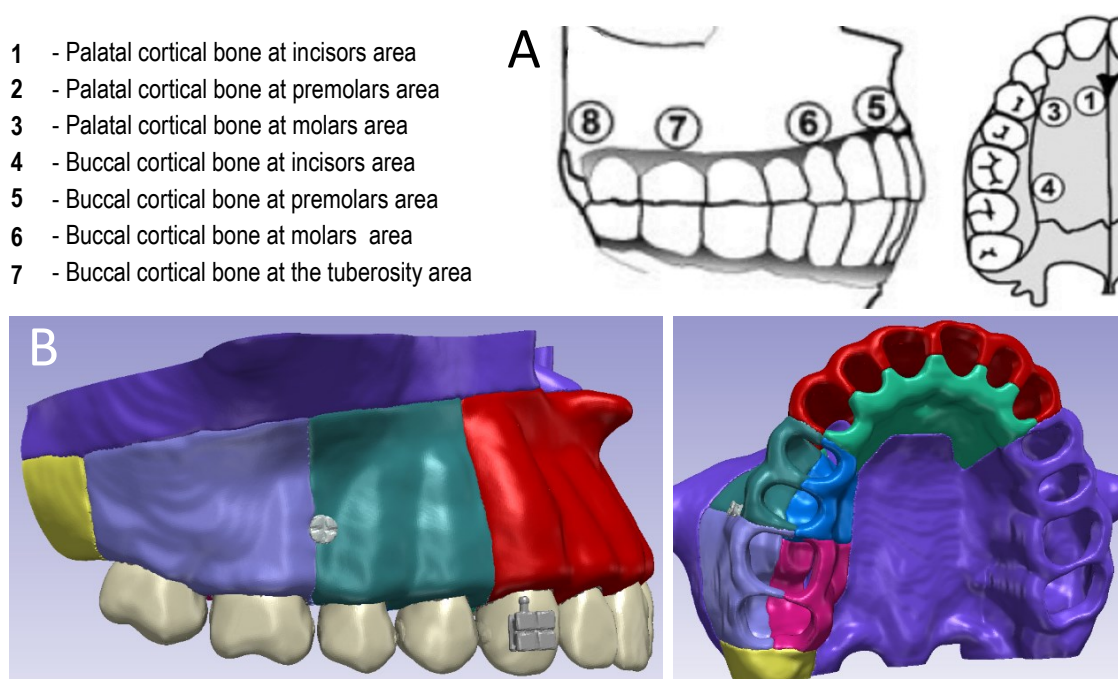


Fig. 3.19: A- Areas of the dentate maxilla (right) with corresponding definitions (After Peterson et al, 2006); B- 3D Model after cortical bone division.

- Thickness variation

The thickness values provided by Peterson et al. (2006) were replicated in the template model (with cortical bone parts) to generate separate models, each belonging to a single cadaver. Three cadavers had three or more missing values; accordingly they were excluded from the sample. For 3 cadavers who had 1 to 3 missing values, the average thicknesses from the total sample were used for the corresponding areas.

Initially, the cortical bone thickness of each part was measured in the template model at 9 sites dispersed around the bone part surface. In each site, 25 to 30 thickness measurements were made on the 2D axial cut sections using ScanIP™ 7.0. A minimum of 200 cortical bone thickness measurements were performed for each cortical bone part (Fig 3.20). Next, the total average was calculated and later used to calculate the amounts of expansion or reduction needed for each mask by subtracting the template model thickness from the cadaver thickness at the same location. Knowing that the pixel size is 0.2 mm (after resampling), the value obtained is multiplied by 0.2 to determine the number of pixels needed to attain the cadaver's thickness. To avoid changing the outer contour of the model, the thickness variation was implemented at the expense of the trabecular bone.

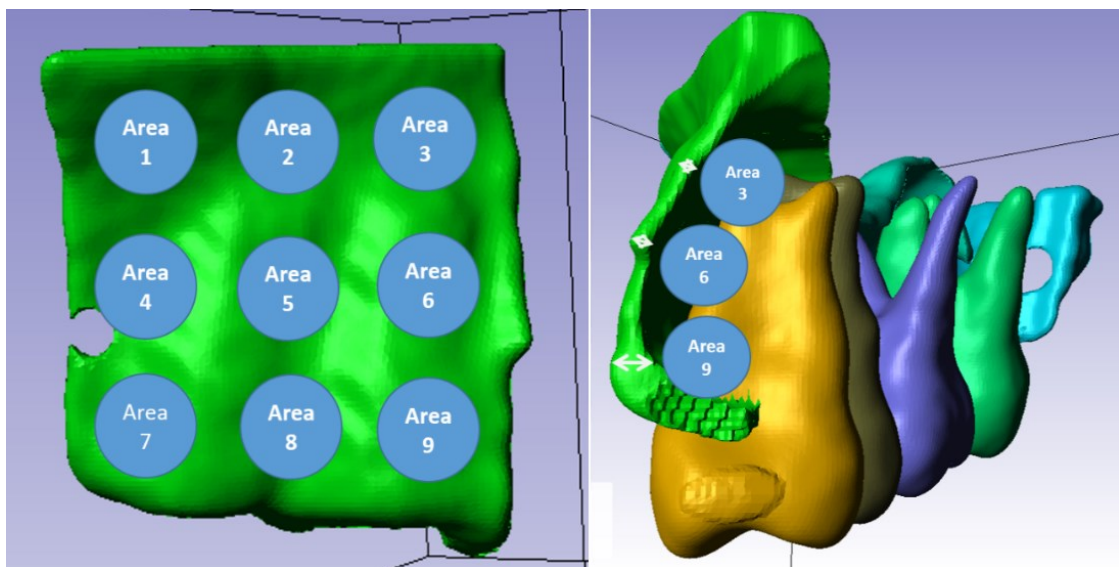


Fig. 3.20: Areas of thickness measurements in the buccal cortical bone part at the premolar area.

Depending on the need to expand or reduce the cortical bone thickness, two methods were used:

- Scenario 1: Template Model Thickness < Cadaver Thickness (Fig. 3.21).

The following workflow was implemented:

1. Duplicate the cortical bone part.
2. Use the Morphological dilate tool by the amount of pixels calculated earlier (the dilation occur on the palatal and buccal side of the cortical bone (mask a)).
3. Use the Intersection Boolean operation between the trabecular bone mask (4) and the dilated cortical bone mask (a) to select the thickness increase that occurred at the inner surface of the cortical bone part (mask b).
4. Use the Union Boolean operation between the mask b and the original cortical bone part (in the template model) to add the thickness increase to the cortical part in the template model.
5. Subtract the trabecular bone mask (4) from the thickened cortical bone part.
6. Manual adjustment.

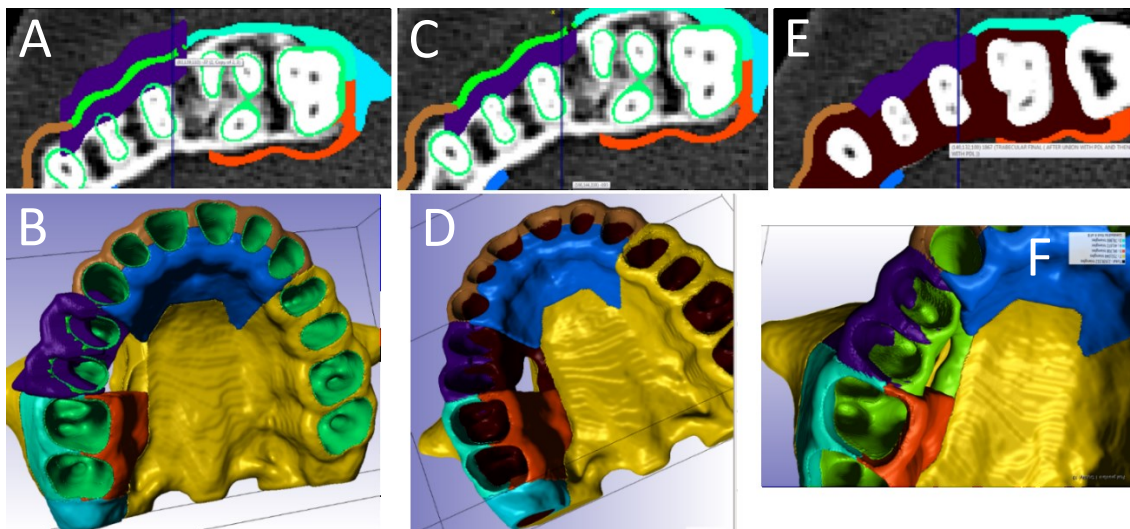


Fig. 3.21: Technique applied to increase cortical bone thickness. **A-B** 2D and 3D images after dilating the premolar cortical bone part by 14 pixels; **C**- After applying “Intersection Boolean operation” with trabecular bone mask; **D-E-F** 2D and 3D images after union with “original cortical bone part”.

- Scenario 2: Template Model Thickness > Cadaver Thickness (Fig. 3.22)

1. Duplicate the cortical bone part
2. Use the '*Morphological dilate*' tool by the amount of pixel difference calculated earlier (the dilation occur on the palatal and buccal side of the cortical bone (mask a))
3. Subtract the trabecular bone mask (4) from the thickened cortical bone part
4. Use the '*Morphological Erode*' tool to shave the mask by as much as calculated (Pixels will be deleted from the buccal and palatal side). The goal at this point was to fill the space between the trabecular bone mask (brown) and the eroded cortical bone part (light blue; Fig. 3.22)
5. Duplicate the trabecular bone mask and unite it with the original cortical bone part.
6. Subtract the eroded cortical part from the newly formed (Trabecular+ Original cortical part) to generate the final trabecular bone mask.

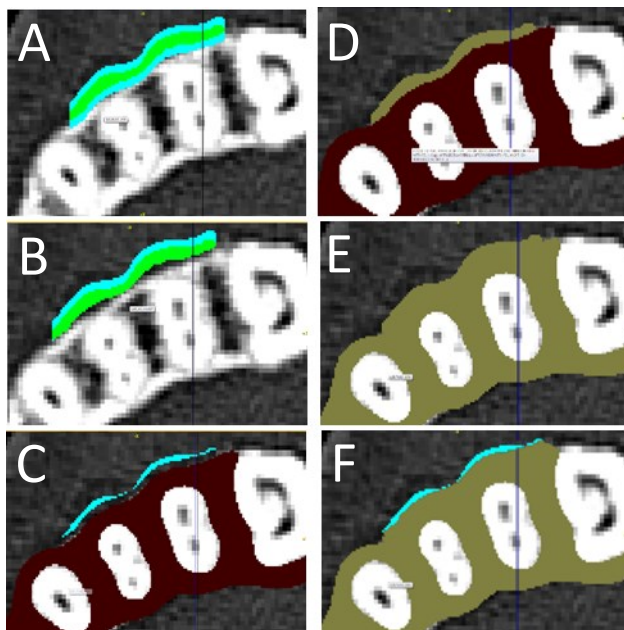


Fig. 3.22: Technique applied to decrease cortical bone thickness. **A-** Buccal premolar cortical bone part dilated by 3 (dilation occurs on both sides of the cortical bone). **B-** Delete the increase that occurred at the inner cortical surface by subtracting the trabecular bone mask from the dilated cortical part; **C-** Application of *Morphological Erode* filter by 3 (mask a); **D-E** Duplicate trabecular bone mask and then unite it with the original cortical bone part (mask b); **F-** Subtract the mask a (eroded cortical bone part) from the mask b (combined trabecular and original cortical bone part).

After applying the above-mentioned steps on the seven areas of each model, twelve 3D models were generated, each corresponding to one cadaver (Fig. 3.23)

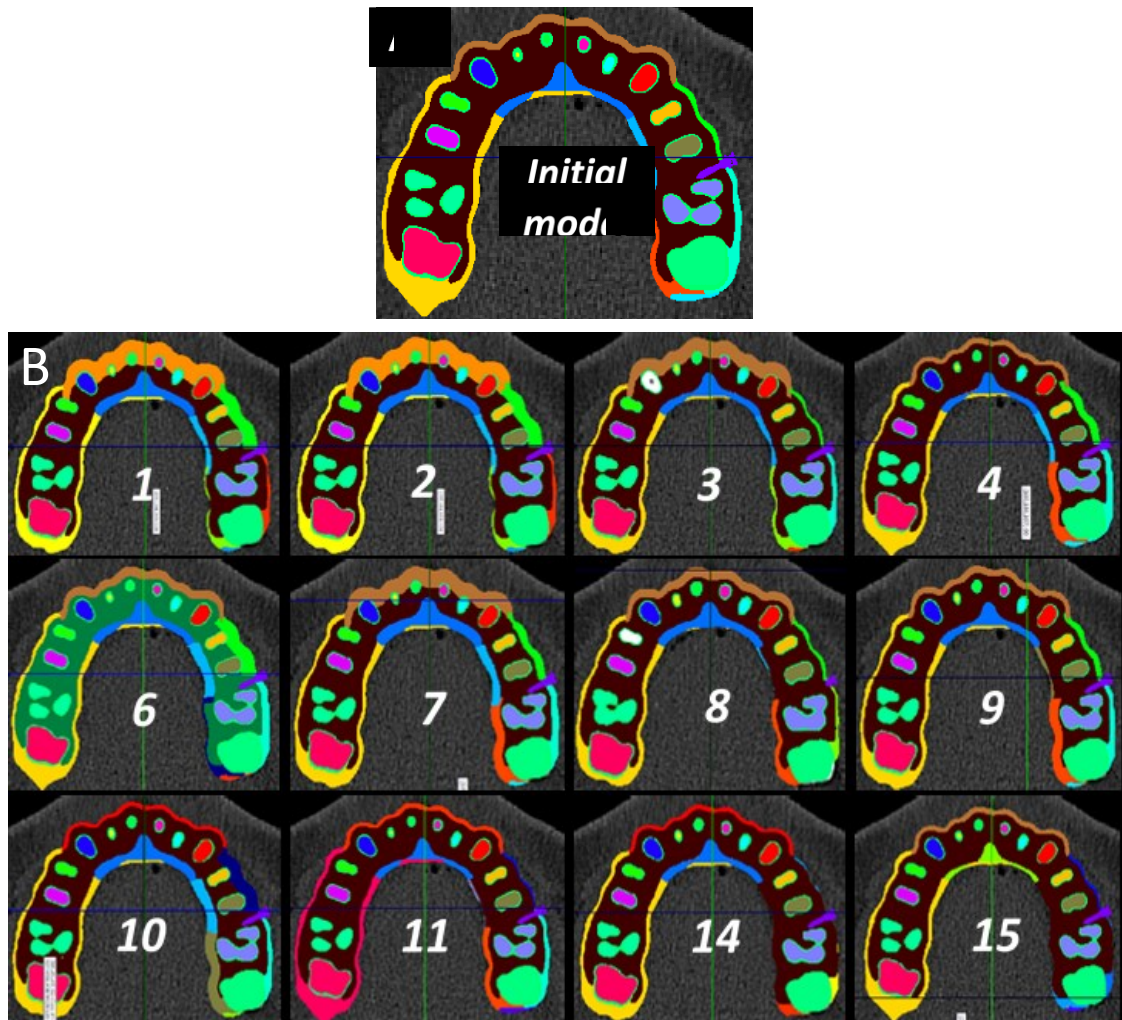


Fig. 3.23: A- TAD level axial cut of the original template model; B- Similar cuts individualized models corresponding to 12 cadavers with modified cortical bone thickness.

3.2.2. *Finite Element Analysis (FEA)*

3.2.2.1. Mesh size / Convergence testing

FEA provides approximate results because theoretical representation is often complicated. The accuracy of the approximation can be improved by increasing the number of elements in the *meshed* model, thus causing an increase in the simulation time. However, the number of elements is not always related to the accuracy of the solution. For this reason, a convergence study was undertaken to determine the least amount of elements that provide the most accurate solution.

Convergence testing was achieved by varying the mesh size in ScanIP™ 7.0 before exporting the FE models. Accordingly, 10 identical FE models differing only in mesh coarseness (19, 25, 28, 31, 34, 36, 40, 43, 47 and 50), with tetrahedral element sizes ranging from 0.2 to 1.3 mm, were exported in “inp.” format.

In Abaqus, the same load (10 N in the Y axis of the TAD) was applied on the different FE models with same boundary conditions and interaction settings until the variation of maximum displacement measured at the level of the maxillary right second molar crown became insignificant.

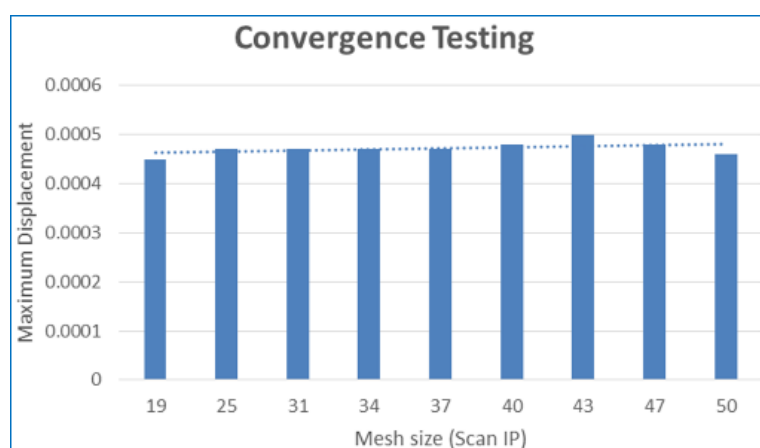


Fig. 3.24: Scatter plot showing the results of the convergence testing (total displacements at the second molar assessed in 9 models with various mesh coarseness size).

A color coded map of displacement helped in determining the location of the maximum displacement: light green color indicated a higher displacement range. Afterwards, the maximum nodal displacement at the crown of the right second molar was recorded and later plotted against the mesh size. In the results, no significant variations existed between the different meshes. This result indicated that similar accuracy outcomes could be obtained in the models with element sizes of 0.2 to 1.3 mm (Fig. 3.24 and Fig. 3.25). Consequently, we were able to choose a mesh size of 0.604 mm (corresponding to coarseness level 36), avoiding large size models that increase the simulation time, without compromising on the accuracy of the results.

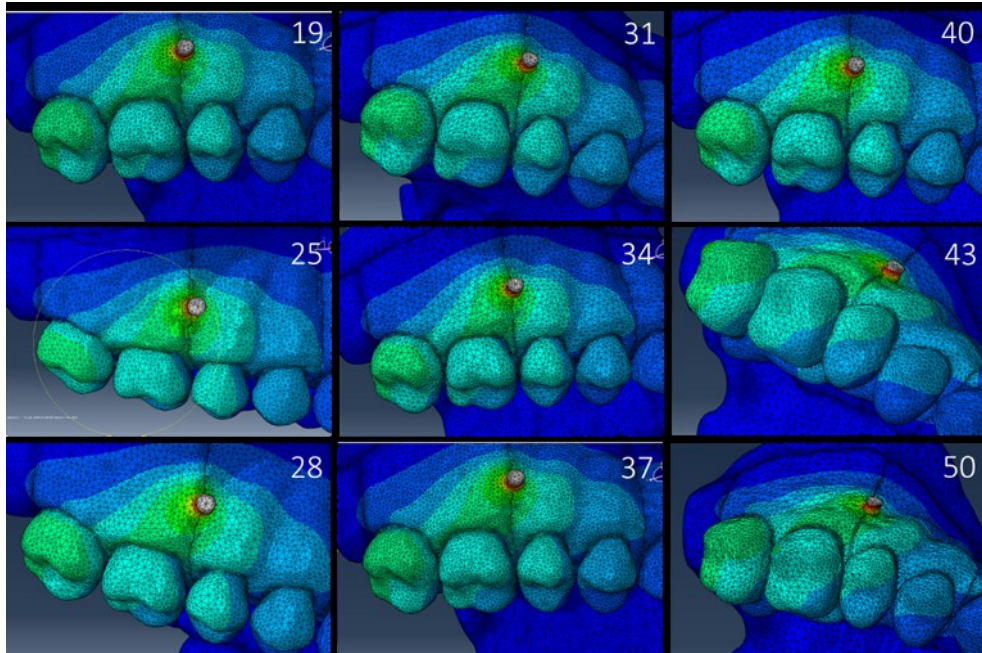


Fig. 3.25: Color coded visualization results of the convergence testing. (Total displacements in 9 models with various mesh coarseness size were assessed).

After defining contact pairs between the connected parts of the models in the configuration settings menu, 13 models (one template model on which stiffness was varied and twelve models with thickness variation) were exported from ScanIP as inp. file format. The template model comprised a total of 1136097 tetrahedral elements (Fig 3.26).

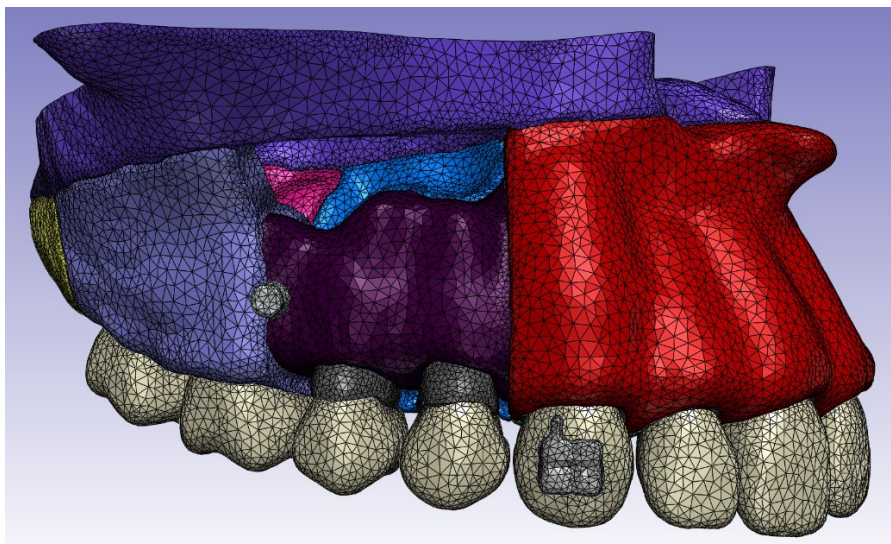


Fig. 3.26: Meshed template model.

3.2.2.2. Definition of material properties

FEA results are only as good as the initial data used to set the parameters of tissue response (Middleton et al. 1996). Therefore, Strait et al. (2005) suggested that modelers should attempt to obtain specific elastic properties data about the species and skeletal elements that are the subjects of their analyses.

Assumptions on all those elements are made on the basis of scientific computations commonly used in FEA applications in orthodontics. Material properties (Young's Modulus of Elasticity and Poisson's ratios) of trabecular bone, teeth, brackets and miniscrew were defined from available data in the literature (Table 3.3). The material property of the PDL was assigned based on the work of Kojima and Fukui (2012). Except for the cortical bone, all materials used in this study were homogeneous, isotropic, and linearly elastic (Field et al., 2009; Lim et al., 2003; Tanne et al., 1987).

Table 3.3: Material properties of various anatomical components commonly used in orthodontic Finite Element Analysis studies*

	Young's modulus (MPa)	Poisson's ratio
Teeth	20 000	0.3
Periodontal ligament (PDL)	0.68	0.45
Trabecular bone	1500	0.33
Cortical bone	Variable	0.33
Brackets and Miniscrew	200 000	0.3

*Field et al., 2009; Kojima et al., 2012; Lim et al., 2003; Tanne et al., 1987

Cortical bone stiffness was modified according to Peterson et al. (2006) to replicate bone qualities found in real patients. Individual material properties provided at the maxillary sites 1, 3, 4, 5, 6, 7 and 8 (locations of interest directly related to our mechanical model) were incorporated into the template FE model. For stiffness variation, unlike other elements of the model, the cortical bone parts were assigned orthotropic material properties providing more detailed information about its behavior

under different loads. In material science and solid mechanics, material properties of an orthotropic material differ when measured from different directions.

Therefore, engineering constants (defined in section 3.1.2.) of Young's modulus of elasticity: E_1 , E_2 , E_3 , Shear Modulus of elasticity G_{12} , G_{31} , G_{32} and Poisson's ratio ν_{12} , ν_{13} , ν_{23} were all incorporated into each cortical bone part (Table 3.4).

Table 3.4: Orthotropic material properties at the site of "buccal cortical bone at incisors area (5)" in the 15 cadavers

	Site 5 (buccal incisors)								
	E1	E2	E3	ν_{12}	ν_{13}	ν_{32}	G12	G31	G23
Patient 1	17140	16918	21567	0.327	0.368	0.123	6603	6889	7175
Patient 2	6762	9888	12219	0.261	0.277	0.489	2879	2667	2455
Patient 3	11380	10731	16861	0.397	0.2	0.357	3990	5426	6862
Patient 4	8343	10246	14033	0.477	0.413	0.116	3229	3701	4173
Patient 6	10825	10006	13323	0.52	0.307	0.264	3453	4626	5799
Patient 7	17129	17209	21765	0.341	0.385	0.365	6411	6594	6777
Patient 9	9188	9143	11113	0.445	0.454	0.227	3198	3443	3688
Patient 10	8301	9263	12943	0.485	0.467	0.066	3098	3490	3882
Patient 11	8993	10380	16675	0.493	0.366	0.176	3292	4141	4990
Patient 14	7129	9636	10967	0.237	0.175	0.424	3114	3362	3610
Patient 15	8550	9582	10798	0.307	0.22	0.343	3395	3792	4189

E1 - E2 - E3: Components of normal stiffness; ν_{12} - ν_{13} - ν_{32} : Poisson's ratio; G12- G31 - G50: Shear stiffness

Sicher and Dubrul (1970) hypothesized that the direction of maximum stiffness was parallel to the long axis of the three pillars of the maxilla and perpendicular to the fronto-maxillary suture. Peterson et al. (2006) confirmed this theory and found that in the 15 maxillary cortical bone areas studied, 7 areas (4 of which included in our model) have a distinct vertical direction of maximum stiffness (section 3.1.2.).

To define the three directions 1, 2 and 3, two user axis systems were constructed in Abaqus, one for the posterior cortical bone parts (sites 3,4,6,7 and 8) and one for the anterior cortical bone parts (sites 1 and 5), (Fig. 3.27).

To rule out the effect of stiffness, the same isotropic material properties were assigned to all cortical bone parts when thickness was varied.

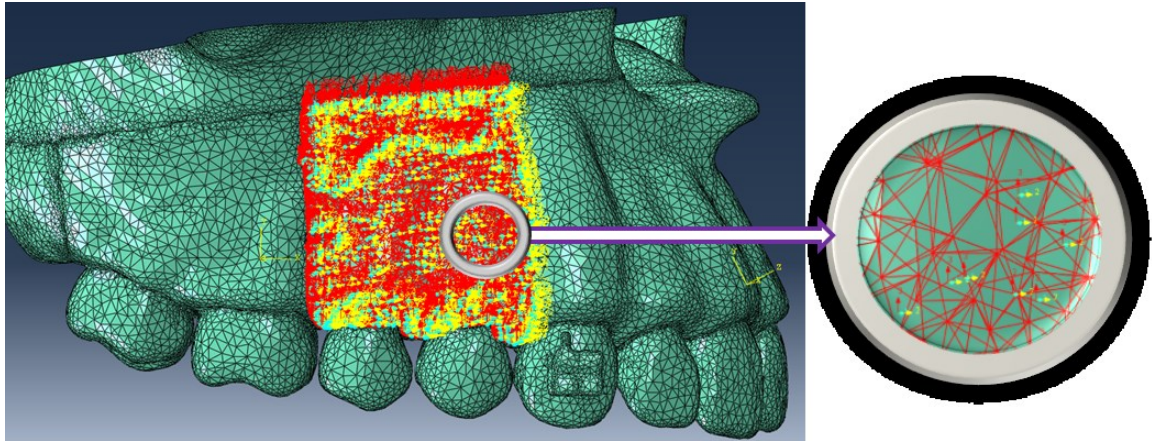


Fig. 3.27: Orthotropic material properties assigned to the buccal premolar area. Each element stiffness is defined in the 3 dimensions. 3: Parallel to the long axis of the three-pillars of the maxilla; 2: within the plane of the cortical plate; 1: through the thickness of the cortical plate.

3.2.2.3. Interactions

The majority of FEA studies applied in orthodontics studied vertical (intrusion) and transverse (expansion) movements of teeth or investigated movements into edentulous areas in the maxilla and mandible (such as canine retraction, incisors retraction and molar protraction into extraction spaces). Unlike distalization, these movements do not require the definition of interaction settings to aid in transmitting the load between adjacent teeth, thus the insufficient literature about this topic.

To accurately represent the transmission of load through the contact point surface, our method involved the following: ScanIP was used to separate the teeth (manually using the *unpaint tool*) by a “dental floss” distance equal to 0.2 to 0.4 mm (1 to 2 pixels). Afterwards, ellipsoid shaped mesial and distal surfaces of each tooth were created using the 3D edit tool of the same software and then exported as surfaces in the inp. format file (Fig. 3.28).

In Abaqus, the exported surfaces act as a separate part from the teeth allowing for “surface to surface” interactions to be defined between the adjacent surfaces. However, in Abaqus the “surface to surface interaction” works only for surfaces in

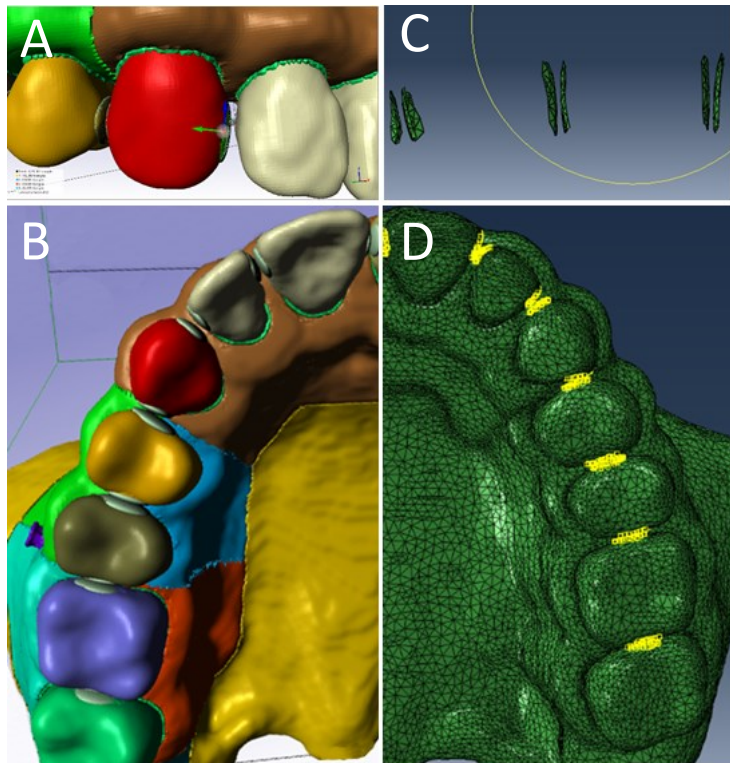


Fig. 3.28: Steps to define surface to surface interaction
A- Creation/positioning of ellipsoid shaped surface at the mesial of the 13 using the 3D edit; **B-** Ellipsoid shaped surfaces between the teeth (in white); **C-** Individual surfaces as viewed in Abaqus; **D-** “Surface to surface” interactions (in yellow) defined between the adjacent surfaces.

contact with each other. To obtain load transmission through the teeth, adjustments to increase the sensibility of the interactions was needed. Thus, we modified the tolerance of each surface to surface interaction to 0.4 to allow communication of nodes at a distance up to 0.4 mm (to account for the maximum distance separating the teeth which is equal to 0.3 mm), (Fig. 3.29).

To validate the use of this interaction setting, we compared a model with “surface to surface interaction” defined between the canine and first premolar only with an identical model in which 5 springs with a total stiffness value equal to 20000 MPa (equal to the stiffness of the teeth) connected the same adjacent surfaces. This set up mimicked dental anatomy whereby the contact area is formed of dental structure. In both models, same boundary conditions and load (of 150 grams applied on the canine) were used. No significant differences were seen in the Von Mises stresses and displacements (U) between the two interaction modalities. The color mapped images

showed similar stress distribution along the teeth and the periodontal ligaments, yet with small differences in the ranges of stress and displacement magnitudes (Fig. 3.30).

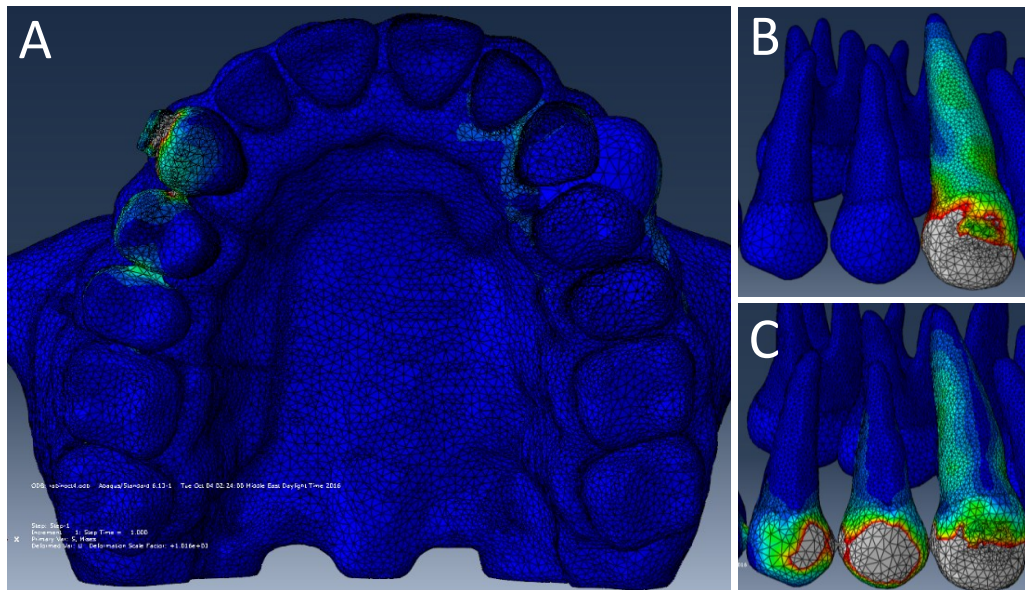


Fig. 3.29: Tolerance testing: Same force applied on both canines. Interaction sensibility increased (tolerance = 0. 4) on the right side only. **A-** Occlusal view of the model; **B-** Lateral view of the left canine and premolars; **C-** Lateral view of the right canine and premolars. Stresses were recorded on the premolars on the right side only.

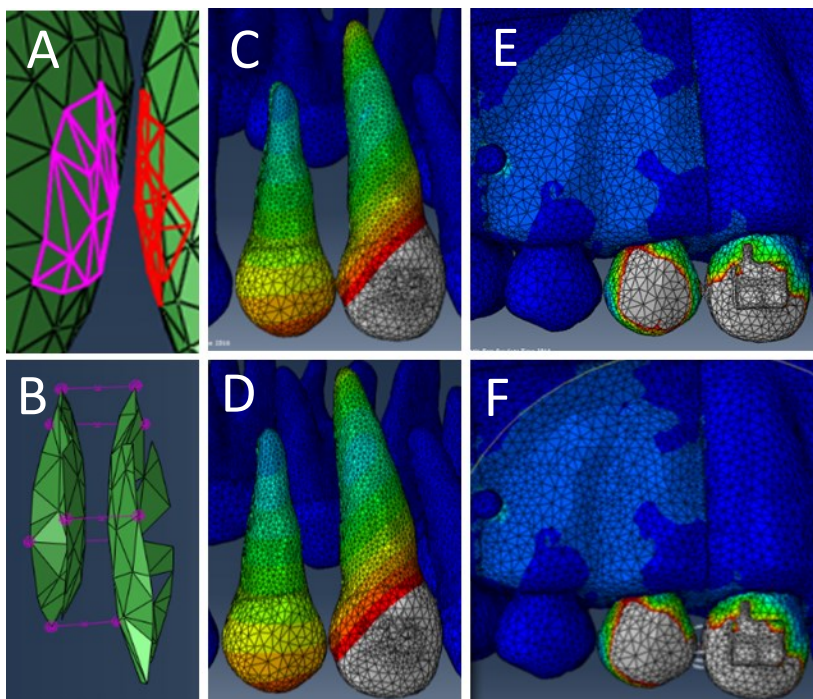


Fig. 3.30: Results of the interaction validation test. Springs (*upper row*) vs surface to surface (*lower row*) interactions placed between the canine and first premolar; **A-B** Zoomed in picture of the two interactions used; **C-D** Color mapped representation of nodal displacements; **E-F** Color mapped representation of Von Mises stresses.

3.2.2.4. Loading scenario

For simplification purposes, the initial and loading conditions used do not accurately represent all the elements encountered in actual orthodontic treatment (e.g. not accounting for friction between bracket and archwire, or representing the canine as rigid in place in the indirect modality when in reality it could move mesially).

Nevertheless, the experiments reflect basic mechanotherapy planning that mirrors the basic tenets of the clinical situation.

- Load

Two prototype models representing the two distalization modalities were generated.

- Prototype 1 (Fig. 3.31) represents the direct anchorage modality.

The miniscrew was inserted in the interradicular bone between the second premolar and the first molar at an angle of 30° (Deguchi et al., 2006) relative to the surface of the cortical bone with the neck/thread interface coincident with the external contour of the cortical bone. An optimal orthodontic force of 150 grams (1.47 Newton) was simulated and directed from the miniscrew to the canine bracket.



Fig. 3.31: Clinical picture showing the direct anchorage modality.

In Abaqus, a concentrated mechanical force was created on the bracket nodes set, comprised of around 1100 nodes, and placed at the right canine crown. The applied

force (150 grams =1.47 Newton) was divided equally on all the nodes of the bracket set.

A datum axis system was constructed using 3 points: the origin of the axis system located at the center of the miniscrew head, a second point located at the center of the bracket helped define the X axis, and a third point was placed perpendicular to the X axis. The direction of the direct loading force followed the X axis with no components in the Y and Z axes (Fig. 3.32).

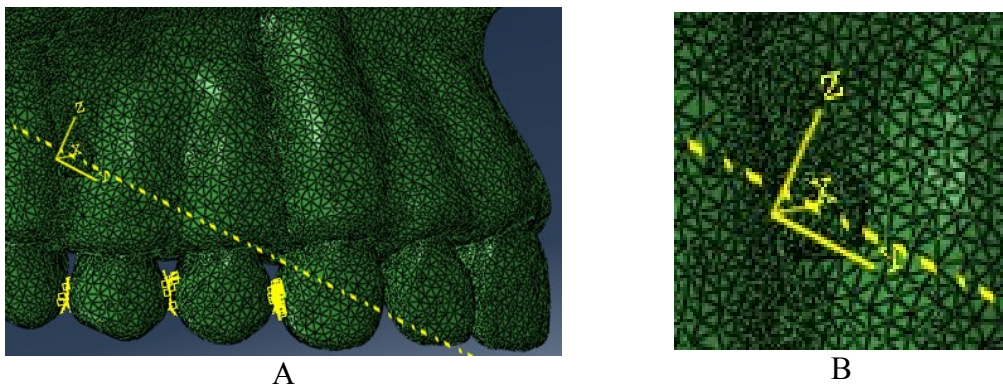


Fig. 3.32: A- Datum axis system used to define the direct load direction. B- Detail of the coordinate system.

- Prototype 2 (Fig 3.33) represent the indirect anchorage modality.

A NiTi open coil spring placed between the second premolar and first molar of a length equal to 1.5 times the distance between these teeth delivered two forces of equal magnitude (150 grams each) but in opposite directions. The miniscrew, placed in the

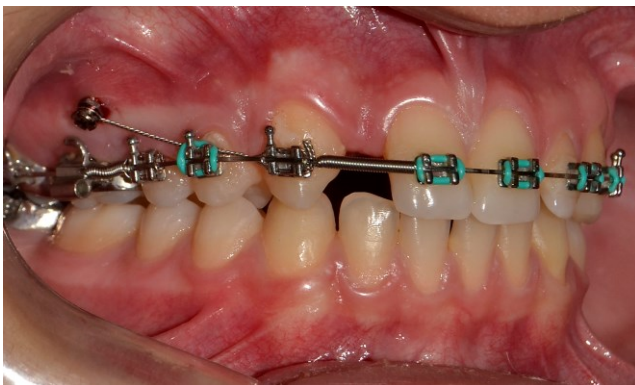


Fig. 3.33: Clinical picture showing the indirect anchorage modality.

same position as in the direct modality, held the maxillary canine in place, negating the unwanted mesial force generated by the open coil.

The opposite forces were equally divided among 10 nodes located at the center of the second premolar and first molar crowns. The direction of the forces followed a datum axis system constructed to have the Y axis follow the long axis of each tooth. These forces have only one component in the X axis which is parallel to the archwire.

- Boundary conditions

Most FEA studies have considered a small part of the maxilla surrounding the area studied. It has been common in these studies to consider the upper and posterior regions of the maxilla fully restrained. This assumption is convincing because the upper and posterior parts of the maxillary bone are fused to the cranial base bones (frontal, ethmoid, sphenoid, malar and nasal bones) and therefore are clamped in all directions (Figs. 3.35, 3.36).

Boundary conditions helped simulate the action of the brackets and archwire. To simulate the movement of the teeth along the archwire, an axis system following the long axis of every tooth was created in Abaqus; 15 to 20 nodes located at the level of the bracket position were assigned a boundary condition that allowed the following movements only (Fig. 3.34):

- Mesio-distal translation movement along the X axis of every tooth (parallel to the archwire).
- Mesio-distal and bucco-lingual tipping around the Z and X axes respectively.
- Rotation around the long axis (Y axis) of each tooth.

In the indirect anchorage modality, the action of the ligature wire connecting the miniscrew to the canine bracket was simulated by placing a pinned

boundary condition on the canine bracket. Pinned supports allow rotation and prevent from normal or tangential translations (Fig. 3.36). Friction and slipping on the archwire were not considered for simplification.

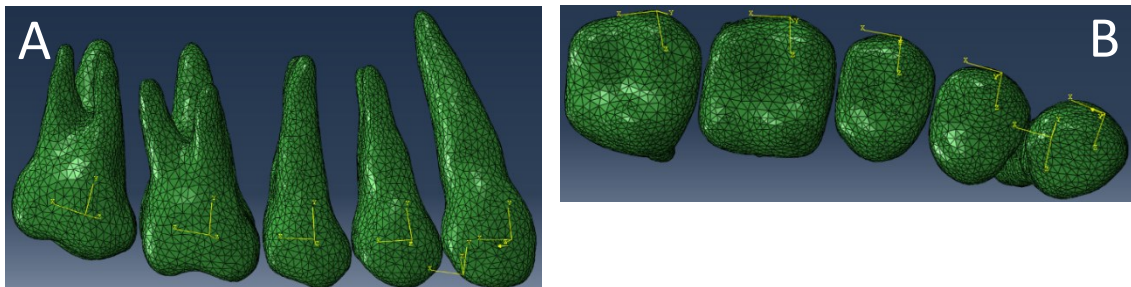


Fig. 3.34: Datum axes systems constructed parallel to the long axis of each tooth, were used to define the direction of the indirect loading and to define boundary condition that mimic the presence of the archwire (See next section). **A-** Lateral view **B-** Occlusal view.

3.2.2.5. Data collection and export

- Measures

FEA can be used to calculate deflection, stress, strains, vibration, displacement, energy storage and many other phenomena. Stress evaluation at the PDL, followed by displacement of the crowns, are the most commonly evaluated measures in dental FEA studies. In orthodontics, stress distribution produced by forces between the periodontal ligament and the bone indicate the location where tooth movement occurs. Therefore, stress at the PDL is assumed to be in proportion to the bone-remodeling rate (Kojima et al., 2012). It also infers about the areas that are more prone to root resorption.

Von Mises stress, evaluated at an element, is a measure of the elasticity of a material, and represents the point at which the elastic limit is exceeded and permanent deformation results. Total displacement includes the sum of the initial translation movements of a node in the X, Y, and Z axes in addition to the rotation movements around the same axes systems.

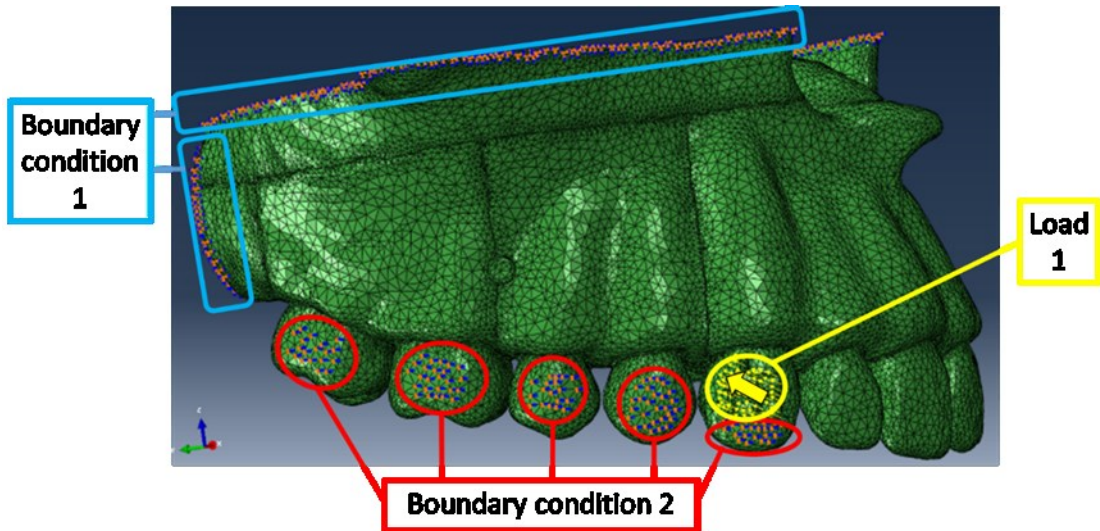


Fig. 3.35: Loading scenario of the direct anchorage modality. **Boundary condition 1:** ENCASTER ($U_1=U_2=U_3=UR_1=UR_2=UR_3=0$) to fully restrain the upper and posterior parts of the maxilla; **Boundary condition 2:** XASYMM ($U_2=U_3=UR_1=0$) simulating the action of the bracket and archwire; **Load 1:** Direct load.

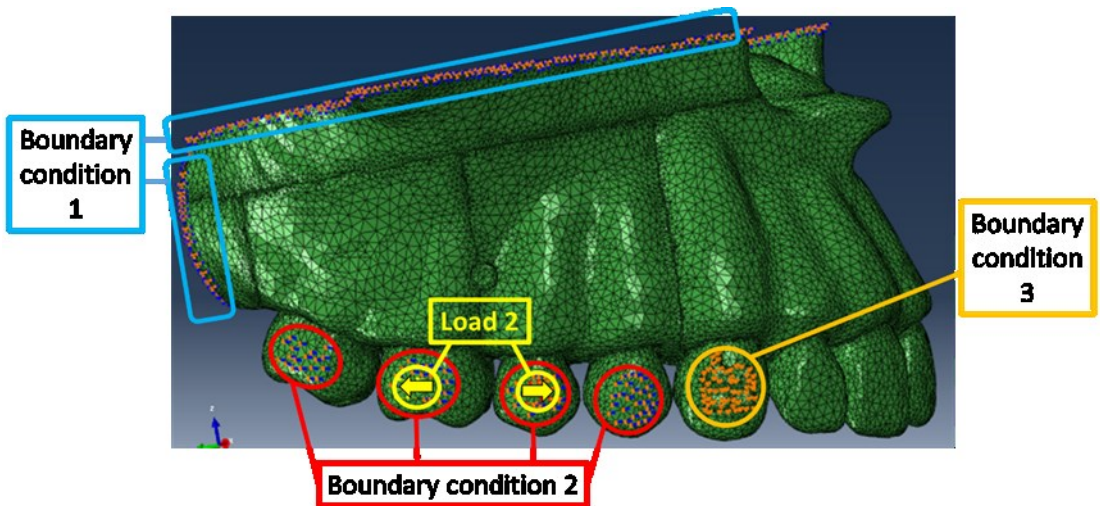


Fig. 3.36: Loading scenario of the indirect anchorage modality. **Boundary condition 1:** ENCASTER ($U_1=U_2=U_3=UR_1=UR_2=UR_3=0$) to fully restrain the upper and posterior parts of the maxilla; **Boundary condition 2:** XASYMM ($U_2=U_3=UR_1=0$) simulating the action of the bracket and archwire; **Boundary condition 3:** PINNED ($U_1=U_2=U_3=0$) to hold the canine in place; **Load 2:** Indirect load.

- Sets

FEA results are usually interpreted by means of color mapped representations and arrows. However, to be able to show individual variations, statistical analysis applied on numerical data is required. Abaqus offers the possibility to collect numerical stresses, displacement and other phenomena at each node or element.

For stress data collection, a set containing randomly selected elements uniformly dispersed along each surface of the periodontal ligament was created. A total of 38 sets, each containing between 70 to 250 elements (depending on area size) was created. The buccal segment teeth (canine, first and second premolars, first and second molars) were represented by a minimum of 4 sets corresponding to the mesial, distal, buccal and palatal areas. Furthermore, to assess the stress distribution along the PDL area, the mesial and distal areas of the PDL of the canine, second premolar and first molar were divided into a cervical, middle and apical areas (Fig. 3.37).

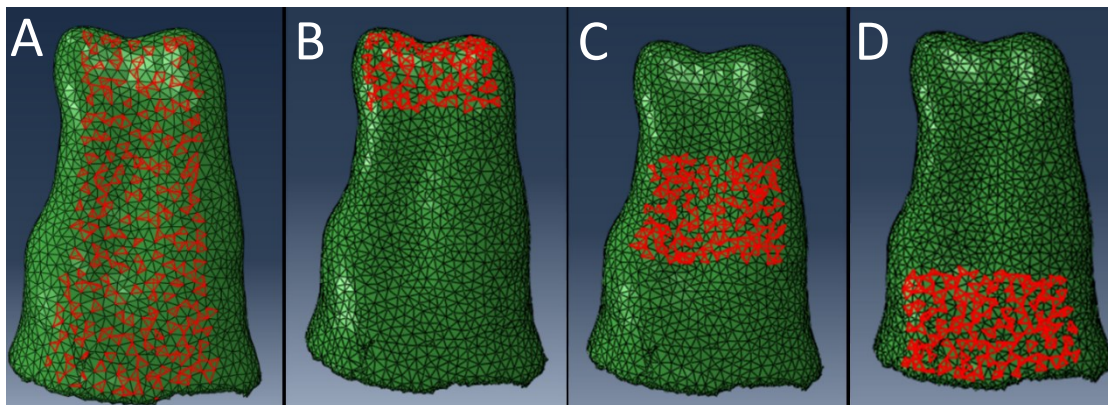


Fig. 3.37: Selection of element sets. **A-** Distal of second premolar (D5); **B-** Apical area of the distal second premolar (D5a); **C-** Middle area of the distal second premolar (D5m); **D-** Cervical area of the distal second premolar (D5c).

As a result, these teeth were represented by 10 sets each. The sets were named as per the following scheme:

Modality/Stiffness or thickness/Tooth surface/Tooth/Root level (Fig. 3.38).

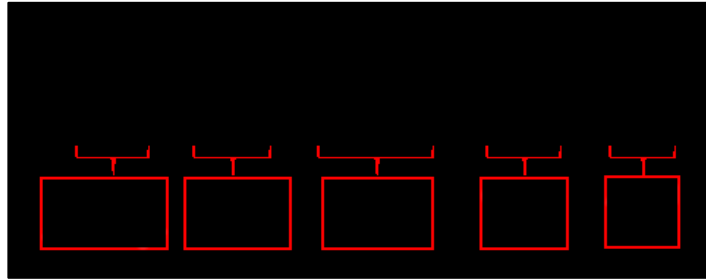


Fig. 3.38: Representative example of labeling of various variables.

Similarly, 9 to 17 nodes (depending on the tooth) were selected at the centroid of the crown of the right canine, premolars and molars. The resulting 5 sets were used to measure the initial displacement. The centroid of each crown was used not to account for the rotation movement that may occur (Fig. 3.39).

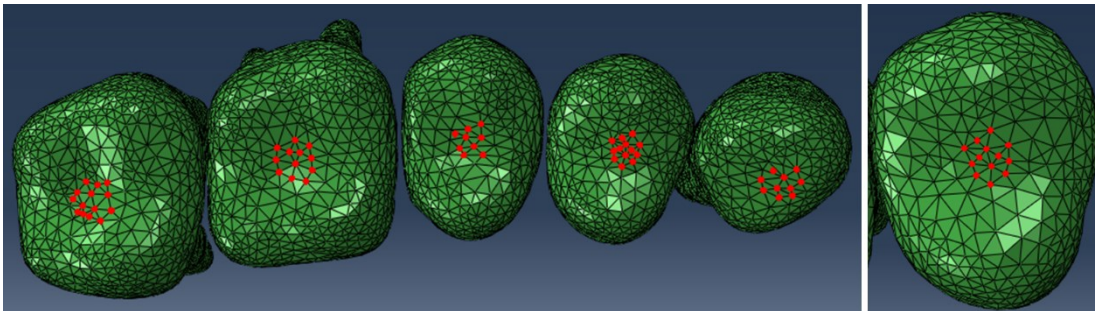


Fig. 3.39: Selection of node sets representing the centroid of each tooth.

After running the finite element analysis, the stress and displacement results were exported as DAT. files into excel where the averages were calculated. Finally, the averages were put in final data sheets.

Four data sheets corresponding to the 4 parts of the study were obtained:

- Part 1: Stiffness variation applied to direct anchorage modality
- Part 2: Stiffness variation applied to indirect anchorage modality

- Part 3: Thickness variation applied to direct anchorage modality
- Part 4: Thickness variation applied to indirect anchorage modality

Stress and displacement data were repeated for the first two cadavers to evaluate intraexaminer reliability.

3.2.3. *Statistical analysis*

Descriptive statistics were generated for the subsamples of both stiffness and thickness variation. Analysis of variance (ANOVA) was used to compare the stresses between the different teeth at all surfaces. All tests were followed by Bonferroni post-hoc analyses for multiple comparisons. Homogeneity of variances was tested for each set of comparisons, and when violated, Welch's robust ANOVA and Games-Howell post hoc tests were reported instead.

The two-tailed paired t-test were performed to compare stresses at the different surfaces obtained in the direct and indirect anchorage modalities. In addition, orthotropic stiffness components (S1, S2 and S3) were compared to the isotropic stiffness commonly used in the literature, and stresses at the PDL (of all teeth) were compared for the two bone material types (orthotropic and isotropic).

The Pearson product moment correlation coefficient (and its equivalent non-parametric Spearman correlation coefficient) was performed to test correlations between the stresses at the mesial, distal, buccal and palatal parts of the periodontal ligament of each tooth with the thickness and stiffness components (S1, S2, S3) of the corresponding palatal and buccal cortical bone areas. The same methods were performed between the stresses at each of the apical, middle and cervical parts of the mesial and the distal surfaces of the canine and first molar. Associations were evaluated

between the average bone stiffness (of S1, S2 and S3) computed for each patient at each area, and the stresses at the first molar and canine. Correlations were also explored between stress amounts resulting from stiffness variation and the stresses resulting from thickness variation. Finally, displacements (in every direction and total) at each tooth were tested for correlation with the stress recorded at the mesial surface.

Bivariate and multivariate regression analyses were used to model the stress response at the mesial and distal PDL of the canine and first molar from the stiffness coefficients and thickness of the corresponding palatal and buccal cortical bone areas. All covariates associated with the outcomes that have a p-value < 0.2 at the bivariate level were included in the multivariate analyses. For all variables included in the final multivariate models, regression coefficients, standard errors, p-values and 95% confidence intervals (CI) were reported. Statistical significance was set at 0.05. The IBM® SPSS statistical software was used to carry out all the statistical analyses.

CHAPTER 4

RESULTS

No differences were noted between the repeated stress and displacement data, indicating intraexaminer reliability.

4.1. Stress comparison between the teeth

Since repeated analyses were done to compare the teeth (3 vs 4 vs 5 vs 6 vs 7), adjustment for the level of significance (α) was required. For each of the two outcomes (1) stress-stiffness variation and (2) stress-thickness variation 8 tests were performed (direct and indirect for each of mesial, distal, palatal and buccal); therefore the adjusted α value was set at $0.05/8 = 0.00625$.

4.1.1. Part 1: Stiffness variation / Direct anchorage modality

In the stiffness variation applied to direct anchorage modality, the Levene's test results were statistically significant for the stress amounts at the distal (SD) and palatal (SP) surfaces, and non-significant for the stresses at the mesial (SM) and buccal (SB) surfaces, (Table 4.1). Therefore, the Welch ANOVA and Games-Howell tests were used for SD and SP and the ANOVA and Bonferroni tests were used for SM and SB.

All stresses were statistically significantly different between adjacent teeth and decreasing in magnitude from the canine (3) to the second molar (7), (Table 4.2). The only exception to this pattern were the palatal and buccal surfaces between the second premolar (5) and the first molar (6), (Table 4.3; Fig 4.1).

**Table 4.1: Descriptive statistics for the stress generated on the 4 surfaces of the buccal teeth (n=11)
(Stiffness variation/Direct anchorage)**

statistics	SD		SP		SM		SB	
	Mean	StD	Mean	StD	Mean	StD	Mean	StD
Canine	0.351	0.002	0.317	0.002	0.318	0.002	0.337	0.002
First Premolar	0.271	0.002	0.304	0.002	0.300	0.002	0.242	0.002
Second Premolar	0.173	0.002	0.173	0.003	0.184	0.003	0.177	0.002
First Molar	0.159	0.003	0.177	0.004	0.201	0.003	0.178	0.003
Second Molar	0.152	0.004	0.168	0.004	0.160	0.004	0.139	0.003
Total	0.221	0.079	0.228	0.068	0.233	0.065	0.215	0.070

Stresses in kPa; **StD**: Standard deviation; **SD**: Stress at distal surface; **SP**: Stress at palatal surface; **SM**: Stress at mesial surface; **SB**: Stress at buccal surface

**Table 4.2: Comparison of stress among the 5 teeth at each surface
(Stiffness/Direct anchorage)**

	3	4	5	6	7	p-value
SD [†]	0.351	0.271	0.173	0.159	0.152	<0.001*
SP [†]	0.317	0.304	0.173	0.177	0.168	<0.001*
SM	0.318	0.300	0.184	0.201	0.160	<0.001*
SB	0.337	0.242	0.177	0.178	0.139	<0.001*

[†]Results obtained with Welch ANOVA

[†]Welch's ANOVA and Games-Howell post hoc *p* values reported because assumption of homogeneity of variances was violated; *Significant at *p* <0.01

SD: Stress at distal surface; **SP**: Stress at palatal surface;

SM: Stress at mesial surface; **SB**: Stress at buccal surface.

3: canine; 4, 5: first, second premolars; 6, 7: first, second molars.

Table 4.3: Pairwise comparisons for stress between the teeth at each surface (n=11)

	3-4	3-5	3-6	3-7	4-5	4-6	4-7	5-6	5-7	6-7
SD [†]	<0.001*	<0.001*	<0.001*	<0.001*	<0.001*	<0.001*	<0.001*	<0.001*	<0.001*	0.002*
SP [†]	<0.001*	<0.001*	<0.001*	<0.001*	<0.001*	<0.001*	<0.001*	0.065	0.042	<0.001*
SM	<0.001*	<0.001*	<0.001*	<0.001*	<0.001*	<0.001*	<0.001*	<0.001*	<0.001*	<0.001*
SB	<0.001*	<0.001*	<0.001*	<0.001*	<0.001*	<0.001*	<0.001*	1	<0.001*	<0.001*

[†] Games-Howell post hoc *p* values reported when assumption of homogeneity of variance violated.

*Significant at *p* <0.001. 3: canine; 4, 5: first, second premolars; 6, 7: first, second molars.

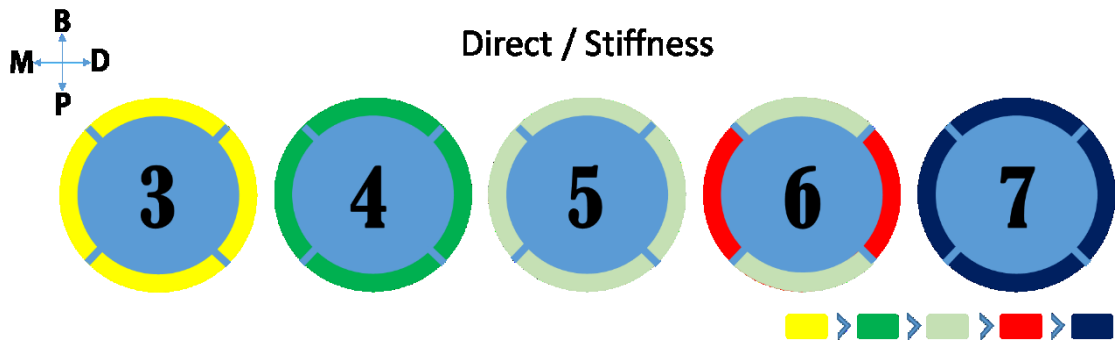


Fig. 4.1: Graphic representation of the buccal teeth response to direct anchorage modality/stiffness variation. Note the similar stresses on the buccal and palatal surfaces of the second premolar (5) and first molar (6). *B: buccal, P: palatal, M: mesial, D: distal surfaces of teeth. Yellow indicates higher severity, dark blue lower severity as per used FEA scale.*

4.1.2. Part 2: Stiffness variation / Indirect anchorage modality

In the stiffness variation applied to the indirect anchorage modality (Part 2), the Levene’s test results were statistically significant for all stress measurements. Therefore, the Welch ANOVA and Games-Howell post hoc tests were used for group comparisons.

Table 4.4: Descriptive statistics for the stress generated on the 4 surfaces of the buccal teeth (n=11) (Stiffness variation/Indirect anchorage)

statistics	N	SD		SP		SM		SB	
		Mean	StD	Mean	StD	Mean	StD	Mean	StD
Canine	11	0.035	0.001	0.059	0.000	0.050	0.000	0.022	0.001
First Premolar	11	0.138	0.001	0.155	0.001	0.163	0.001	0.141	0.002
Second Premolar	11	0.274	0.003	0.205	0.003	0.277	0.002	0.319	0.002
First Molar	11	0.457	0.010	0.442	0.013	0.580	0.014	0.559	0.012
Second Molar	11	0.461	0.014	0.518	0.014	0.472	0.013	0.396	0.013
Total	55	0.273	0.172	0.276	0.177	0.308	0.197	0.287	0.191

Stresses in kPa; **StD**: Standard deviation; **SD**: Stress at distal surface; **SP**: Stress at palatal surface; **SM**: Stress at mesial surface; **SB**: Stress at buccal surface.

All stresses were statistically significantly different when comparing each tooth to its adjacent, decreasing in magnitude from the second molar (7) to the canine (3) for palatal (SP) and distal (SD) surfaces. For the buccal (SB) and mesial (SM) surfaces, stress amounts were highest on the first molar and diminished in magnitude

toward the canine (Table 4.5). The only exception to this pattern were the distal surfaces between the first and second molars (6-7), (Table 4.6; Fig. 4.2).

Table 4.5: Comparison of stress among the 5 teeth at each surface (Stiffness/Indirect anchorage)

	3	4	5	6	7	p-value
SD [†]	0.035	0.138	0.274	0.457	0.461	<0.001*
SP [†]	0.059	0.155	0.205	0.442	0.518	<0.001*
SM [‡]	0.050	0.163	0.277	0.580	0.472	<0.001*
SB [‡]	0.022	0.141	0.319	0.559	0.396	<0.001*

[†]Results obtained with Welch ANOVA

[†]Welch's ANOVA and Games-Howell post hoc *p* values reported because assumption of homogeneity of variances was violated; *Significant at *p* <0.01

SD: Stress at distal surface; **SP**: Stress at palatal surface;

SM: Stress at mesial surface; **SB**: Stress at buccal surface.

3: canine; 4, 5: first, second premolars; 6, 7: first, second molars.

Table 4.6: Pairwise comparisons for stress between the teeth at each surface (n=11)

	3-4	3-5	3-6	3-7	4-5	4-6	4-7	5-6	5-7	6-7
SD [‡]	<0.001*	<0.001*	<0.001*	<0.001*	<0.001*	<0.001*	<0.001*	<0.001*	<0.001*	0.969
SP [‡]	<0.001*	<0.001*	<0.001*	<0.001*	<0.001*	<0.001*	<0.001*	<0.001*	<0.001*	<0.001*
SM [‡]	<0.001*	<0.001*	<0.001*	<0.001*	<0.001*	<0.001*	<0.001*	<0.001*	<0.001*	<0.001*
SB [‡]	<0.001*	<0.001*	<0.001*	<0.001*	<0.001*	<0.001*	<0.001*	<0.001*	<0.001*	<0.001*

[‡] Games-Howell post hoc *p* values reported when assumption of homogeneity of variance violated.

*Significant at *p* <0.001. 3: canine; 4, 5: first, second premolars; 6, 7: first, second molars.

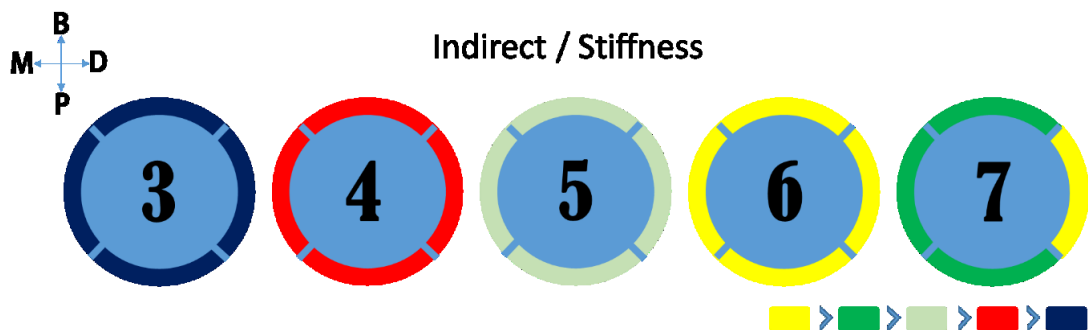


Fig. 4.2: Graphic representation of the buccal teeth response to the indirect anchorage modality/stiffness variation. Note the similar stresses between the distal of the first molar and second molar. *B*: buccal, *P*: palatal, *M*: mesial, *D*: distal surfaces of teeth. Yellow indicates higher severity, dark blue lower severity as per used FEA scale.

4.1.3. Part 3: Thickness variation / Direct anchorage modality

In the thickness variation applied to the direct anchorage modality (Part 3), the Levene's test results were not statistically significant for all stress measurements. Therefore, the ANOVA and Bonferroni post hoc tests were used for group comparisons (Table 4.7).

Table 4.7: Descriptive statistics for the stress generated on the 4 surfaces of the buccal teeth (n=13) (Thickness variation/Direct anchorage)

statistics	N	TD		TP		TM		TB	
		Mean	StD	Mean	StD	Mean	StD	Mean	StD
Canine	13	0.308	0.031	0.253	0.037	0.273	0.028	0.290	0.028
First Premolar	13	0.271	0.054	0.294	0.063	0.289	0.056	0.241	0.041
Second Premolar	13	0.171	0.023	0.180	0.025	0.191	0.029	0.181	0.025
First Molar	13	0.160	0.027	0.181	0.041	0.202	0.037	0.181	0.032
Second Molar	13	0.147	0.016	0.163	0.020	0.157	0.020	0.134	0.014
Total	65	0.212	0.073	0.214	0.064	0.222	0.062	0.205	0.061

Stresses in kPa; **StD**: Standard deviation; **TD**: Stress at distal surface; **TP**: Stress at palatal surface; **TM**: Stress at mesial surface; **TB**: Stress at buccal surface

All stresses were statistically significantly different for successive adjacent teeth, progressively decreasing in magnitude from the canine (3) to the second molar (7), (Table 4.8). Deviating from this pattern were the distal, palatal and mesial surfaces of the first premolar (4), in addition to all surfaces of the first molar (6) and the distal and palatal surfaces of the second molar (7). The stress amounts therefore stopped decreasing past the second premolar (Table 4.9; Fig. 4.3).

Table 4.8: Comparison of stress among the 5 teeth at each surface (Thickness/Direct anchorage)

	3	4	5	6	7	p-value
TD	0.308	0.271	0.171	0.160	0.147	<0.001*
TP	0.253	0.294	0.180	0.181	0.163	<0.001*
TM	0.273	0.289	0.191	0.202	0.157	<0.001*
TB	0.290	0.241	0.181	0.181	0.134	<0.001*

*Results obtained with ANOVA

TD: Stress at distal surface; **TP**: Stress at palatal surface;

TM: Stress at mesial surface; **TB**: Stress at buccal surface

3: canine; 4, 5: first, second premolars; 6, 7: first, second molars.

Table 4.9: Pairwise comparisons for stress between the teeth at each surface (n=13)

	3-4	3-5	3-6	3-7	4-5	4-6	4-7	5-6	5-7	6-7
TD	0.058	<0.001*	<0.001*	<0.001*	<0.001*	<0.001*	<0.001*	1	0.59	1
TP	0.104	<0.001*	<0.001*	<0.001*	<0.001*	<0.001*	<0.001*	1	1	1
TM	1	<0.001*	<0.001*	<0.001*	<0.001*	<0.001*	0	1	0.18	0.022*
TB	0.001*	<0.001*	<0.001*	<0.001*	<0.001*	<0.001*	<0.001*	1	0	0.001*

* Games-Howell post hoc p values reported when assumption of homogeneity of variance violated.

*Significant at p <0.001 3: canine; 4, 5: first, second premolars; 6, 7: first, second molars.

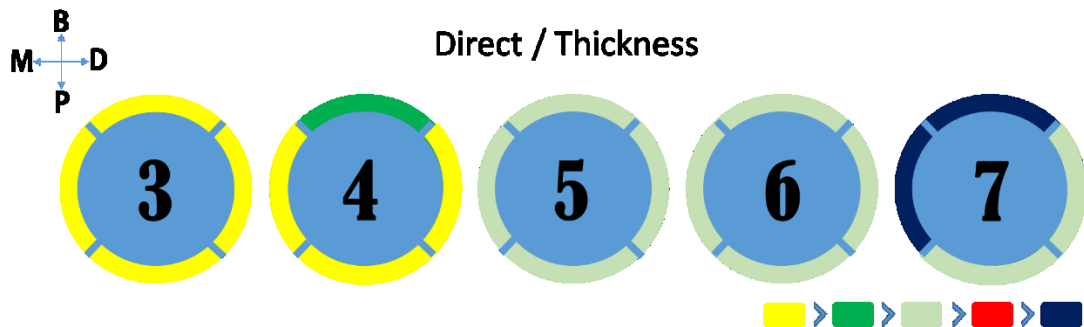


Fig. 4.3: Graphic representation of the buccal teeth response to direct anchorage modality/thickness variation. Note the similar stresses between the canine (3) and the first premolar (4) and between the second premolar (5), first molar (6) and second molar (7). *B*: buccal, *P*: palatal, *M*: mesial, *D*: distal surfaces of teeth. Yellow indicates higher severity, dark blue lower severity as per used FEA scale.

4.1.4. Part 4: Thickness variation / Indirect anchorage modality

In the thickness variation applied to the indirect anchorage modality (Part 4), the Levene’s test results were statistically significant for the stresses at the buccal surface (TB) and TP (stresses at palatal surface in the thickness variation part) and non-significant for stress amounts at the mesial (TM) and distal (TD) surfaces, (Table 4.10).

Table 4.10: Descriptive statistics for the stress generated on the 4 surfaces of the buccal teeth (n=13) (Thickness variation/Indirect anchorage)

Statistics	N	TD		TP		TM		TB	
		Mean	StD	Mean	StD	Mean	StD	Mean	StD
Canine	13	0.034	0.003	0.054	0.005	0.046	0.004	0.023	0.005
First Premolar	13	0.103	0.021	0.132	0.031	0.119	0.022	0.086	0.010
Second Premolar	13	0.200	0.021	0.125	0.017	0.225	0.017	0.289	0.022
First Molar	13	0.400	0.079	0.364	0.076	0.524	0.110	0.515	0.096
Second Molar	13	0.383	0.053	0.431	0.063	0.383	0.058	0.321	0.042
Total	65	0.224	0.154	0.221	0.156	0.259	0.184	0.247	0.184

Stresses in kPa; **StD**: Standard deviation; **TD**: Stress at distal surface; **TP**: Stress at palatal surface; **TM**: Stress at mesial surface; **TB**: Stress at buccal surface.

Therefore, the Welch ANOVA and Games-Howell post were used for TB and TP while the ANOVA and Bonferroni tests were used for TM and TD. All stress amounts were statistically significantly different across adjacent teeth, decreasing in magnitude from molars to canine (3). The first molar recorded higher stress than the second molar (Table 4.11). The palatal surface of the second premolar (5) and the distal and palatal surfaces of the second molar (7) deviated from this pattern. (Table 4.12; Fig. 4.4).

Table 4.11: Comparison of stress among the 5 teeth at each surface (Thickness/Indirect anchorage)

	3	4	5	6	7	p-value
TD	0.034	0.103	0.200	0.400	0.383	<0.001*
TP [‡]	0.054	0.132	0.125	0.364	0.431	<0.001*
TM	0.046	0.119	0.225	0.524	0.383	<0.001*
TB [‡]	0.023	0.086	0.289	0.515	0.321	<0.001*

[‡]Results obtained with Welch ANOVA

[‡]Welch's ANOVA and Games-Howell post hoc *p* values reported because assumption of homogeneity of variances was violated; *Significant at *p* <0.01

SD: Stress at distal surface; **SP**: Stress at palatal surface;

SM: Stress at mesial surface; **SB**: Stress at buccal surface.

3: canine; 4, 5: first, second premolars; 6, 7: first, second molars

Table 4.12: Pairwise comparisons for stress between the teeth at each surface (Thickness/Indirect anchorage)

	3-4	3-5	3-6	3-7	4-5	4-6	4-7	5-6	5-7	6-7
TD	<0.001*	<0.001*	<0.001*	<0.001*	<0.001*	<0.001*	<0.001*	<0.001*	<0.001*	1
TP [‡]	<0.001*	<0.001*	<0.001*	<0.001*	0.94	<0.001*	<0.001*	<0.001*	<0.001*	0.14
TM	0.02*	<0.001*	<0.001*	<0.001*	<0.001*	<0.001*	<0.001*	<0.001*	<0.001*	<0.001*
TB [‡]	<0.001*	<0.001*	<0.001*	<0.001*	<0.001*	<0.001*	<0.001*	<0.001*	0.2	<0.001*

[‡] Games-Howell post hoc *p* values reported when assumption of homogeneity of variance violated. *Significant at *p* <0.001

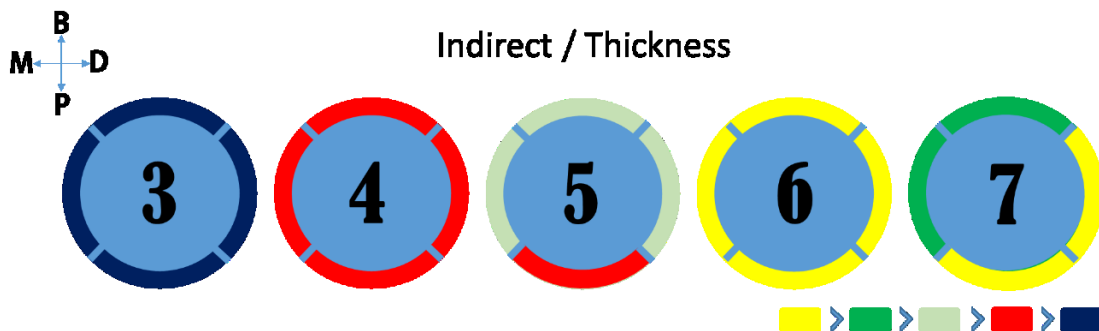


Fig. 4.4: Graphic representation of the buccal teeth response to indirect anchorage modality/thickness variation. Note the similar stresses between the palatal surface of the first (4) and second (5) premolars, and the palatal and distal surfaces between the first (6) and second molars (7). *B*: buccal, *P*: palatal, *M*: mesial, *D*: distal surfaces of teeth. Yellow indicates higher severity, dark blue lower severity as per used FEA scale.

4.2. Comparison between direct and indirect anchorage modalities

Repeated analyses were performed to compare anchorage (direct vs indirect) multiple times, prompting adjustment for the p-value. For each of the two outcomes, (1) stress-stiffness variation and (2) stress-thickness variation, 20 tests were conducted, one for each of the 4 surfaces and for each of the 5 teeth; accordingly, the critical p value was set at $0.05/20 = 0.0025$.

The results showed statistically significant differences for all pairs on all the teeth. The p-values were all below 0.001, except for the pair dTD5 – iTD5 where the p-value was equal to 0.029 (Table 4.13).

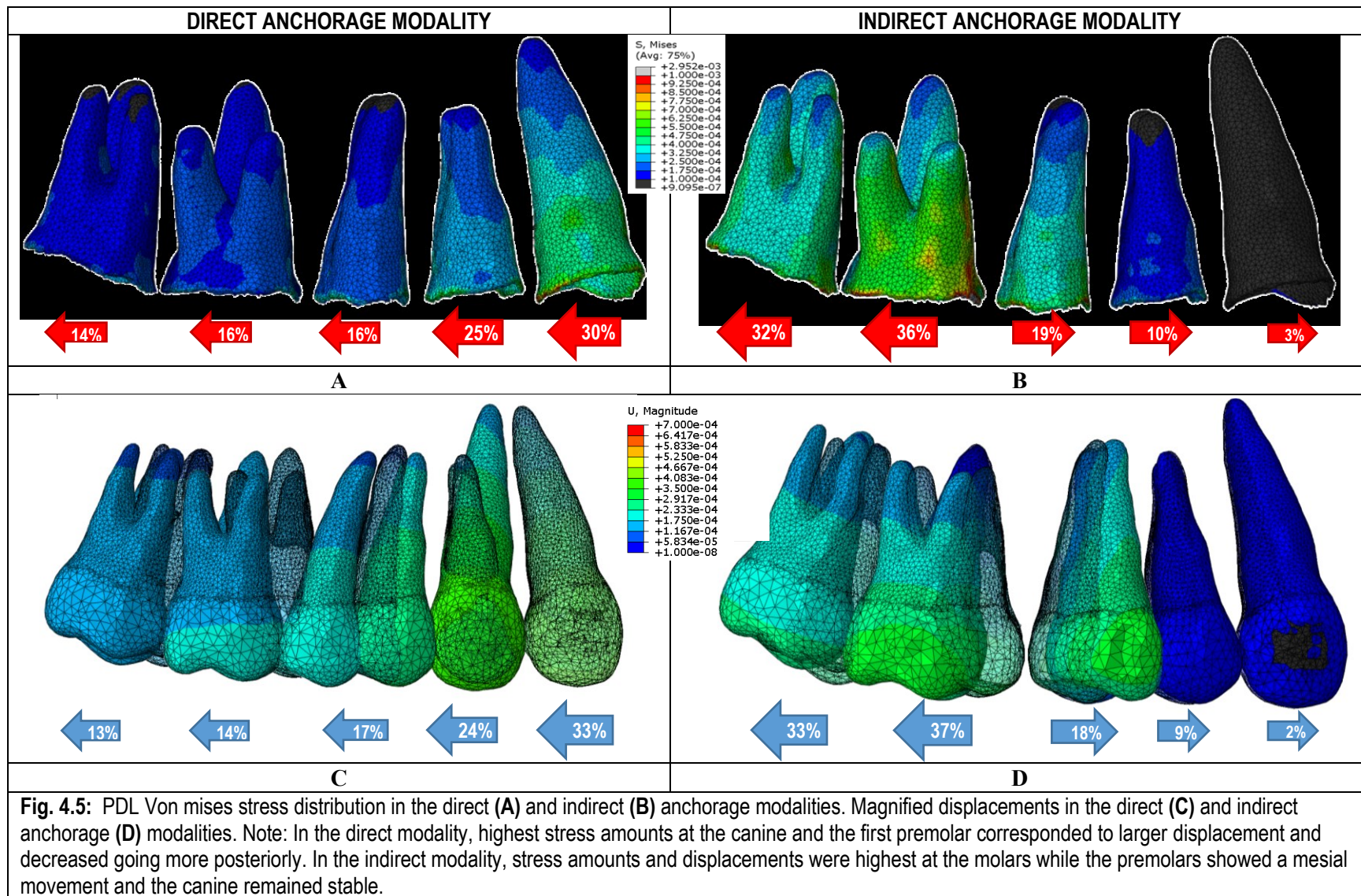
Table 4.13: Results of the paired t-tests to compare direct vs indirect anchorage modalities

Tooth		Paired Differences		Sig. (2-tailed)
		Mean	SD	
3	dSD - iSD	0.32	0.00	<0.001*
	dSP - iSP	0.26	0.00	<0.001*
	dSM - iSM	0.27	0.00	<0.001*
	dSB - iSB	0.32	0.00	<0.001*
	dTD - iTD	0.27	0.03	<0.001*
	dTP - iTP	0.20	0.04	<0.001*
	dTM - iTM	0.23	0.03	<0.001*
	dTB - iTB	0.27	0.03	<0.001*
4	dSD - iSD	0.13	0.00	<0.001*
	dSP - iSP	0.15	0.00	<0.001*
	dSM - iSM	0.14	0.00	<0.001*
	dSB - iSB	0.10	0.00	<0.001*
	dTD - iTD	0.17	0.03	<0.001*
	dTP - iTP	0.16	0.04	<0.001*
	dTM - iTM	0.17	0.04	<0.001*
	dTB - iTB	0.15	0.03	<0.001*
5	dSD - iSD	-0.10	0.00	<0.001*
	dSP - iSP	-0.03	0.00	<0.001*
	dSM - iSM	-0.09	0.00	<0.001*
	dSB - iSB	-0.14	0.00	<0.001*
	dTD - iTD	-0.03	0.04	0.029*
	dTP - iTP	0.06	0.03	<0.001*
	dTM - iTM	-0.03	0.03	0.001*
	dTB - iTB	-0.11	0.03	<0.001*
6	dSD - iSD	-0.30	0.01	<0.001*
	dSP - iSP	-0.27	0.01	<0.001*
	dSM - iSM	-0.38	0.01	<0.001*
	dSB - iSB	-0.38	0.01	<0.001*
	dTD - iTD	-0.24	0.05	<0.001*
	dTP - iTP	-0.18	0.05	<0.001*
	dTM - iTM	-0.32	0.07	<0.001*
	dTB - iTB	-0.33	0.07	<0.001*
7	dSD - iSD	-0.31	0.01	<0.001*
	dSP - iSP	-0.35	0.01	<0.001*
	dSM - iSM	-0.31	0.01	<0.001*
	dSB - iSB	-0.26	0.01	<0.001*
	dTD - iTD	-0.24	0.04	<0.001*
	dTP - iTP	-0.27	0.05	<0.001*
	dTM - iTM	-0.23	0.04	<0.001*
	dTB - iTB	-0.19	0.03	<0.001*

*Significant at $p < 0.0025$; 3: Canine; 4: First premolar; 5: Second premolar; 6: First molar; 7: Second molar.

The opposite directions of stress amounts in the direct and indirect modalities, as well as the corresponding displacements are illustrated in Fig. 4.5. PDL stress is nearly equal in percentage at the canine in the direct (30%) and molar in the indirect (36%). However, while the stress distribution in the direct modality decreases to nearly half of the amount on the canine at the level of the second premolar and molars, in the indirect modality stress values diminish progressively to nearly half at the first premolar, then almost nil at the canine (3%), which was originally set up as stationary. Displacement mirrored the progression of percentages in stress distribution in both direct and indirect modalities.

The color mapped representations of Von mises stress (Fig 4.5; A - B) showed higher stress at the coronal part of the PDL compared to the apical part. Similarly, the magnified displacements (Fig 4.5; C - D) showed more displacement at the crown level.



4.3. Correlation between stress and displacement

In the direct anchorage modality, significantly high correlations (>0.8) were present between the mesial stress amounts of each buccal tooth and the total displacement. High correlations also existed with the displacements in the x axis (in the horizontal plane perpendicular to the archwire), y axis (parallel to the archwire) and z axis (vertical to the archwire). Negative correlations were observed between the stresses and the displacements in the x axis (Table 4.14).

Similarly, in the indirect anchorage modality, significantly high correlations (>0.82) were found between mesial stress of the second premolar and molars and the total displacement of these teeth, as well as their displacements in the x axis (parallel to the archwire), y axis (vertical to the archwire) and z axis (in the horizontal plane perpendicular to the archwire). Slightly lower significant correlations (>0.73) existed at the first premolar; no significant correlations were found at the canine (Table 4.15).

Table 4.14: Correlation between stress amounts at the mesial surfaces of every tooth and the corresponding displacements in the direct modality

		dSU3	dSU3x	dSU3y	dSU3z
dSM3	Pearson	.864**	-.875**	.872**	.800**
	Sig. (2-tailed)	0.001	<0.001	<0.001	0.003
dSM4		dSU4	dSU4x	dSU4y	dSU4z
	Pearson	.821**	-.821**	.820**	.827**
	Sig. (2-tailed)	0.002	0.002	0.002	0.002
dSM5		dSU5	dSU5x	dSU5y	dSU5z
	Pearson	.930**	-.950**	.944**	.863**
	Sig. (2-tailed)	<0.001	<0.001	<0.001	0.001
dSM6		dSU6	dSU6x	dSU6y	dSU6z
	Pearson	.982**	-.982**	.982**	.957**
	Sig. (2-tailed)	<0.001	<0.001	<0.001	<0.001
dSM7		dSU7	dSU7x	dSU7y	dSU7z
	Pearson	.987**	-.981**	.986**	0.315
	Sig. (2-tailed)	<0.001	<0.001	<0.001	0.345

† Significant at the: *0.05, **0.01.

Table 4.15: Correlation between stress amounts at the mesial surfaces of every tooth and the corresponding displacements in the indirect modality

		iSU3	iSU3x	iSU3y	iSU3z
		iSM3	Pearson	-0.438	0.508
	Sig. (2-tailed)	0.178	0.111	0.11	0.511
		iSU4	iSU4x	iSU4y	iSU4z
		iSM4	Pearson	-.756**	.759**
	Sig. (2-tailed)	0.007	0.007	0.007	0.01
		iSU5	iSU5x	iSU5y	iSU5z
		iSM5	Pearson	-.957**	.959**
	Sig. (2-tailed)	<0.001	<0.001	<0.001	<0.001
		iSU6	iSU6x	iSU6y	iSU6z
		iSM6	Pearson	.997**	-.997**
	Sig. (2-tailed)	<0.001	<0.001	<0.001	<0.001
		iSU7	iSU7x	iSU7y	iSU7z
		iSM7	Pearson	.998**	.936**
	Sig. (2-tailed)	<0.001	<0.001	<0.001	<0.001

*Significant at the: *0.05, **0.01.

4.4. Correlation between cortical bone properties and stress

4.4.1. Correlations with cortical bone thickness

No significant or high correlations were found between the stress values at the canine and the buccal and palatal thicknesses (TPinc- TBinc), (Table 4.16), nor between the stresses at the first molar and the buccal and palatal thicknesses (TPmol - TBmol), (Table 4.17).

Table 4.16: Correlations between stresses and thickness of the cortical bone at palatal and buccal incisors/canine areas in both distalization modalities

	Direct anchorage modality				Indirect anchorage modality			
	dTD3	dTP3	dTM3	dTB3	iTD3	iTP3	iTM3	iTB3
TPinc	0.151	0.006	0.099	0.161	-0.064	0.253	0.113	-0.254
TBinc	0.072	0.022	-0.076	0.093	0.003	-0.226	-0.225	-0.313

Significant at *0.05, **0.01. P-values are listed in brackets and only for significant correlations.

Table 4.17: Correlations between stresses and thickness of the cortical bone at palatal and buccal molar areas in both distalization modalities

	Direct anchorage modality				Indirect anchorage modality			
	dTD6	dTP6	dTM6	dTB6	iTD6	iTP6	iTM6	iTB6
TPmol	0.28	0.135	0.292	0.308	0.298	0.291	0.262	0.291
TBmol	0.384	0.114	0.286	0.294	0.289	0.177	0.287	0.286

Significant at *0.05, **0.01. P-values are listed in brackets and only for significant correlations.

4.4.2. Correlations with cortical bone stiffness

No significant or high correlations were found between the stresses at the canine and the stiffness components of the corresponding cortical bone areas (S1Pinc- S2Pinc - S3Pinc- S1Binc - S2Binc - S3Binc), (Tables 4.18). On the contrary, high ($-0.68 < r < 0.72$) and significant correlations ($p\text{-value} < 0.05$) existed between stress amounts at the first molar on all surfaces, and the S3Bmol in the direct and indirect anchorage modalities.

Table 4.18: Correlations between stresses and stiffness values of the cortical bone at palatal and buccal incisors and canine areas.

	Direct anchorage modality				Indirect anchorage modality			
	dSD3	dSP3	dSM3	dSB3	iSD3	iSP3	iSM3	iSB3
S1Pinc	0.235	0.131	0.229	0.232	0.314	0.374	0.347	0.274
S2Pinc	-0.038	-0.118	0.019	-0.016	0.172	0.056	0.12	0.222
S3Pinc	-0.134	-0.124	-0.097	-0.173	-0.134	-0.036	-0.114	-0.116
S1Binc	0.211	-0.05	0.357	0.368	0.074	-0.319	-0.07	0.333
S2Binc	0.198	-0.057	0.356	0.373	0.091	-0.165	0.042	0.386
S3Binc	0.077	-0.155	0.239	0.253	0.057	-0.267	0.012	0.457

Significant at *0.05, **0.01. P-values are listed in brackets and only for significant correlations

The Pearson correlation coefficients were higher in the indirect anchorage modality compared to the direct anchorage modality. Moreover, in the indirect anchorage modality, the stresses at all surfaces significantly correlated with the S1Bmol and S2Bmol, but were lower and not significant for the direct anchorage modality. In addition, it is important to note that:

- A statistically significant correlation existed between the stresses at the distal of the first molar and the S3Pmol in the indirect anchorage modality.
- Moderate correlations ($0.5 < r < 0.6$) with borderline significance existed between the stresses at all surfaces in both modalities with the S1 and S3 of the palatal cortical bone stiffness (S1Pmol, S3Pmol).

All these correlations were negative, denoting the association of high stress with low stiffness (Table 4.19).

Table 4.19: Correlations between stresses and stiffness values of the cortical bone at palatal and buccal molar areas in both distalization modalities.

	Direct anchorage modality				Indirect anchorage modality			
	dSD6	dSP6	dSM6	dSB6	iSD6	iSP6	iSM6	iSB6
S1Pmol	-0.575	-0.53	-0.558	-0.595	-0.592	-0.575	-0.564	-0.558
S2Pmol	-0.53	-0.435	-0.473	-0.571	-0.495	-0.467	-0.472	-0.461
S3Pmol	-0.553	-0.536	-0.538	-0.561	-0.603* (0.049)	-0.586	-0.599	-0.585
S1Bmol	-0.372	-0.569	-0.5	-0.378	-.729* (0.011)	-.787** (0.004)	-.780** (0.005)	-.760** (0.007)
S2Bmol	-0.511	-0.472	-0.481	-0.59	-.690* (0.019)	-.685* (0.02)	-.706* (0.015)	-.707* (0.015)
S3Bmol	-.687* (0.019)	-.720* (0.012)	-.725* (0.012)	-.700* (0.016)	-.816** (0.002)	-.813** (0.002)	-.822** (0.002)	-.808** (0.003)

Significant at *0.05, **0.01. P-values are listed in brackets and only for significant correlations.

4.4.3. Correlation with vertical sections of the mesial and distal surfaces

While similar correlation patterns would be expected between stiffness and stress, the partition of the distal and mesial surfaces into 3 vertical areas revealed more detailed information regarding the section of the surface responsible for the correlation and the part that did not correlate with cortical bone stiffness. Moreover, in some instances this categorization showed that small areas of the PDL correlated with the bone stiffness, but when the entire surface was considered, the correlation diminished.

4.4.3.1. Thickness

In both distalization modalities, no significant or high correlations were found between the apical, middle and cervical stresses (mesial and distal) and the thickness of the buccal and palatal cortical bone areas that correspond to the canine (TPinc- TBinc) and first molar (TPmol - TBmol), (Table 4.20 and 4.21).

Table 4.20: Correlations of apical, middle and cervical canine stresses with thickness of the cortical bone at palatal and buccal incisors areas in both distalization modalities

		Distal vertical parts			Mesial vertical parts		
		dTD3a	dTD3m	dTD3c	dTM3a	dTM3m	dTM3c
Direct anchorage	TPinc	-0.353	0.022	0.306	-0.359	-0.202	0.225
	TBinc	-0.191	-0.04	0.233	-0.25	-0.132	0.161
		iTD3a	iTD3m	iTD3c	iTM3a	iTM3m	iTM3c
Indirect anchorage	TPinc	0.017	0.067	-0.093	0.143	0.068	0.185
	TBinc	-0.365	-0.376	0.048	-0.187	-0.333	-0.353

Significant at the: *0.05, **0.01. P values are listed in brackets and only for significant correlations.

Table 4.21: Correlations of apical, middle and cervical molar stresses with thickness of the cortical bone at palatal and buccal molar areas in both distalization modalities

		Distal vertical parts			Mesial vertical parts		
		dTD6a	dTD6m	dTD6c	dTM6a	dTM6m	dTM6c
Direct anchorage	TPmol	0.176	0.288	0.366	0.194	0.267	0.329
	TBmol	0.156	0.317	0.401	0.168	0.282	0.338
		iTD6a	iTD6m	iTD6c	iTM6a	iTM6m	iTM6c
Indirect anchorage	TPmol	0.297	0.276	0.298	0.282	0.296	0.261
	TBmol	0.142	0.21	0.266	0.248	0.303	0.309

Significant at the: *0.05, **0.01. P values are listed in brackets and only for significant correlations.

4.4.3.2 Stiffness

At the canine, no significant correlations were found between the apical, middle and cervical stresses (mesial and distal) with the stiffness of the corresponding buccal and palatal bone areas. The only exception was the correlation between the apical stress at the distal of the canine in the indirect anchorage modality (iSD3a) and the S1 and S2 components of the stiffness at the buccal molar area (S1Bmol, S2Bmol). When the total distal surface was studied, this correlation was not significant, (Table 4.22).

For the first molar, in both the direct and indirect anchorage modalities, the regional stresses (apical, middle and cervical) showed relatively similar patterns of correlation to the total stresses at the mesial and distal surfaces. However, in some instances the dissection of the distal and mesial surfaces into 3 vertical areas revealed

more detailed information regarding which part of the surface was responsible of the correlation and which part did not correlate with the cortical bone stiffness.

Table 4.22: Correlations of apical, middle and cervical molar stresses with the stiffness values of the cortical bone at palatal and buccal incisors/canine areas in both distalization modalities

		Distal vertical parts			Mesial vertical parts		
		dSD3a	dSD3m	dSD3c	dSM3a	dSM3m	dSM3c
Direct anchorage	S1Pinc	-0.114	0.038	0.465	-0.098	0.129	0.379
	S2Pinc	-0.423	-0.28	0.315	-0.388	-0.117	0.245
	S3Pinc	-0.306	-0.262	0.07	-0.316	-0.188	0.058
	S1Binc	-0.244	-0.098	0.553	-0.115	0.222	0.553
	S2Binc	-0.141	-0.058	0.458	-0.03	0.249	0.507
	S3Binc	-0.288	-0.192	0.395	-0.187	0.123	0.419

		Distal vertical parts			Mesial vertical parts		
		iSD3a	iSD3m	iSD3c	iSM3a	iSM3m	iSM3c
Indirect anchorage	S1Pinc	-0.28	0.248	0.382	0.089	0.314	0.381
	S2Pinc	-0.202	0.046	0.275	-0.182	0.08	0.188
	S3Pinc	-0.118	-0.193	-0.062	-0.2	-0.139	-0.07
	S1Binc	.621* (0.042)	-0.038	0.126	-0.354	-0.091	-0.008
	S2Binc	.644* (0.032)	0.036	0.119	-0.254	0.024	0.087
	S3Binc	0.564	-0.01	0.104	-0.404	-0.019	0.089

Significant at *0.05 level, **0.01. P values are listed in brackets and only for significant correlations

The correlation differences relative to stress on the total surface were:

1. In the direct anchorage modality:
 - Stress on the apical areas at the mesial and distal of the first molar (dSM6a and dSD6a respectively) correlated with the S1 component of the stiffness at the palatal molar area (S1Pmol).
 - Stress at the cervical part of the distal surface (dSD6c) did not correlate significantly with S3Bmol.
2. In the indirect anchorage modality:
 - None of the vertical parts of the distal area (iSD6a, iSD6m and iSD6c) correlated with S3Pmol, while the latter was correlated with the total surface stress (iSD6).

- The cervical part of the mesial surface (iSM6c) correlated significantly with S3Pmol, but the total surface (iSM6) did not.
- The iSD6c did not correlate with any of the stiffness components of the buccal molar area (S1Bmol, S2Bmol and S3Bmol), (Table 4.23).

Table 4.23: Correlations of apical, middle and cervical molar stresses with the stiffness values of the cortical bone at palatal and buccal incisors areas in both distalization modalities

		Distal vertical parts			Mesial vertical parts		
		dSD6a	dSD6m	dSD6c	dSM6a	dSM6m	dSM6c
Direct anchorage	S1Pmol	-.601* (0.05)	-0.588	-0.455	-.629* (0.038)	-0.576	-0.442
	S2Pmol	-0.525	-0.511	-0.501	-0.535	-0.495	-0.353
	S3Pmol	-0.586	-0.565	-0.458	-0.581	-0.548	-0.451
	S1Bmol	-0.53	-0.492	-0.01	-0.514	-0.493	-0.482
	S2Bmol	-0.493	-0.487	-0.467	-0.492	-0.49	-0.434
	S3Bmol	-.760** (0.007)	-.734* (0.01)	-0.476	-.755** (0.007)	-.729* (0.011)	-.656* (0.028)

		Distal vertical parts			Mesial vertical parts		
		iSD6a	iSD6m	iSD6c	iSM6a	iSM6m	iSM6c
Indirect anchorage	S1Pmol	-0.574	-0.582	-0.098	-0.575	-0.564	-0.561
	S2Pmol	-0.472	-0.477	-0.266	-0.473	-0.468	-0.476
	S3Pmol	-0.595	-0.595	-0.41	-0.596	-0.594	-.605* (0.049)
	S1Bmol	-.773** (0.005)	-.767** (0.006)	0.091	-.772** (0.005)	-.779** (0.005)	-.781** (0.005)
	S2Bmol	-.670* (0.024)	-.673* (0.023)	-0.187	-.681* (0.021)	-.702* (0.016)	-.720* (0.012)
	S3Bmol	-.821** (0.002)	-.818** (0.002)	-0.098	-.820** (0.002)	-.820** (0.002)	-.826** (0.002)

Significant at *0.05 level, **0.01. P values are listed in brackets and only for significant correlations

4.4.4. Correlation of stresses with the average stiffness

4.4.4.1. Canine

The only statistically significant correlation was found in the indirect anchorage modality between stress amounts at the level of the apical part of the canine distal surface (iSD3a) and the average stiffness at the buccal incisor area (SBinc). The same correlation was found with the S1 and S2 stiffness components of the same cortical bone area (S1Binc - S2Binc), (Table 4.24).

4.4.4.2. First molar

As shown previously, first molar stresses in general correlated more with the buccal (SBmol) than the palatal (SPmol) cortical bone average stiffness. The average buccal cortical bone stiffness (SBmol) correlated with all the stresses at the different surfaces in the direct and indirect anchorage modalities. The only exceptions were the cervical part of the distal surface (dSD6c and iSD6c) in both distalization modalities.

The average palatal cortical bone stiffness (SPmol) at the first molar in the direct anchorage modality correlated with the stresses at: the mesial and distal apical areas (dSM6a and dSD6a), the middle distal area (dSD6m) and the buccal surface (dSB6). In the indirect anchorage modality, the average palatal cortical bone stiffness (SPmol) correlated with the stresses at: the middle part and total distal surface (iSD6m and iSD6); and the apical and cervical mesial surfaces (iSM6a and iSM6c) of the molar.

When we compared the correlations using the average bone stiffness to those using all the stiffness components (S1, S2, and S3), we observed the following:

- No change in the correlations relating buccal cortical bone at the molar area (SBmol) with the average stiffness value (SBmol) or the different stiffness components (S1Bmol, S2Bmol, S3Bmol).
- The number of correlations related to palatal cortical bone stiffness (SPmol) increased. In the direct anchorage modality, dSD6m and dSB6 correlated with SPmol, but did not correlate with S1Pmol, S2Pmol or S3Pmol. In the indirect anchorage modality iSD6m and iSM6a correlated with SPmol, but did not correlate with S1Pmol, S2Pmol or S3Pmol (Table 4.25).

Table 4.24: Correlations between the canine stresses at the different surfaces and the average cortical bone stiffness.

		Distal				Mesial					
Direct		dSD3	dSD3a	dSD3m	dSD3c	dSP3	dSM3	dSM3a	dSM3m	dSM3c	dSB3
	SPinc	-0.009 (0.978)	-0.324 (0.331)	-0.21 (0.536)	0.275 (0.413)	-0.064 (0.851)	0.027 (0.936)	-0.31 (0.353)	-0.091 (0.791)	0.22 (0.516)	-0.018 (0.959)
	SBinc	0.161 (0.635)	-0.239 (0.48)	-0.126 (0.713)	0.48 (0.135)	-0.094 (0.783)	0.321 (0.336)	-0.122 (0.722)	0.198 (0.56)	0.503 (0.114)	0.335 (0.314)
		Distal				Mesial					
Indirect		iSD3	iSD3a	iSD3m	iSD3c	iSP3	iSM3	iSM3a	iSM3m	iSM3c	iSB3
	SPinc	0.094 (0.783)	-0.202 (0.551)	0.003 (0.993)	0.183 (0.591)	0.105 (0.759)	0.091 (0.79)	-0.132 (0.699)	0.056 (0.87)	0.145 (0.671)	0.111 (0.745)
	SBinc	0.075 (0.828)	.623* (0.041)	-0.007 (0.984)	0.119 (0.727)	-0.264 (0.433)	-0.008 (0.982)	-0.355 (0.284)	-0.032 (0.925)	0.057 (0.868)	0.406 (0.216)

Significant at *0.05, **0.01. P values are listed in brackets.

Table 4.25: Correlations between the first molar stresses at the different surfaces and the average cortical bone stiffness.

		Distal				Mesial					
Direct		dSD6	dSD6a	dSD6m	dSD6c	dSP6	dSM6	dSM6a	dSM6m	dSM6c	dSB6
	SPmol	-0.602 (0.05)	-.623* (0.04)	-.605* (0.048)	-0.511 (0.108)	-0.549 (0.08)	-0.572 (0.066)	-.634* (0.036)	-0.589 (0.056)	-0.456 (0.158)	-.626* (0.04)
	SBmol	-.647* (0.031)	-.720* (0.012)	-.694* (0.018)	-0.426 (0.191)	-.702* (0.016)	-.689* (0.019)	-.713* (0.014)	-.693* (0.018)	-.631* (0.037)	-.686* (0.02)
		Distal				Mesial					
Indirect		iSD6	iSD6a	iSD6m	iSD6c	iSP6	iSM6	iSM6a	iSM6m	iSM6c	iSB6
	SPmol	-.618* (0.043)	-0.601 (0.05)	-.605* (0.048)	-0.294 (0.379)	-0.596 (0.053)	-0.599 (0.051)	-.602* (0.05)	-0.596 (0.053)	-.602* (0.05)	-0.588 (0.057)
	SBmol	-.877** (<0.001)	-.883** (<0.001)	-.882** (<0.001)	-0.098 (0.775)	-.889** (<0.001)	-.900** (<0.001)	-.887** (<0.001)	-.897** (<0.001)	-.908** (<0.001)	-.888** (<0.001)

Significant at *0.05, **0.01. P values are listed in brackets.

4.5. Multiple regression analysis

4.5.1. *Canine*

At the level of the canine, none of the cortical bone stiffness values at the incisor/canine area (S1Pinc, S2Pinc, S3Pinc and S1Binc, S2Binc, S3Binc) was associated at a p -value <0.2 with the stresses at the mesial (dSM3, iSM3) or distal (dSD3, iSD3) surfaces of the canine PDL in both distalization modalities.

Moreover, none cortical bone thickness value at the incisor/canine area (TPinc, TBinc) was associated at a p -value <0.2 with the stresses at the mesial (dTM3, iTM3) and distal (dTD3, iTD3) of the canine PDL in both distalization modalities.

As a result, no multivariate equations were run for the canine stresses because none of the bivariate p -values were statistically significant at $p<0.2$.

4.5.2. *First molar*

4.5.2.1. Stress prediction from thickness values

None of the cortical bone thickness values at the area of the molars (TPmol, TBmol) was associated at a p -value <0.2 with the stress values at the mesial (dTM6, iTM6) and distal (dTD6, iTD6) surfaces of the first molar PDL in both distalization modalities. Therefore, no multivariate equations were run.

The only exception was the p -value of TBmol in the direct anchorage modality that was equal to 0.195 but was not statistically significant. The resulting multivariate equation and its predictors were not statistically significant.

4.5.2.2. Mesial stress prediction from stiffness values

In the direct anchorage modality, S3Bmol correlated significantly with the mesial stress amounts (dSM6) at the bivariate level (p -value =0.012). The only

statistically significant multivariate equation that predicted stress at the mesial area in the direct anchorage modality was determined by S1Bmol and S3Bmol with a coefficients of association equal to $-2.79\text{e-}07$ and $-5.42\text{e-}07$, respectively. Although the overall equation was significant ($p\text{-value} = 0.0423$; $r^2 = 0.5464$), none of the predictors were significant (Table 4.26).

Table 4.26: Bivariate and multivariate analyses for the prediction of the stresses at the mesial of the first molar in the direct anchorage modality

Outcome: dSM6					
	Assoc. Var.	Coef.	Std. Err.	95% CI	p-value
Bivariate equations	S1Pmol	-6.67e-07	3.31e-07	-1.42e-06; 8.15e-08	0.075
	S2Pmol	-5.99e-07	3.72e-07	-1.44e-06; 2.42e-07	0.141
	S3Pmol	-5.1e-07	2.66e-07	-1.11e-06; 9.17e-08	0.087
	S1Bmol	-8.21e-07	4.75e-07	1.9e-06; 2.52e-07	0.118
	S2Bmol	-5.49e-07	3.33e-07	-1.30e-06; 2.05e-07	0.134
	S3Bmol	-6.17e-07	1.98e-07	-1.06e-06; -1.75e-07	0.012
Multivariate equations	S1Bmol	-2.79e-07	4.58e-07	-1.33e-06; 7.76e-07	0.559
	S3Bmol	-5.42e-07	2.37e-07	-1.09e-06; 4.36e-09	0.051
	Constant	0.212	0.043	0.202; 0.222	0.001*
	F (2,8)	4.82			
	Prob > F	0.0423*			
	R ²	0.5464			
	Adjusted R ²	0.4330			

Significant at *0.05, **0.01. P values are listed in brackets and only for significant correlations.

† p-value < 0.2 and included in multivariate analysis; **Coef:** Coefficient; **Std. Err.:** Standard error; **CI:** Confidence interval.

In the indirect anchorage modality, S1Bmol, S2Bmol and S3Bmol correlated significantly with the mesial stresses (iSM6) at the bivariate level ($p = 0.005$, 0.015 and 0.002 respectively). At the multivariate level, the stress at the mesial area was predicted by S1Pmol, S1Bmol and S3Bmol with coefficients of association equal to $-1.97\text{e-}06$, $-4.40\text{e-}06$ and $-1.15\text{e-}06$, respectively. The first two predictors (S1Pmol, S1Bmol) were statistically significant ($p\text{-value} = 0.019$ and 0.002 respectively), while S3Bmol was not ($p=0.07$). The overall equation was statistically significant and highly predictive ($p=0.0002$; $r^2 = 0.9341$), (Table 4.27).

Table 4.27: Bivariate and multivariate analyses for the prediction of the stresses at the mesial of the first molar in the indirect anchorage modality

Outcome: iSM6					
	Assoc. Var.	Coef.	Std. Err.	95% CI	p value
Bivariate equations	S1Pmol	-2.98e-06	1.46e-06	-6.27e-06; 3.12e-07	0.071
	S2Pmol	-2.64e-06	1.64e-06	-6.36e-06; 1.08e-06	0.143
	S3Pmol	-2.50e-06	1.12e-06	-5.03e-06; 2.33e-08	0.052
	S1Bmol	-5.67e-06	1.52e-06	-9.09e-06; -2.24e-06	0.005*
	S2Bmol	-3.56e-06	1.19e-06	-6.25e-06; -8.63e-07	0.015*
	S3Bmol	-3.10e-06	7.14e-07	-4.71e-06; -1.48e-06	0.002*
Multivariate equations	S1Pmol	-1.97e-06	6.48e-07	-3.50e-06; -4.37e-07	0.019*
	S1Bmol	-4.40e-06	8.74e-07	-6.47e-06; -2.33e-06	0.002*
	S3Bmol	-1.15e-06	5.39e-07	-2.43e-06; 1.22e-07	0.070
	Constant	0.662	0.008	0.641; 0.681	0.001*
	F (3,7)	33.08			
	Prob > F	0.0002*			
	R ²	0.9341			
	Adjusted R ²	0.9059			

Significant at the: *0.05, **0.01. P values are listed in brackets and only for significant correlations.

† p-value < 0.2 and included in multivariate analysis; **Coef.**: Coefficient; **Std. Err.**: Standard error; **CI**: Confidence interval.

4.5.2.3. Distal stress prediction from stiffness values

At the distal surface, the bivariate and multivariate analyses were very similar to the mesial surface.

In the direct anchorage modality, S3Bmol correlated significantly with the distal stress values (dSD6) at the bivariate level ($p = 0.019$). The only statistically significant multivariate equation that determined stress at the distal area was predicted by S1Pmol and S3Bmol with coefficients of association equal to $-2.95e-07$ and $-3.90e-07$, respectively. While the overall equation was significant ($p = 0.0489$; $r^2 = 0.5298$), none of the predictors were significant (Table 4.28).

In the indirect anchorage modality, S3Pmol, S1Bmol, S2Bmol and S3Bmol correlated significantly with the distal stress amounts (iSD6) at the bivariate level (p -value = 0.049, 0.011, 0.019 and 0.002, respectively). At the multivariate level, the stress at the distal area was predicted by S1Pmol, S1Bmol and S3Bmol with coefficients of association equal to $-1.97e-06$, $-4.40e-06$ and $-1.15e-06$, respectively. The first two

predictors (S1Pmol, S1Bmol) were statistically significant (p-value= 0.039 and 0.009 respectively) while S3Bmol was not (p = 0.127). The overall equation was statistically significant and highly predictive (p = 0.0009; $r^2 = 0.8927$) (Table 4.29).

Table 4.28: Bivariate and multivariate analyses for the prediction of the stresses at the distal of the first molar in the direct anchorage modality

Outcome: dSD6					
	Assoc. Var.	Coef.	Std. Err.	95% CI	p value
Bivariate equations	S1Pmol	-5.92e-07	2.81e-07	-1.23e-06; 4.38e-08	0.064
	S2Pmol	-5.78e-07	3.08e-07	-1.28e-06; 1.19e-07	0.093
	S3Pmol	-4.51e-07	2.27e-07	-9.63e-07; 6.16e-08	0.078
	S1Bmol	-5.27e-07	4.38e-07	-1.52e-06; 4.65e-07	0.260
	S2Bmol	-5.02e-07	2.82e-07	-1.14e-06; 1.35e-07	0.108
	S3Bmol	-5.04e-07	1.78e-07	-9.06e-07; -1.02e-07	0.019*
Multivariate equations	S1Pmol	-2.95e-07	2.98e-07	-9.81e-07; 3.92e-07	0.351
	S3Bmol	-3.90e-07	2.12e-07	-8.79e-07; 9.83e-08	0.103
	Constant	0.168	0.003	0.161; 0.175	0.001*
	F (2,8)	4.51			
	Prob > F	0.0489*			
	R ²	0.5298			
	Adjusted R ²	0.4122			

Significant at the: *0.05, **0.01. P values are listed in brackets and only for significant correlations.

‡ p-value < 0.2 and included in multivariate analysis; **Coef:** Coefficient; **Std. Err.:** Standard error; **CI:** Confidence interval.

Table 4.29: Bivariate and multivariate analyses for the prediction of the stresses at the distal of the first molar in the indirect anchorage modality

Outcome: iSD6					
	Assoc. Var.	Coef.	Std. Err.	95% CI	p value
Bivariate equations	S1Pmol	-2.16e-06	9.80e-07	-4.38e-06; 5.84e-08	0.055
	S2Pmol	-1.91e-06	1.12e-06	-4.44e-06; 6.19e-07	0.122
	S3Pmol	-1.74e-06	7.67e-07	-3.48e-06; -5.75e-09	0.049
	S1Bmol	-3.65e-06	1.14e-06	-6.24e-06; -1.06e-06	0.011*
	S2Bmol	-2.40e-06	8.39e-07	-4.30e-06; -5.00e-07	0.019*
	S3Bmol	-2.12e-06	5.01e-07	-3.25e-06; -9.87e-07	0.002*
Multivariate equations	S1Pmol	-1.45e-06	5.71e-07	-2.80e-06; -1.00e-07	0.039*
	S1Bmol	-2.75e-06	7.70e-07	-4.57e-06; -9.29e-07	0.009*
	S3Bmol	-8.21e-07	4.75e-07	-1.94e-06; 3.01e-07	0.127
	Constant	0.512	0.007	0.494; 0.530	0.001*
	F (3,7)	19.41			
	Prob > F	0.0009*			
	R ²	0.8927			
	Adjusted R ²	0.8467			

Significant at the: *0.05, **0.01. P values are listed in brackets and only for significant correlations.

‡ p-value < 0.2 and included in multivariate analysis; **Coef:** Coefficient; **Std. Err.:** Standard error; **CI:** Confidence interval.

4.6. Stiffness variation stress vs Thickness variation stress

Overall thickness did not correlate significantly with the stiffness values in the different areas studied except for (Table 4.30):

- The buccal incisor/canine area (site 5): thickness (TBinc) correlated significantly with all stiffness values: S1Binc ($r=0.613$), S2Binc ($r=0.679$) and S3Binc ($r=0.625$).
- The palatal premolar area (site 3): thickness (TPpmol) correlated significantly with S2Ppmol ($r=0.669$) and S3Ppmol ($r=0.781$).

At the buccal premolar area (site 6), thickness (TBpmol) correlated significantly with S2Bpmol ($r= -0.638$).

Table 4.30: Correlation between stiffness and thickness of each cortical bone part

Buccal incisors/canine (site 5)				Palatal incisors/canine (site 1)			
	S1Binc	S2Binc	S3Binc		S1Pinc	S2Pinc	S3Pinc
TBinc	.613* (0.045)	.679* (0.022)	.625* (0.04)	TPinc	0.113 (0.742)	0.182 (0.593)	0.314 (0.347)
Buccal premolars (site 6)				Palatal premolars (site 3)			
	S1Bpmol	S2Bpmol	S3Bpmol		S1Ppmol	S2Ppmol	S3Ppmol
TBpmol	-0.337 (0.31)	-.638* (0.035)	-0.087 (0.799)	TPpmol	0.324 (0.332)	.669* (0.025)	.781** (0.005)
Buccal molars (site 7)				Palatal molars (site 4)			
	S1Pmol	S2Pmol	S3Pmol		S1Bmol	S2Bmol	S3Bmol
TPmol	0.201 (0.553)	0.013 (0.97)	0.093 (0.785)	TBmol	0.157 (0.645)	-0.543 (0.084)	-0.455 (0.159)

Significant at the: *0.05, **0.01. P-values are listed in brackets and only for significant correlations.

4.7. Effect of cortical bone material property type on the PDL stresses

For all cortical bone sites, the average S3 (related to vertical stiffness) was larger than S2 (in the plane of the bone), which in turn was larger than S1 (through bone). The isotropic material property was very close to S3 albeit slightly greater (Table 4.31).

Table 4.31: Averages of the S1, S2 and S3 at each site (n=11)

	S1	S2	S3
site 1	8939.7	12093.3	14614.8
site 3	10055.5	13485.6	16814.8
site 4	8953.5	10944.3	15623.6
site 5	10340	11182	14751.3
site 6	7188.4	8724.5	12205.5
site 7	10171.5	11588.7	16598.3
Average (exc. site 8)	9274.8	11336.4	15101.4
Template	15750		

Site 1: Palatal incisor area; **Site 3:** Palatal premolar area; **Site 4:** Palatal molar area; **Site 5:** Buccal incisor area; **Site 6:** Buccal premolar area; **Site 7:** Buccal molar area; **Site 8:** Tuberosity area; **Template:** Model where isotropic material properties taken from the literature were used.
S1 - S2 -S3: Different stiffness components.

When evaluating these values for each cortical bone part, the same pattern (Isotropic > S3 >S2 >S1) emerged except for the palatal premolar (site 3) and the buccal molar areas (site 7) where the average S3 is larger than the isotropic value (Fig. 4.6).

In the direct anchorage modality, average orthotropic stresses were very similar (0.035 to 0.041 kPa higher) on all surfaces to the isotropic model. The only dissimilarities were found in the stress values recorded at the canine (all surfaces) and at the palatal surface of the first molar (Fig. 4.7).

In the indirect anchorage modality, the stress variations of the template model were parallel to and lower than the average orthotropic stresses, but were similar at the canine (Fig. 4.8).

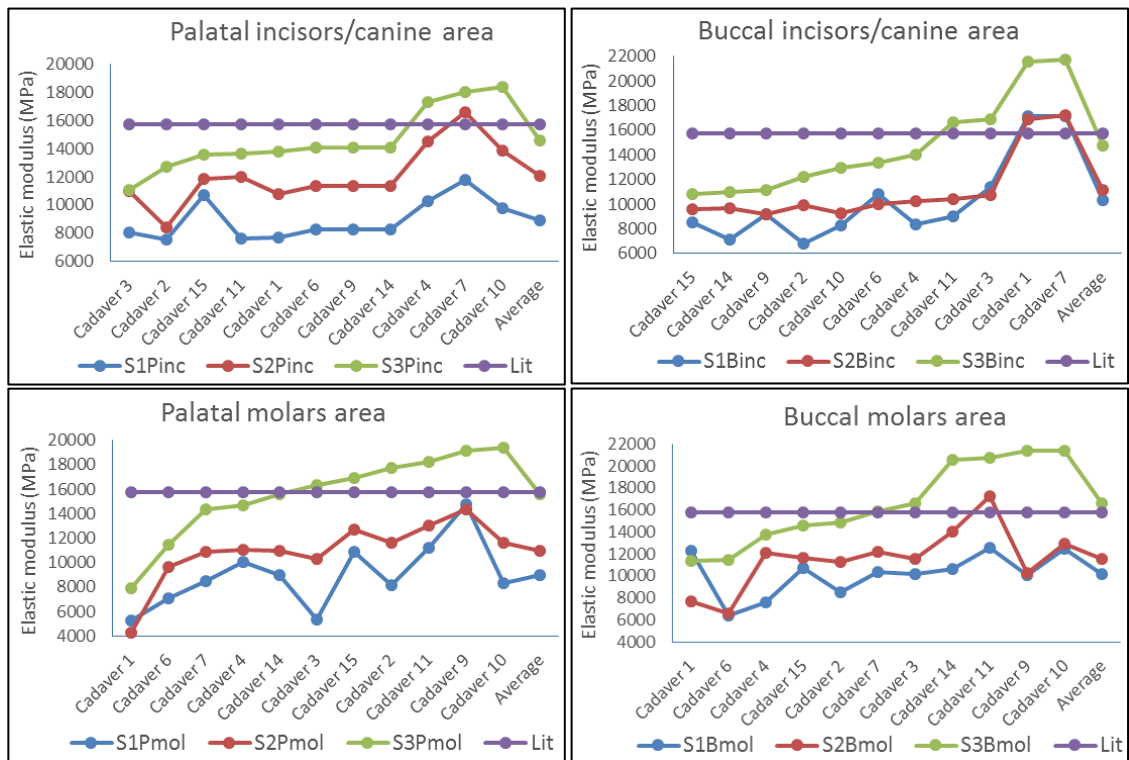


Fig 4.6: Graph showing the S1, S2 and S3 for every cadaver at every cortical bone area compared to the isotropic material property value used.

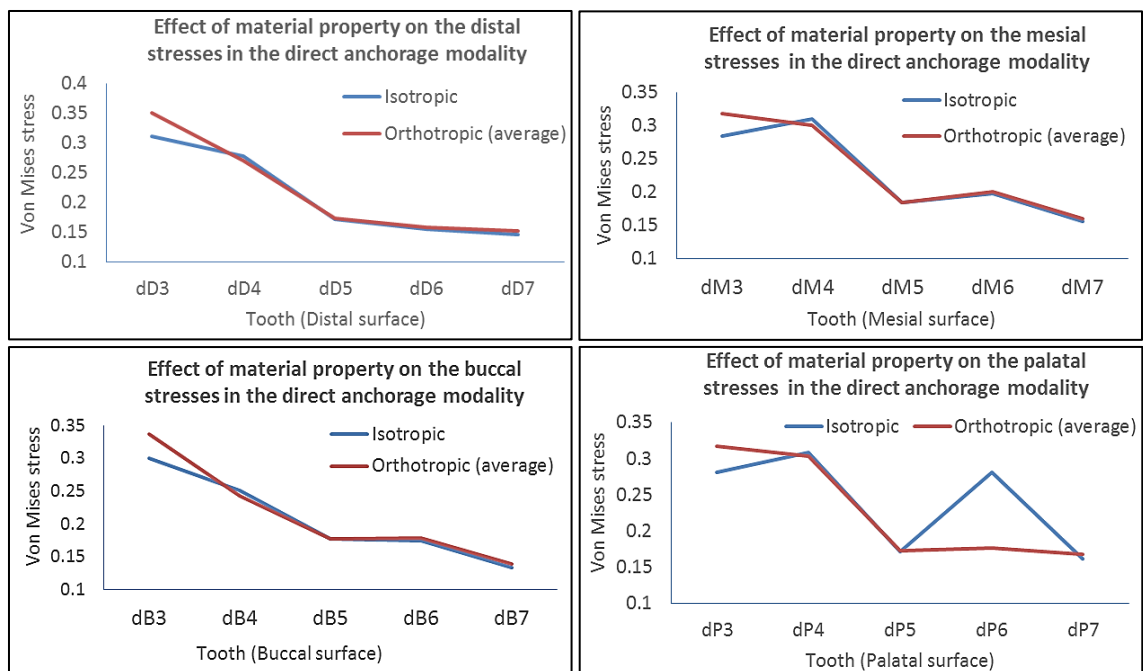


Fig 4.7: Line graph showing the stress amounts recorded at the different buccal teeth in the direct anchorage modality with material properties assumptions (isotropic and orthotropic).

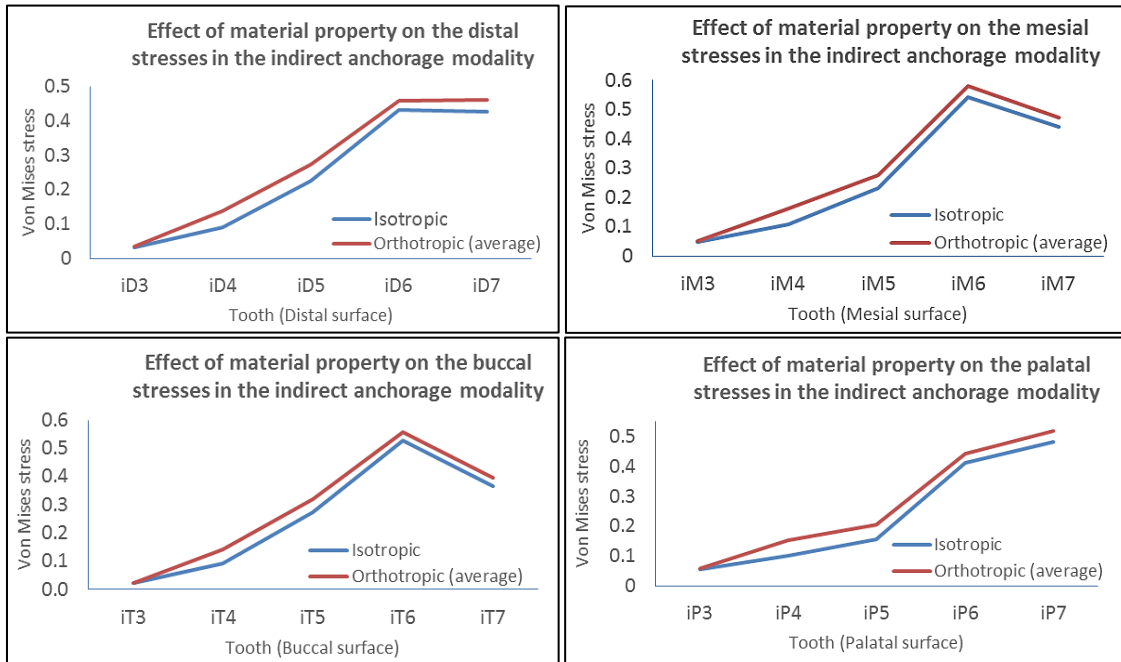


Fig 4.8: Line graph showing very similar stresses recorded at the different buccal teeth in the indirect anchorage modality with material properties assumptions (isotropic and orthotropic).

The mesial surface stresses of all buccal teeth were plotted along with the isotropic model stresses in a bar chart. Stress values at the mesial of the canine were lower in the isotropic model compared to all orthotropic models. Conversely, the isotropic model and orthotropic models showed similar stresses at the mesial surface of the molar (Fig. 4.9).

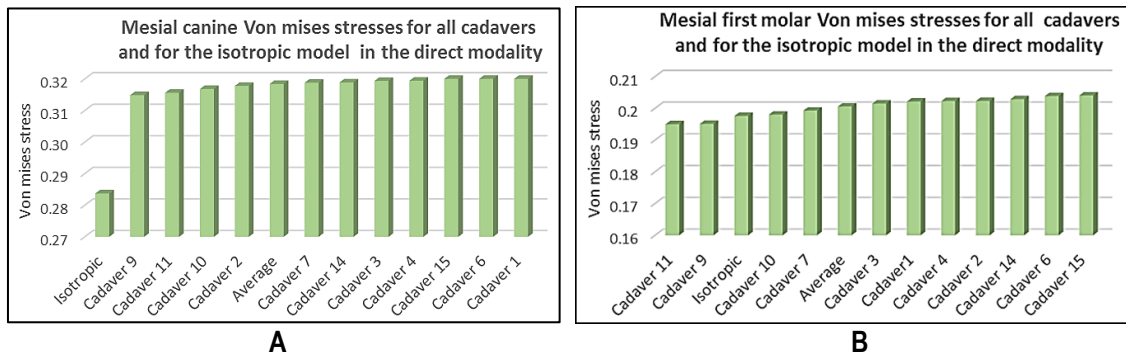


Fig 4.9: Bar chart showing the stresses obtained at the mesial surface for all the models evaluated (11 orthotropic and 1 isotropic) in the direct anchorage modality. **A-** At the canine; **B-** At the first molar.

For the indirect anchorage modality, the isotropic model showed less stress at the level of the canine and first molar (Fig.4.10). The maximum variation between the template and orthotropic models (in both modalities) was minimal (51Pa).

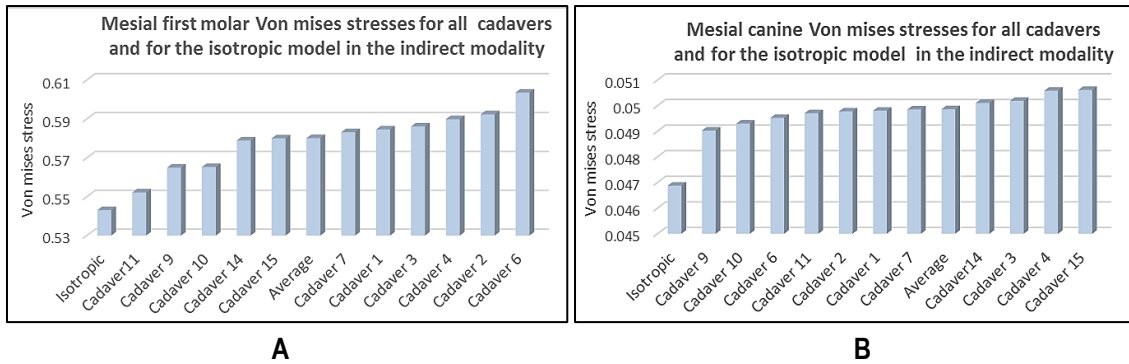


Fig 4.10: Bar chart showing the stresses obtained at the mesial surface for all the models evaluated (11 orthotropic and 1 isotropic) in the indirect anchorage modality. **A-** At the canine; **B-** At the first molar.

CHAPTER 5

DISCUSSION

5.1. Strengths

We have established in this study modalities heretofore not used or documented. We have illustrated the strengths in their relevant contexts in the different chapters, but list them in a comprehensive summary in this section.

5.1.1. *Individual variation*

Most FEA studies applied in engineering generated inferences and readings from a single mathematical solution, corresponding to one single set-up or simplified fractioned clinical scenario. However, in the medical and dental fields individual variations lead to different results for a similar clinical problem, thus the need to study larger samples to determine not only central tendencies but also potential outliers. Any FEA application may not be carried out directly in living organs. Accordingly, the best available reconstructions have been simplified with segmented elements of anatomy. To merge both principles, accounting for individual variation and applying engineering methods, we have incorporated cortical bone stiffness and thickness that were investigated in studies of real cadavers to simulate variations existing between real patients. This approach is the closest to date to achieve a link between the virtual finite element models and actual clinical situations.

The inclusion of a biologic sample with individual variations facilitated the application of statistical analyses that disclosed the effect of variances on a number of

outcome measures, leading to some definite conclusions or allowing the enunciation of new hypotheses.

5.1.2. Effect of bone characteristics on tooth movement

Various rates of tooth movement have been reported during distalization ((Iwasaki, Haack, Nickel, & Morton, 2000). Accounting for this variation, different factors have been incriminated, such as position, anatomy, physiology and metabolism of the involved systems (bone, teeth, PDL).

Unlike other types of tooth movements (e.g. torque before retraction of incisors; impacted canines) where positional variations may lead to different dental response to the same load applied, variation in dental alignment is not a primary cause of variation because teeth are usually leveled and aligned before distalization.

While physiology and metabolism cannot be studied in a static FEA, this analysis provides an excellent tool to exclusively study anatomical differences and their ability to affect tooth movement, because it has the capability to control all other variables.

While other authors attempted to determine the contribution of bone and dental anatomy to tooth movement in two-dimensional FEA studies (Choy et al, 2000), including the determination in clinical investigations of the differences between trabecular and cortical bone (Roberts et al. 1996), such differentiation was not established in FE analysis prior to this investigation, in which the effects of stiffness and thickness (two important characteristics of cortical bone) on the distal movement of the maxillary teeth were evaluated.

5.1.3. Orthotropic material properties

Because orthodontic tooth movement is considered a periodontally driven mechanism, the focus of most FEA studies was on validating the assumption on its material properties. The other oral tissues were assumed to have homogeneous isotropic material properties.

Yet, in orthopedics where bone is studied in more depth, bone is considered far from being homogeneous and isotropic. Lindh et al. (2004) found extreme variations in the density of the trabecular bone tissue of the edentulous maxilla. Chugh et al. (2013) showed variations in the density of cortical bone in the interradicular areas of dentate maxilla. Gačnik et al. (2014) went as far as considering that each bone particle has a different elastic property than its adjacent and used a bone mapping technique to assign a material property to each voxel according to its Hounsfield Unit value read on the CT scan.

Moreover, Schwartz-Dabney and Dechow (2003) showed that bone is an anisotropic material (material properties differ by direction) with material properties varying in 3 perpendicular directions X, Y and Z and confirmed its orthotropic behavior. Cowin et al. (1990) showed that local anisotropy and regional variations in skeletal material properties can have drastic effects on the relationship between stress and strain (Cowin & Hart, 1990).

Based on this wealth of information, we have described in our study the material properties of the cortical bone as accurately as possible by defining its properties as orthotropic, and implemented the stress components S1, S2 and S3 corresponding to different directions.

5.1.4. Complete 3D model

Building a complete and accurate FE model requires significant effort and time. In the majority of studies, modelling of the investigated structures was compromised. Some used incomplete models containing a segment of bone with 2 to 3 teeth surrounded by the PDL assuming fixed boundary conditions all around (Nihara et al., 2015). Others did not differentiate between the trabecular and cortical bones (Sung et al., 2015; Yu et al., 2014), or built cortical bone assuming a certain thickness that might not match the reality (Nihara et al., 2015). Moreover, some authors have constructed complete FE models that were based on a dentoform rather than radiographic images, therefore presenting many anatomical flaws (Sung et al., 2015). In comparison, our model was more complete, constructed on the basis of a CT scan of a patient and contains all structures except for the enamel, dentin and pulp (for simplification purposes). The data of each human cadaver was inserted in this model, replicating the individual variations.

5.2. Comparison with FEA distalization studies

Finite element analysis was most frequently used in movements of teeth into edentulous areas such as canine retraction, molar protraction and incisors retraction. The main reasons were the easier interpretation of the results and to avoid complicating the model with interaction settings between the teeth.

Distalization is a difficult movement with an indeterminate force system, in which moments and forces cannot be readily measured and evaluated, thus its amenability to study with FEA. As a result, only the studies by Kang et al. (2016), Sung et al. (2015) and Yu et al. (2012) tackled maxillary distalization of teeth using the FEA.

Our study differed from these studies in many aspects: the evaluated distalization modalities, model construction and set up, aims, data collection, and consequently results obtained. The methodological differences and similarities are outlined in this section, and results compared where pertinent.

5.2.1. *Distalization modalities*

Kang et al. (2016) compared distalization using palatal miniscrews (bone anchored pendulum and palatal anchorage plate) to molar distalization with headgear. Applying the force from the palatal side instead of the buccal side, as in our study, generated different dental responses because the force point of application and vectors were different (Proffit et al., 2013).

Sung et al. (2015) evaluated the influence of force vectors, determined by the height and antero-posterior position of the retraction arm, on the “en masse” distalization of the whole maxillary arch.

The distalization modalities employed by Yu et al. (2012) are the closest to our study because they compared 3 distalization approaches using a palatal plate, direct anchorage and indirect anchorage. However, their direct and indirect anchorage modalities differed from ours in the following:

- In both modalities, the second premolar was not bonded and the force was transmitted from the first premolar to the first molar through an opencoil spring.
- In the indirect modality, the first premolar rather than the canine was attached to the miniscrew, which was placed between the second premolar and the first molar. The short span, added to a more vertical direction of pull, yield less effective anchorage compared to the more horizontal pull to the canine.

Even though the first two differences can create side effects in a real clinical setting, they might not affect the FEA results because they can be controlled by the FEA solver; the software can be used to stabilize the teeth and avoid the extrusive and mesial movements. However, the next difference can be the cause for divergence of results between the two studies.

- Yu et al. simulated a TP bar linking the maxillary first molars to each other in both distalization modalities. This addition affects the type of dental movements allowed in the FE simulations. Basically, molar rotation is inhibited, distal crown tipping is limited and translation movement is hindered because the anchorage value of the posterior unit is increased. In contrast, the movements in our study were dictated by local boundary conditions to allow all movements except translation in the horizontal and vertical planes (See section 3.2.2.4).
- We included the second molar in our set up mirroring the clinical situation. Yu et al did not in either the direct or indirect anchorage modalities evaluated.

In addition, force magnitude differed between the studies. Yu et al. (2012) and Kang et al. (2016) used a force magnitude of 150 grams while Sung et al. (2015) used a heavier force of 200 grams, possibly to account for the higher resistance to dental movement by the whole maxillary dentition. In our study, the direct anchorage force as well as the 2 forces (in opposite direction generated by the opencoil spring) in the indirect anchorage were of 150 grams each. Global boundary conditions to constrain the posterior and upper parts of the maxilla in all directions were applied similarly in all studies including our study.

5.2.2. Model construction and set up

5.2.2.1. Bone

The 3D model creation in the study by Kang et al (2016) was similar to our method. They used an image processing and digital reconstruction software (MIMICS version 15.01; Materialise, Leuven, Belgium) to extract a 3D model from computed tomography (CT) images of a dry skull of an adolescent. However, the same 3D model used in the studies by Sung et al. (2015) and Yu et al. (2012) was constructed on the basis of a dentoform (Nissin Dental Products, Kyoto, Japan) via laser scanning of the maxillary dentition, assuming the existence of only trabecular bone (without differentiating between the trabecular and cortical bones).

Accordingly, in both studies, the bone part was given a material property that correspond to the trabecular bone (Young's Modulus of elasticity = 2000 MPa). This assumption was based on the fact that during initial displacement, teeth may not come close to the cortical bone making it irrelevant in their studies. However, cortical bone is in direct contact with the PDL and is not separated by trabecular bone at the coronal and interdental areas (Fig. 5.1).

The average range of variation (between maximum and minimum stiffness at each area) of the mean cortical bone stiffness (average of S1, S2, and S3) was equal to 7056.5 MPa. This variation is equal to half of the difference between the trabecular and cortical bones material properties most frequently used in the literature (1970 MPa for trabecular and 15750 MPa for cortical therefore the difference is equal to 13780 MPa). This observation would imply an even larger variation of the stress and displacement results than the variations observed in our study. As a consequence, modelling of the

cortical bone is a must in any FEA study evaluating orthodontic tooth movement even if only initial displacement is studied.

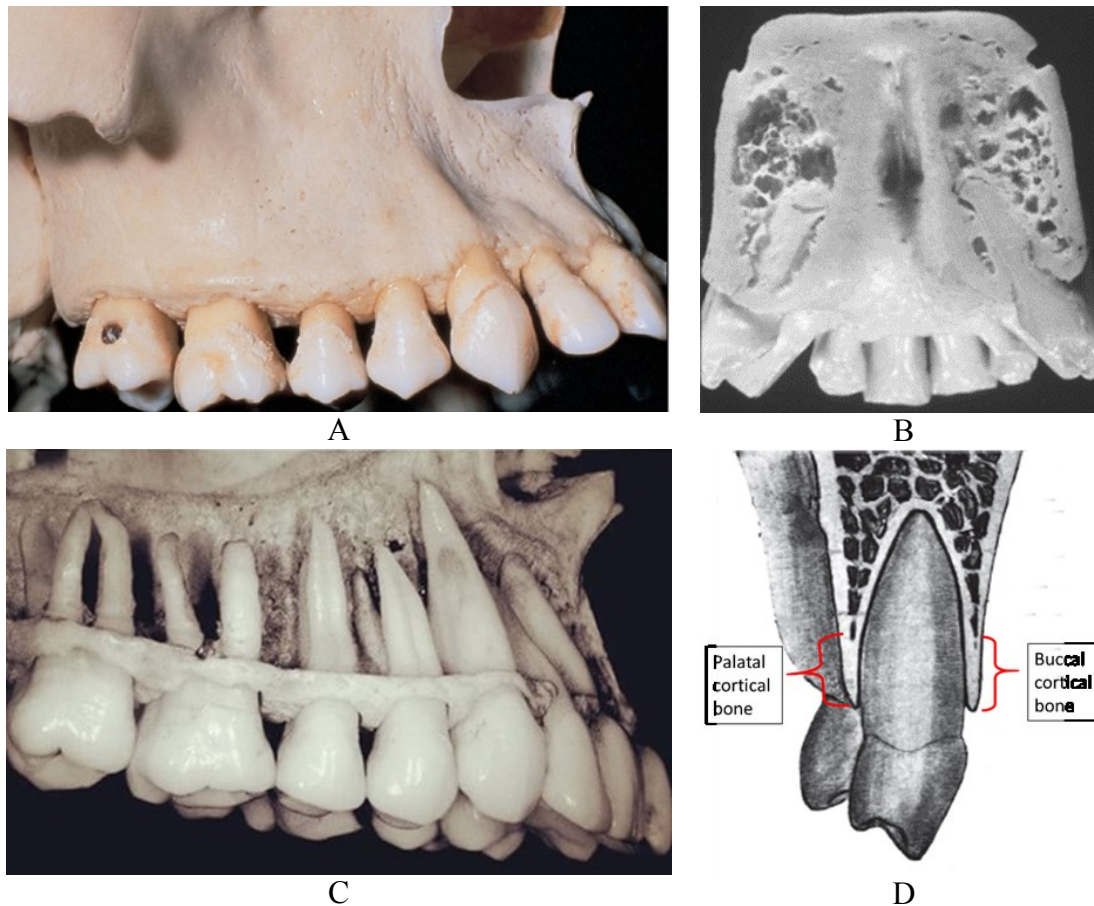


Fig. 5.1: Different views of the cortical bone buccal (A) and palatal (B) envelope around the maxillary teeth. Extraction of the outer layers reveals the compact bone around the cervical (interdental) and apical areas of the teeth (C). Illustration of direct contact with the PDL at the lower third of a premolar (D) (Choy et al. 2000).

5.2.2.2. PDL

In the same context, another important cause of divergence of the quantitative results is related to the material property definition of the PDL.

The variation in the PDL properties is common among dental FEA studies and was addressed in a systematic review by Fill et al. (2012) who showed that a myriad of modelling approaches were used to configure the PDL material properties. Moreover, Rees and Jacobsen (1997) found that elastic moduli of the PDL ranged from 0.07 to

1750 MPa. Despite using isotropic homogeneous material properties for the PDL in all 4 studies, differences in the range of the young's moduli used are present.

Yu et al. (2012) and Sung et al. (2015) used a Young's modulus of 0.05 MPa, while the PDL stiffness in the study by Kang et al (2016) was equal to 50 MPa. In our study, we assumed a material property equal to 0.68 MPa, more commonly used in FEA studies (Kojima et al., 2012), and potentially more comparable. Although the PDL in our study is closer to the studies by Yu et al. (2012) and Sung et al. (2015), it remains more than 13 times stiffer.

The stiffness of the PDL unquestionably affects the stress, strain or displacement responses obtained from the FEA, particularly during the initial tooth movement when the tooth actually moves into the periodontal ligament space.

5.2.2.3. Interaction settings

Sung et al (2015). and Yu et al. (2012) defined dental interactions via contact at an individual (finite) element located at the contact point area of the adjacent teeth. In essence, this definition amounts to joining the teeth together, which represents an anatomical inaccuracy. As a result, the FEA solver treats them as one object and the force applied anteriorly does not dissipate gradually in a posterior direction, maintaining the same magnitude on all the teeth. This issue was not problematic for Sung et al. because they studied distalization of the entire maxillary dentition, unlike our investigating only the movement of buccal teeth.

Therefore, joining the teeth is an artificial assumption when they should be represented as independent structures, if only tested through the insertion of dental floss

between contact points. We adopted the latter course and evaluated the reaction of each tooth of the buccal segment.

Kang et al (2016) allowed a small sliding condition and used the Lagrange multiplier method to define the contact interface, where contacts between teeth were assumed to be frictionless.

In our method, we used the “surface to surface” interaction which assumes the presence of a rigid connection between the teeth without any sliding. Our rationale, mimicking the clinical setting, was that distalization is often applied on a heavy rectangular wire to reduce the distal tipping movement and avoid archform changes due to the application of force buccal to the center of resistance of the tooth. The heavy rectangular wire increases the friction and limits the play between the archwire and the bracket, hindering sliding of teeth (refer to Methods, section 3.2.2.2.3. Fig. 3.28).

5.2.3. Aims

Unlike the 3 distalization studies mentioned above, we measured displacement only at the centroid of the crown, and not on the apices, because our focus was not to vary loading scenarios and describe in details the corresponding type and magnitude of the responses. We aimed to evaluate the effect of cortical bone properties on the various responses observed clinically by incorporating individual bone stiffness and thickness from real human material into the model. Meanwhile, we implemented specific boundary conditions to mimic the clinical circumstance, by guiding the teeth into movement tracks defined by the archwire buccally, negating extrusion, intrusion, and bucco-lingual translation. Accordingly, our outcome measures would include mesio distal translation and tipping movements, bucco-palatal tipping and rotations, all potentially comparable with similar displacements in the other studies.

In our methods, displacements were recorded and then correlated with the stresses (at the mesial surface of the PDL) to provide for a clinical interpretation of the PDL stress / cortical bone stiffness correlation results. This interpretation was facilitated by the high and significant correlations found between displacements (in all directions) and stresses at the mesial surfaces of the corresponding teeth (Tables 4.14 and 4.15).

5.2.4. Data collection

FEA studies regularly assess stresses and displacements at different parts of the model. In the three FEA distalization studies, stresses were addressed differently. Yu et al. (2012) did not assess stresses, while Kang et al. (2016) evaluated stresses at the alveolar bone and at the appliances used (headgear, bone anchored pendulum and MPAP appliance). Our study and the study by Sung et al. (2014) were the only ones to record stresses at the PDL during distalization.

Displacements were gauged differently between our study and the other 3 studies, in which data in the 3 directions were obtained from nodes located at the crown and at the apex:

- Sung et al. (2014) considered the root apices and buccal cusps of all the teeth.
- Kang et al. (2016) only studied the molars and the central incisor at root apices (only palatal root for molars), incisor edge, and mesiolingual and distobuccal cusps of molars.
- Yu et al. (2012) evaluated nodal displacement at the apex and the middle of the incisal edge of the central incisor and at the 4 cusp tips and palatal root apex of the first molar.

Moreover, Yu et al. (2012) and Sung et al (2014) reported that only transitional degrees of freedom were allowed. Movements involving rotation around an axis such as

dental tipping was interpreted when the nodal displacement at the level of the apex was less than at the crown. Likewise, bucco-palatal rotation of the molar was interpreted when the displacements at the mesial and distal cusps were different.

As noted above, we recorded crown displacements to correlate them with the stresses at the PDL. Displacements at the centroid of the crown reflected the true distal movement disregarding bucco-palatal rotations that can under or over-estimate movement magnitude.

5.2.5. Results

In dental FEA studies, comparing the absolute stress and displacement values to other studies is not relevant to draw conclusions because many factors come into play and affect these quantitative data. In contrast, comparing the results of different FEA simulations obtained from the same study is more appropriate to draw conclusions because similar assumptions and settings were used.

For this reason, we limit the comparison of our results to the FEA distalization studies to qualitative findings. Such comparison should also determine if the types of tooth movements implemented in our models were based on assumptions of dental movements similar to their results.

Nevertheless, we carried the quantitative comparison on the premise that even if the quantitative ranges were different, numerical data comparisons aided the qualitative comparison and underscored the reasons of the deviation.

5.2.5.1. Qualitative comparison

In the only distalization study where PDL stresses were reported (Sung et al., 2014), and of the different “en masse” distalization modalities recorded, only one was

clinically close to our direct anchorage modality, having in common the point of force application at the level of the wire (vertically) and mesial to the canine. The color mapped representations of the stresses at the PDL of all teeth were similar to our results: lowest at the molars and highest at the canine/first premolar area. The notable difference is the presence of stresses at the incisors in their modality because the whole maxillary dentition was moved distally while in our model only the buccal teeth were moved distally (Fig. 5.2).

In the study by Yu et al. (2012), the resulting displacements at the level of the first molar in the direct and indirect anchorage modalities were similar to the displacements assigned to the teeth in our study:

The nodes at the crown level showed distal tipping movement (more displacement at the crown than root apex), with minor buccal expansion and extrusion movements, despite the use of a TP bar, which prevented bucco-palatal rotations. Rotations were not prevented in our study as we did not include a TP bar; buccal expansion and extrusion were not implemented.

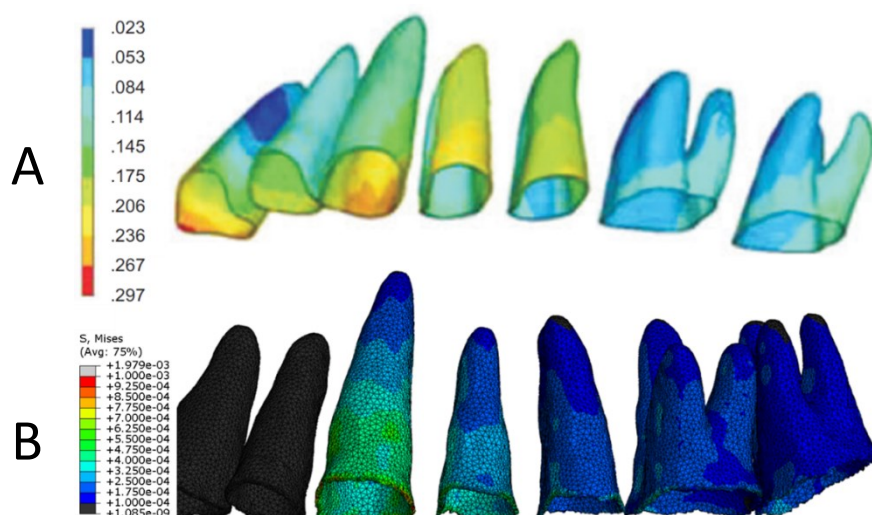


Fig. 5.2: Color mapped representations of the Von mises stress recorded at the PDL. **A-** Condition 1 in the study by Sung et al. 2015; **B-** Direct anchorage modality in our study.

Similar to our findings, they found more initial displacement of first molar in the indirect modality than the direct anchorage.

5.2.5.2. Quantitative assessment

The numerical data support the qualitative color mapped representation of stresses. The maximum stresses obtained in the “en masse” distalization by Sung et al. (2015) were recorded anteriorly and the minimum stresses recorded posteriorly. The same pattern in our study coexisted with a range of stresses (between 0.1145 to 0.3918 kPa - in the isotropic template model) much higher than that recorded by Sung et al. (0.0086 kPa and 0.0272 kPa).

In contrast, the maximum displacements found in our study were lower than the maximum displacements reported in all the 3 studies; however, the minimum displacements were in similar ranges. Nevertheless, in the study by Yu et al. (2012) where the displacements were the highest, no unit of displacement measurement was indicated, suggesting a possible magnification of the numbers by using other than the millimeter unit for easier interpretation (Table 5.1). Also, in the indirect anchorage the anterior displacements (at the incisors or canine) have a different sign than the posterior displacement (molars) proving that the posterior and anterior teeth move in opposite directions.

While the same factors affecting the stress response contribute to the displacement differences, other factors are specific to the displacement variation such as the measurement of the crown displacement at the cusp tips rather than at the centroid (taking into account rotation movements).

Table 5.1: Magnitude of maximum and minimum sagittal displacements recorded in the different FEA distalization studies

Study	Type of distalization	Maximum displacement	Location of maximum displacement	Minimum displacement	Location of minimum displacement
Sung et al. (2014) (In mm)	En masse (7 erupted) (Modality 1: Force applied to the wire)	0.024	IE of 1	0.0023	BC of 7
Yu et al. (2012) (No unit of measurement)	Indirect (7 not erupted)	0.018	DBC of 6	0.027	IE of 1
	Direct (7 not erupted) (3 modalities: vertical hooks at 1,4,7 mm)	0.182	DPC of 6 (in hook height = 7 mm)	0.0000152	IE of 1 (in hook height = 1 mm)
	PP (7 not erupted) (3 modalities: vertical hooks at 4,7,10 mm)	0.116	MPC of 6 (in hook height = 4 mm)	0.0016	IE of 1 (in hook height = 7 mm)
	PP (7 erupted) (1 modality: vertical hook at 10 mm)	0.024	DPC of 6	0.0013	IE of 1
Kang et al. (2016) (In mm)	CPHG (7 erupted)	0.01	DBC of 6	0.0002	IE of 1
	BAP (7 erupted)	0.007	MPC of 6	0.0001	IE of 1
	MPAP (7 erupted)	0.01	MPC of 6	0.00181	IE of 1
Present study. (In mm)	Direct	0.00029	Cent of 3	0.00013	Cent of 7
	Indirect	0.00045	Cent of 6	0.000028	Cent of 3

PP: Palatal plate – CPHG: Cervical pull headgear – BAP: Bone anchored pendulum – MPAP: Modified palatal anchorage plate
 BC: Buccal cusps - DBC: Distobuccal cusp - DPC: Distopalatal cusp - MPC: Mesio palatal cusp - IE: Incisal edge - Cent: Centroid.
 1: central incisor - 3: Canine - 6: First molar - 7: Second molar.

However, the most influential factor justifying the different quantitative results may be related to the different material properties used for the bone and in particular the PDL, because during the initial stage of tooth movement, the tooth actually moves into the ligament (see 5.2.2.2). The differential weights of the PDL Young's modulus could account for the differences (modulus in our model 13 folds stiffer than Sung et al's and Yu et al's; 73 times lesser than Kang et al's).

Table 5.2: Summary of the differences between the 4 different studies

	Yu et al. (2012)	Sung et al. (2015)	Kang et al. (2016)	Present study
Distalization modalities	- PP - Indirect anchorage - Direct anchorage	- En-masse distalization of the whole arch with different retraction hook height	- CPHG - MPAP - BAP	- Direct - Indirect
Bone construction / material properties	- No differentiation between cortical and trabecular bones - Isotropic and homogenous - Young's modulus = 2000 MPa	- No differentiation between cortical and trabecular bones - Isotropic and homogenous - Young's modulus = 2000 MPa	- Isotropic and homogenous - Young's modulus: Cortical bone: 13 700 MPa Trabecular bone: 7900 MPa	-Young's modulus: Cortical bone: Individual Variation / Orthotropic material Trabecular bone: 1970 MPa
PDL material properties	Homogenous and Isotropic Young's modulus = 0.05 MPa	Homogenous and Isotropic Young's modulus = 0.05 MPa	Homogenous and Isotropic Young's modulus = 50 MPa	Homogenous and Isotropic Young's modulus = 0.68 MPa
Interaction settings	Teeth joined at an individual (finite) element	Teeth joined at an individual (finite) element	- Small sliding allowed - Lagrange multiplier method to define the contact interface	Surface to surface interaction with tolerance adjustment / teeth separated
Aim	Variation of loading scenarios and description of the corresponding type and magnitude of movement	Variation of loading scenarios and description of the corresponding type and magnitude of movement	Description of dental movements in various loading scenarios at different stages of eruption of molars	Test the effect of cortical bone properties (stiffness and thickness) on movement in different individuals
Data collection	- Displacements only at: Central incisor: IE and RA First Molar: 4 cusp tips and PRA	- Stress values at PDL - Displacements at root apices and buccal cusps of all the teeth.	- Stresses at appliances and bone - Displacements at: Central incisor: IE and RA First molar: MPC, DBC and PRA	- Stress values at PDL - Displacements at: Centroid of the buccal teeth
Comparative results	- Type of movements found in both direct and indirect modalities: distal tipping movement, minor buccal expansion and extrusion - More displacement of first molar in the indirect than direct modality	- Stress values: - Lowest at the molars / highest around the anterior teeth - Highest displacement at the central incisor	- More displacement at the molar than incisor in all appliances	- Direct modality targets the canine - Indirect modality targets the molars - Allowed movements (by local boundary condition) correspond to FEA and clinical studies findings
Conclusion	- The PP appliance provoke less distal tipping movement and less displacement of the incisors - Buccal distalization cause distal tipping and minor extrusion of the first molar.	- Occlusal plane rotated according to the relationship between the line of force (determined by the height of retraction arm) and the center of resistance of the maxillary arch.	- MPAP cause more root than crown movement - BAP cause intrusion, distal and buccal tipping. - Presence of second not third molar delay distal movement of first molar.	- Cortical bone stiffness not thickness affected the PDL stresses - Stress and displacement correlated - Preferences between indirect and direct must consider anatomical conditions.

PP: Palatal plate – CPHG: Cervical pull headgear – BAP: Bone anchored pendulum – MPAP: Modified palatal anchorage plate

BC: Buccal cusps - DBC: Distobuccal cusp - DPC: Distopalatal cusp - MPC: Mesiopalatal cusp - IE: Incisal edge – PRA: Palatal root apex - RA: Root apex

5.3. Correlation between stress and displacement

From a clinical perspective, the correlations between stress and displacement provide for the following observations:

1. In the direct modality, mesial stress values were positively and highly correlated with displacement in the Y axis, which corresponds to the anteroposterior movement. Based on the assumption that high stress values translate to more movement, we may conclude that the direct anchorage targets the canine and first premolar while the indirect anchorage targets the molars.
2. In the direct anchorage, an optimal force of 150 grams resulted in low stress and displacement at the molars. Therefore, higher forces should be applied for molar movement with the direct modality (Fig. 5.3).

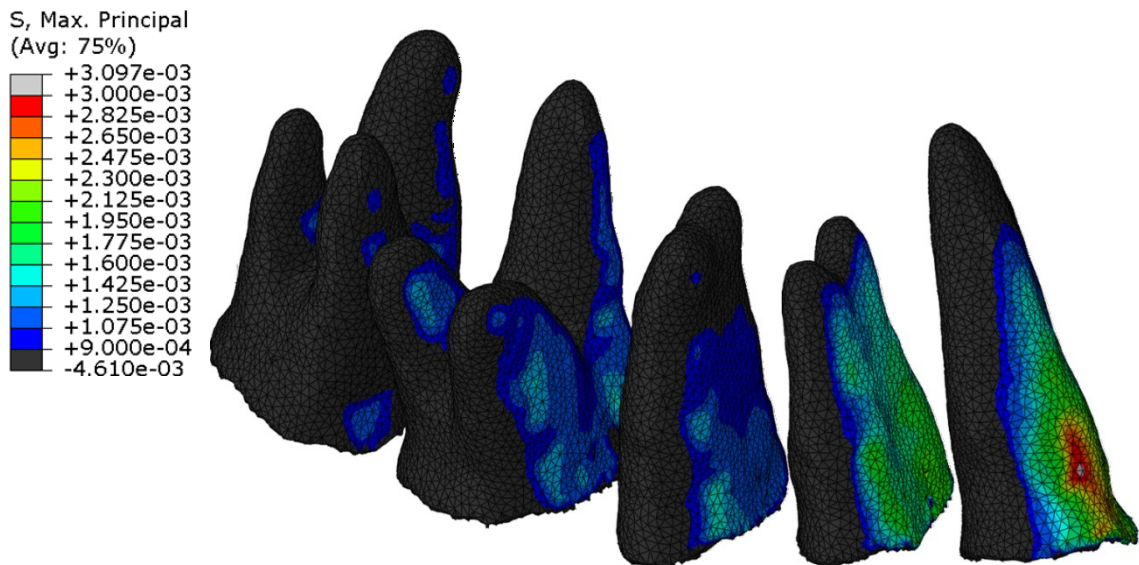


Fig. 5.3: Tension stress (principal stress) at the PDL in the direct anchorage modality. Note the low stress values at the second molar indicating minimal movement.

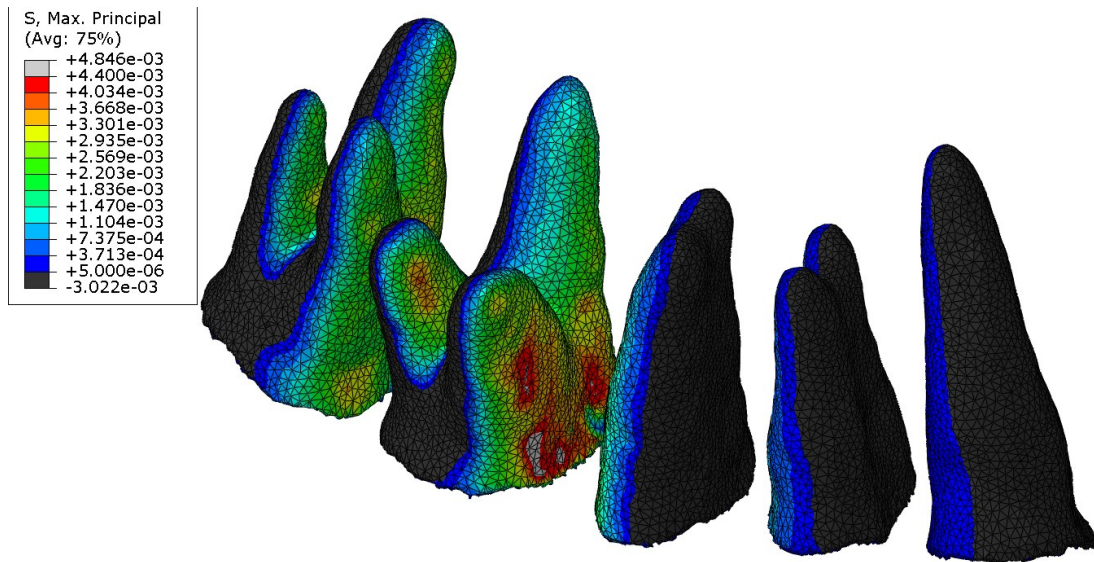


Fig. 5.4: Tension stress (principal stress) at the PDL in the indirect anchorage modality. Note the high stress values located at the mesial of the molars but distal of premolars and the low stresses at the canine indicating minimal movement.

3. In the indirect anchorage, the stress/displacement correlations were also significant but had different signs (positive/negative) at different teeth (e.g. positive for molars, negative for premolars), probably denoting the direction of movement of the corresponding teeth. At the canine, the correlation was low and not significant. Given that high correlations between stress and displacement indicate dental movement, a non-significant and low correlation may signal no movement. Indeed, in the indirect anchorage modality, the canine was stabilized (Fig. 5.4).
4. In the same context, and within the indirect anchorage experiment, the highest percentage of stress and concomitant displacement was at the molars (36%, 37%, respectively at the first molar; 32%, 33%, respectively at the second molar), and nearly nil as expected at the anchoring canine (Fig. 4.5). The stress and corresponding displacement at the second premolar, subjected to the same amount of force as the first molar (150 grams), was nearly half of that at the molars (19%, 18% respectively). These findings suggest that initial displacement in the PDL

occurred in the anchoring unit of teeth (premolars and canine). Longer-term time dependent movement should explore the dynamic displacement beyond the initial response within the PDL to determine whether and how anchorage may be absolute in the indirect setting.

5. Considering both modalities, stress values were highest on the first molar during the indirect modality (higher than the stress at the canine, which was highest in the direct mode). Given that stress not only correlates with distal movement but also with bucco-lingual and vertical movements, more unwanted side effects are expected at the first molar in the indirect anchorage modality.

5.4. Correlation between stress and bone properties (stiffness and thickness)

Stiffness of bone (particularly at the buccal side) correlated significantly with stress values at different areas of the molar. Comparatively, the absence of correlations between stress and thickness (at the canine and molar) suggests that thickness of the cortical bone does not impact initial movement as much as stiffness.

Two possible theories may account for the way stiffness may have affected the stresses.

5.4.1. Theory 1: Maxilla is a composite material

By definition, a composite material (also called composite) is made from two or more constituent materials with significantly different physical or chemical properties that, when combined, produce a material with characteristics different from the individual components (Fig. 5.5).

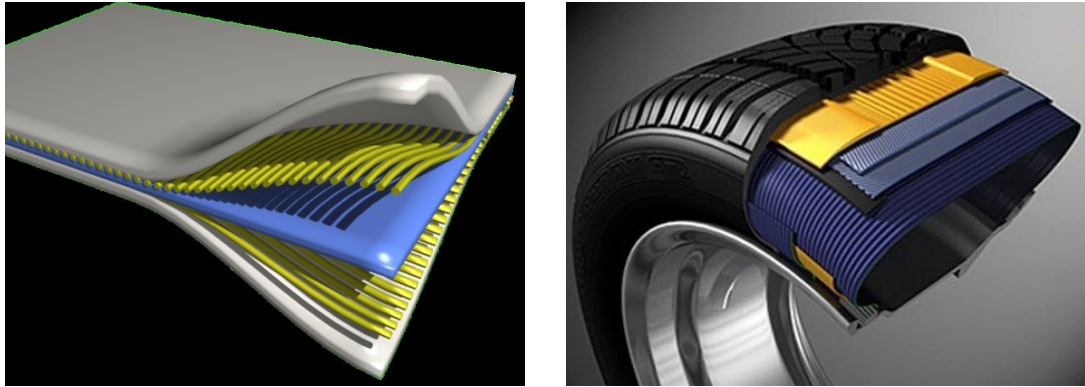


Fig. 5.5: Composite material formed from multiple layers of materials with different physical and mechanical properties (<http://www.wikipedia.com> - accessed January 18, 2017).

In this perspective, the maxilla can be considered as a composite material with a high stiffness component on the outer surface and softer components in the deeper zones (trabecular bone then PDL) (Fig. 5.6). If one of the maxillary components is removed or if its physical or chemical properties are altered (in this instance the cortical bone), then the stiffness of the whole composite material will differ. Since stresses analyzed at one component of the composite material (here PDL) are related to the stiffness of the composite material:

$$\text{Stress } (\sigma) = \text{stiffness } (E) \times \text{strain } (\epsilon).$$

We can expect different stresses at the PDL when cortical bone stiffness is changed.

Accordingly, the representation of the cortical bone is a must in any FEA study even though only initial displacement is studied.

5.4.2. Theory 2: Presence of direct contact between PDL and cortical bone

Ten Hove et al. (1977) studied intrusion of maxillary incisors utilizing laminography and concluded that when the retroclined maxillary incisors approximate the palatal cortex, this bone would bend and remodel but not allow for a significant amount of palatal movement of the root. In this setting, when a palatal root torque is

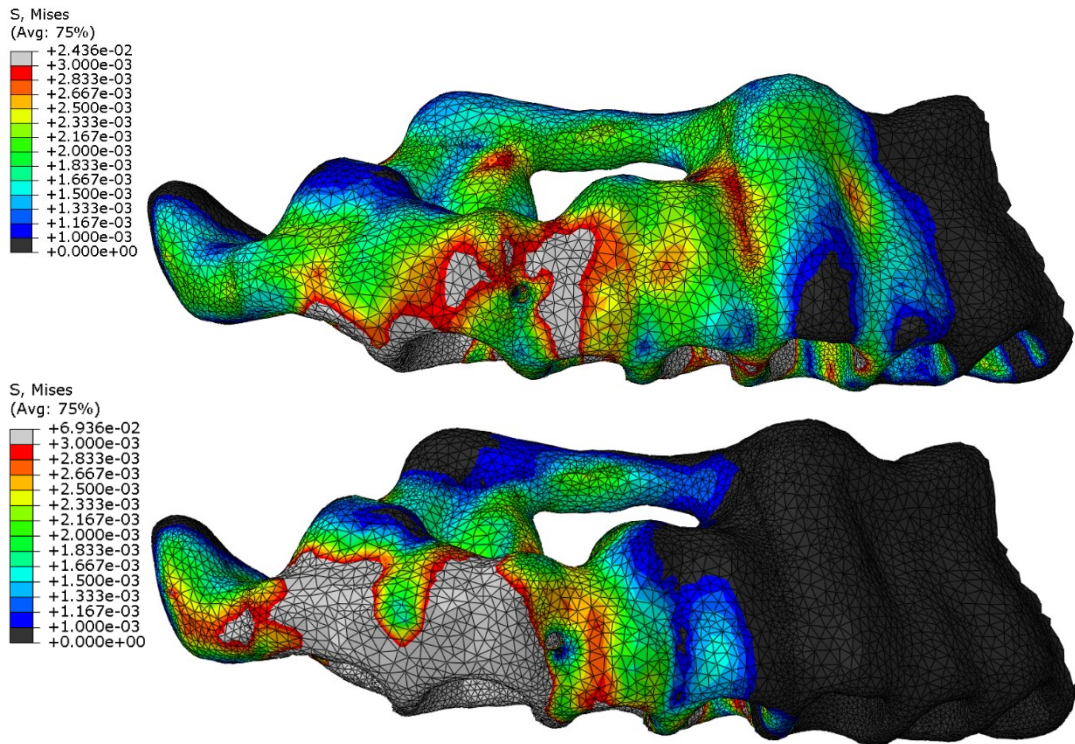


Fig. 5.6: Color mapped visualization of the Von mises stresses recorded at the trabecular bone showing the transmission of the stresses from the PDL through the trabecular bone before reaching the cortical bone highlighting the composite nature of the maxillary complex (Theory 1). **A-** Direct anchorage; **B-** Indirect anchorage. In the indirect modality, greater stresses (gray color) recorded around the molars indicate more buccal tipping movement. Note in the direct anchorage, the lower stresses at the canine compared to the molar although the load was applied on the canine.

applied to correct the inclination of the tooth, the root tip remains stationary and the crowns would move anteriorly, with root resorption as another side effect (Fig 5.7).

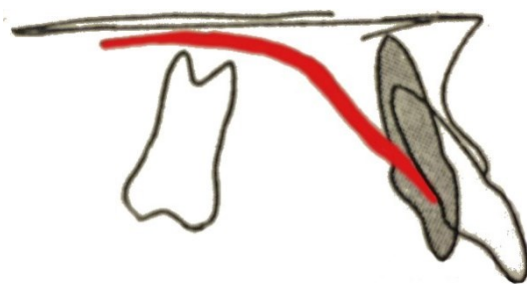


Fig 5.7: Proximity of the maxillary incisor root (in white) to the palatal cortex (in red) preventing palatal root torque movement. After intrusion (in gray), the tooth is bordered by trabecular bone facilitating the same movement. (adapted from Ten Hoope et al. 1977)

The authors recommended the intrusion of the incisors in trabecular bone prior

to torque to avoid severe retroclination of the tooth and avoid abutting the root against the palatal cortex. In this perspective, and to better translate these findings in the context of our results, a series of observations are warranted:

1. While stress at the PDL and stiffness at the molar exhibited high correlations, they were negative ($-0.68 < r < -0.82$), indicating an inverse relationship: stress is higher at the PDL with a less hard cortical bone. This finding is in line with the equation between stiffness, stress, and displacement: the higher the stiffness, the lower the stress and displacement, and vice versa (Table 5.3).
2. At the cortical bone, stress values increased, suggesting absorption of part of the stress by the periodontal ligaments. Unlike this reaction at the PDL, higher stress at cortical bone suggests resistance to movement because of the higher material properties (Young's modulus - Fig. 5.8). This explanation would support Ten Hoeve et al.'s theory and associated clinical implications. By extension, the principle of distancing the tooth from the cortical bone, regardless of its thickness, may be a direct clinical implication of our study and would warrant focused research.
3. Based on the above-mentioned negative correlations between stiffness and stress, the question arises whether higher stress would be generated at the less stiff (softer) trabecular bone. If so, greater displacement would be projected, unlike the expectation of higher resistance from the cortical bone.
4. These premises are based on and limited by the conditions of our experiments, reflecting the initial response at the level of the PDL and displacement within the PDL space. Only time-dependent FEA investigating real-time motion of teeth would allow the proper testing of these hypotheses.

Table 5.3: Cortical bone impact on PDL stress and crown displacement based on the correlation results

Cortical bone stiffness	PDL stress	Crown displacement
↗	↘	↘
↘	↗	↗

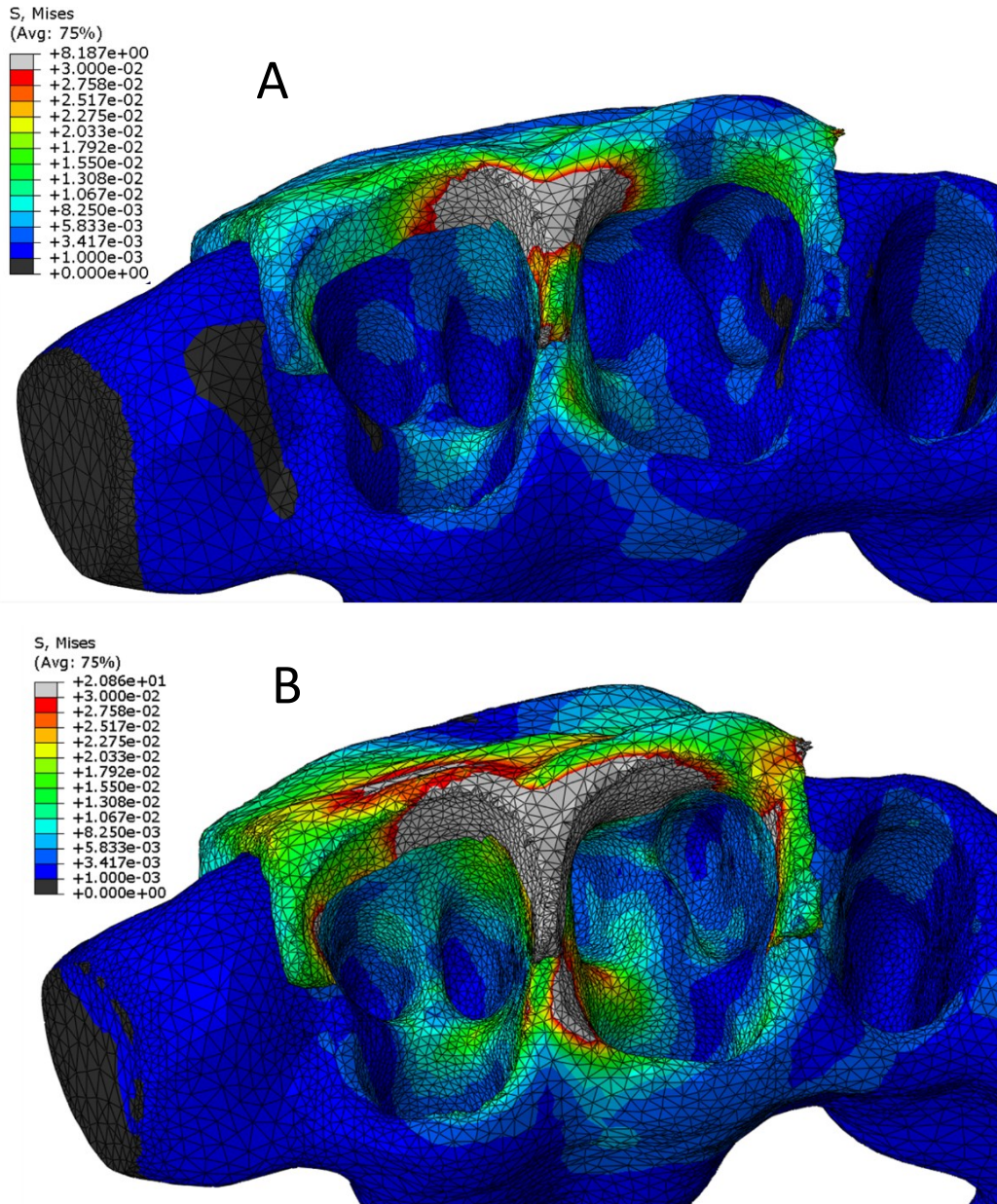


Fig. 5.8: Occlusal view showing the trabecular bone and the buccal molar cortical part. Note the higher stresses at the occlusal and interdental cortical bone highlighting the direct transmission of stress from the PDL to the buccal cortex (Theory 2). Higher stresses present in the indirect anchorage (**B**) compared to the direct anchorage (**A**). Unlike at the PDL, higher stresses at the cortical bone level suggest resistance to movement because of the higher material property value.

5.4.3. Synthesis based on theories 1 and 2

Based on the two previous theories, and on the significant stress/stiffness correlations we observed, we suggest the following explanations:

1. The higher number of significant correlations observed at the buccal cortical bone area of the molar than at the palatal area was probably related to the buccal tipping

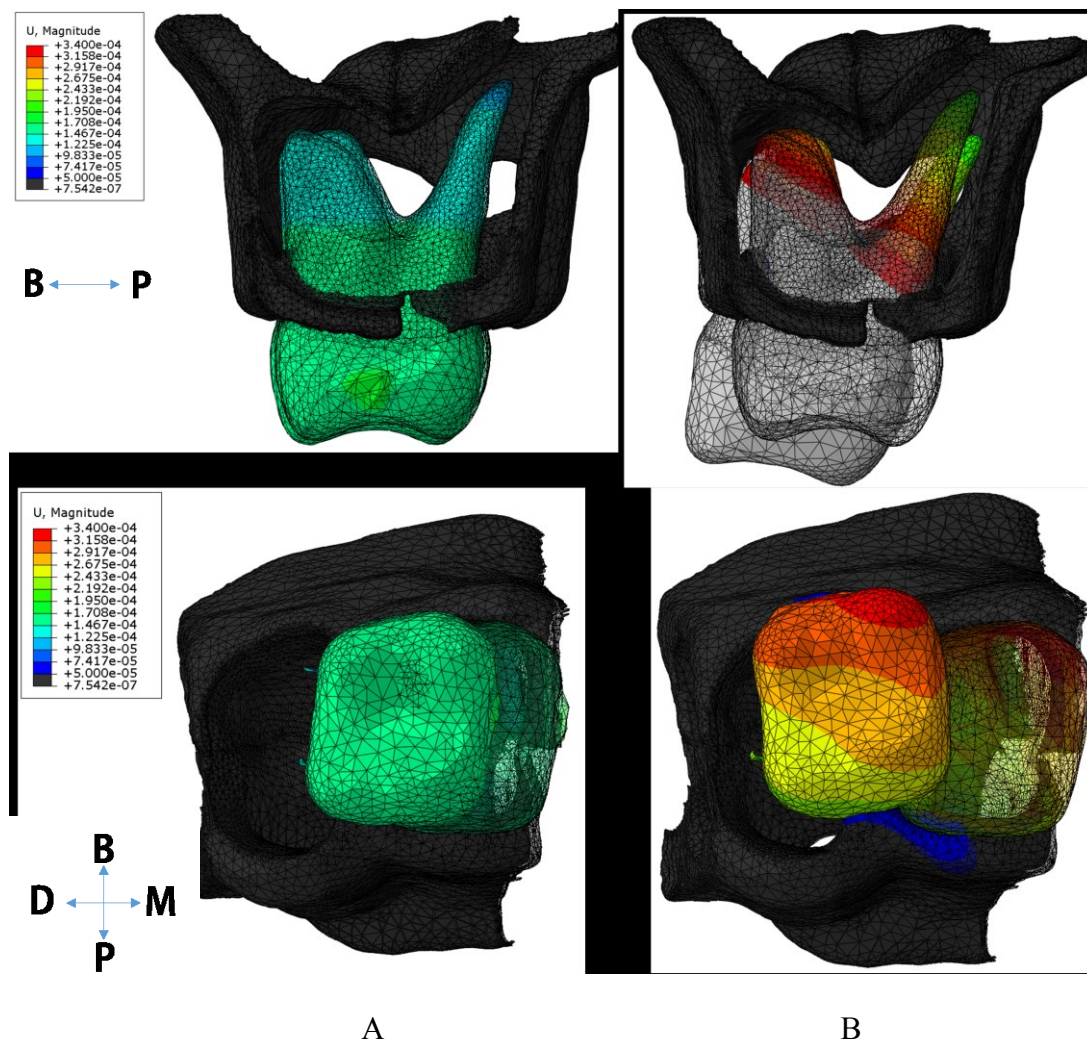


Fig. 5.9: First molar displacement (magnified) seen on an axial cut mesial to the first molar (top row) and occlusal view (lower row). The transparent mesh corresponds to the initial tooth position; the colored mesh corresponds to the final position. **A-** Direct anchorage modality: note the mild extrusion and buccal tipping. **B-** Indirect anchorage: note the severe extrusion, mesiobuccal rotation, distal movement; the higher tooth contact with the buccal cortical bone accounts for the higher number of significant correlations between PDL stresses and cortical bone stiffness. The closeness of the palatal root to the palatal cortex explains the significant correlation of the apical part of both the mesial and distal PDL with the stiffness of the palatal cortex.

movement of this tooth because the force was applied buccal to its center of resistance. Moreover, more correlations were present in the indirect than in the direct modalities, suggesting more buccal tipping (side effects) with this modality, mainly because the point of application of the force is closer to the first molar (Figs. 5.8, 5.9; Table 4.23).

2. The highest stress values were observed at the cervical of the mesial and distal surfaces of the PDL because these areas are in direct contact with occlusal and interdental cortical bone. However, correlations were found only at the mesial cervical area, and not on the distal cervical side, suggesting a possible mesiobuccal rotation movement that displaces the mesial of the first molar buccally and the distal surface palatally into the trabecular bone (Fig. 5.9, 5.10; Table 4.23).

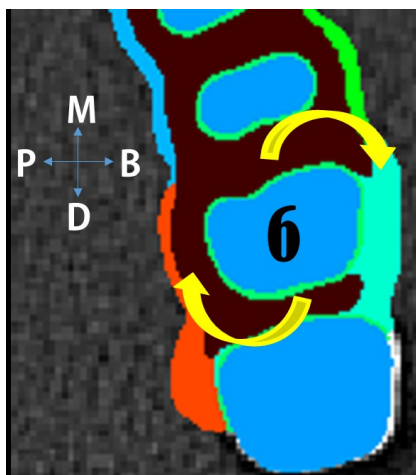


Fig 5.10: Occlusal horizontal cut showing the effect of a mesio-buccal rotation of the first molar bringing the mesial surface of the tooth into the buccal cortex and the distal surface into the palatal trabecular bone.

3. In the direct anchorage experiment, the apical areas of the mesial and distal parts correlated highly and significantly with the stiffness of the palatal cortical bone. This association may be explained by the contact of the palatal root apex with the cortical of the floor of the nose corresponding to the palatal bone area of the first molar (Fig. 5.11; Table 4.23).

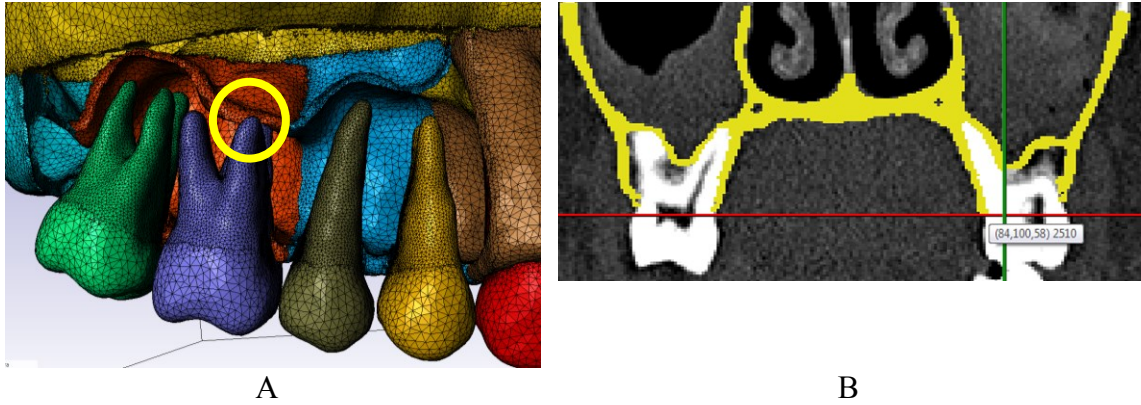


Fig. 5.11: **A-** 3D model and **B-** 2D axial cut at the molar level showing a contact of the palatal root with the palatal cortical area. This can justify the presence in the direct anchorage modality, of significant correlation between stresses at the apical part of mesial and distal surfaces with the stiffness at the palatal cortical bone area.

4. At the canine, the smaller bucco-lingual width and mesio-distal width of the crown and the presence of only one thin and tapered root (vs 3 for the molar) helped steer its movement in the trabecular bone with minimal contact with the cortical bone. This finding would explain the absence of any correlation of the PDL stresses with the cortical bone (Figs. 5.6, 5.12)

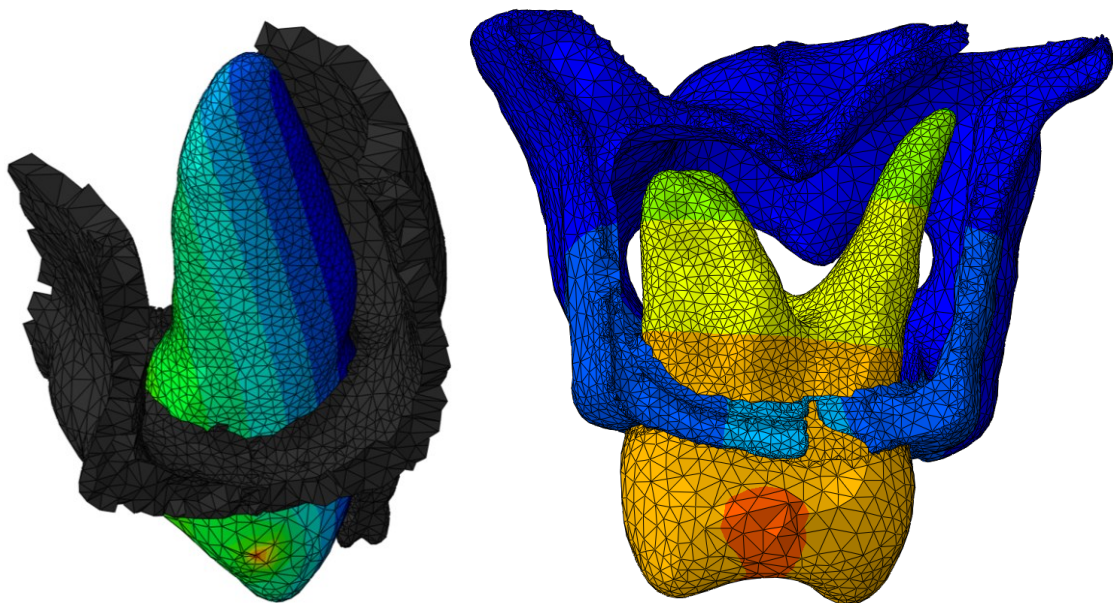


Fig. 5.12: Anatomical differences between the canine and the molar possibly explaining the absence of significant correlation between stress and cortical stiffness.

5.5 Correlation between thickness and stiffness of cortical bone parts

Buccal cortical bone usually has a thinner but stiffer cortex (Peterson et al. 2006). Meanwhile, the palatal cortical bone is intermediate in some features and is generally similar to the cortical bone from the alveolar region.

However, cortical bones near the incisors and canines (sites 3, 5, and 6) follow a slightly different pattern: they have a greater thickness than at other alveolar sites, while their density and stiffness are intermediate. This configuration is in concordance with our results whereby thickness did not correlate with stiffness at any alveolar site except at the sites 3, 5 and 6 (Table 4.30).

This finding further supports our interpretation of the results that the stiffness not the thickness is of greater influence on the stresses and displacement: the thicker but less stiff cortex at the canine bone areas did not affect the stress values recorded at the PDL of the canine while the thinner but stiffer cortex at the molar (especially the buccal cortex) influenced the first molar PDL stresses significantly.

5.6. Effect of material property type on results

Peterson et al (2006) reported that the majority of sites within the dentate maxilla were moderately anisotropic with ratios ranging from 0.69 to 0.85. When we compared the stresses at the PDL obtained in both modalities, orthotropic (type of anisotropic material where the stiffness differs along three mutually-orthogonal twofold axes) models did not differ from the isotropic model. Since the maximum difference found was equal to 51 Pa, we may conclude that orthotropic material definition did not significantly influence the stresses at the PDL, further suggesting that isotropic representation of the cortical bone in FEA studies of initial tooth movement may be an acceptable assumption.

5.7. Clinical implications

The implications are drawn from the interpretation of data and would require independent research for confirmation. Ideally, the conditions should be part of treatment planning when all components are investigated, including the definition of cortical bone thickness, stiffness, width of the trabecular trough in which the tooth is being moved, posterior crowding of teeth, occlusal interferences and muscle activity (Table 5.4).

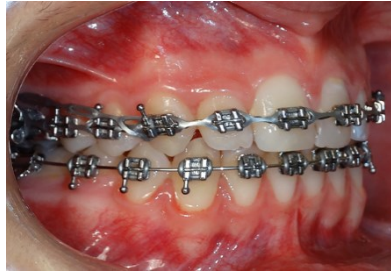
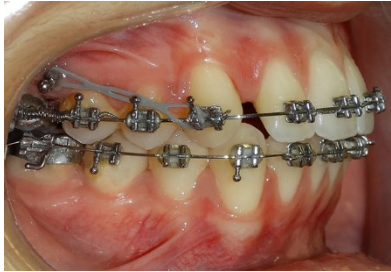


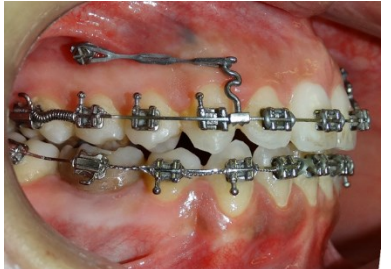
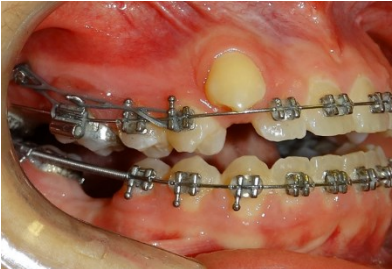
High inverted correlations between stress and buccal stiffness ($r=-0.9$ in indirect anchorage; $r=-0.7$ in direct anchorage) at the molar indicate that stress increase (thus more displacement) when stiffness decreases and vice versa. This finding, along with the lack of similar correlations at the palatal side, indicates that the buccal cortex offers resistance to initial movement. If this rationale holds throughout force application, the clinical control of this side effect would suggest the use of:

- Posterior box elastics.
- Use of heavy wire to maintain the molars in the middle of the alveolus especially in the indirect anchorage modality.
- Coordination of wire to the initial archform to avoid moving the molars into the buccal cortex.
- Incorporation of an inset bend mesial to the molar when the distalization rate is slow.

Moreover a palatal force to distalize the molar may help avoid a mesiobuccal rotation of this tooth.

Table 5.4: Working guidelines in molar distalization against miniscrews*

Condition	Possible reason	Additional diagnostic aids	Recommended mechanics	Clinical tips
Failed distalization with indirect anchorage (posterior teeth not moving)	Contact with the buccal cortical bone	- CBCT/3D assessment and measurements (thickness and density) - Indirect gauging during initial placement of mini-screws	Mechanics to move the molar into the trabecular bone (possibly including palatal miniscrew)	<i>Use of posterior box elastics</i>
	Cortical bone stiffer and/or thicker at the molars (including second molar)		Distalize the second molar first (C) then the first molar and subsequently other mesial teeth	<i>Heavy wire to maintain the molars in the middle of the alveolus</i>
	Large sinus extending to the molar roots		Sequential distalization may decrease resistance to movement	<i>Coordinate archwire to initial arch form</i>
No molar movement with the direct modality	Force is not transmitted to the molar	CBCT/3D assessment and measurements may be needed	Shift to indirect, particularly if increased forces (either to canine or both canine and first premolar) do not improve the situation	<i>Incorporation of an inset bend mesial to the molar when the distalization rate is slow.</i>
Either direct or indirect anchorage	Presence of posterior crowding	Panoramic x-ray, clinical assessment	Extract posterior teeth if surgically indicated or shift to sequential distalization starting with second molar separately	<i>Palatal force to distalize the molar may help avoid a mesiobuccal rotation of this tooth</i>
	Occlusion / muscles activity	Clinical evaluation	Raise the bite (clear posterior occlusion)	

Clinical situations related to above listed working guidelines.	LOW RESISTANCE			MODERATE RESISTANCE			HIGH RESISTANCE		
		 <p>A En masse distalization of the maxillary arch</p>	 <p>C Combined direct and indirect distalization modality</p>	 <p>E Multiple forces applied to the premolar and to the canine</p>	 <p>B Distalization of molars and premolars</p>	 <p>D Combined direct and indirect distalization modality</p>	 <p>F Distalize the second molar alone then the other mesial teeth</p>		

*Assumption: both first and second molars banded and aligned.

5.8. Limitations

Numerous approaches were used to model the PDL ranging from linear-elastic, viscoelastic, hyperelastic and multiphase approaches (Fill et al., 2012). The lack of experimental studies and absence of modern technologies to measure the properties of the oral tissues has prevented researchers from confirming the correct assumption that accurately simulates the role of the PDL. Our study was in line with the majority of dental FEA studies to use an isotropic and homogeneous material property for the PDL, which may lead to simplistic and inaccurate outcomes.

Moreover, this study provides a “snap-shot” view of the initial conditions (e.g. stresses, displacement) within the model and does not depict changes that occur over time, such as bone remodeling, healing, friction etc. These initial results represent the initial dental movement whereby the tooth is pushed into the PDL space before the main phases of bone resorption/apposition occur. Subsequent clinical results may not be similar to the initial ones. A change in the onset and rate of tooth movement may normally occur. Roberts et al (1996) analyzed four similar cases of mandibular molar protraction in adult patients over time and showed a decrease in the rate of molar protraction from 0.6 mm/month during the first 8 months to 0.33 mm/month after.

Ideally, time-dependent (continuous/dynamic) finite element model for tooth movement should be implemented to reach the timepoint when FEA becomes an integral part of planning orthodontic mechanotherapy. Although such model was introduced since 1996 (Middleton et al.), accurate mathematical simulation of the biological process of tooth movement (including the PDL and bony reactions) over time has not been possible with FEA to date (Ammar et al., 2011). Significant resources should be invested in this necessary field of research.

One aspect of this process was initiated by Cheng et al (2014) by constructing a FE model from one patient and incorporated the average rate of canine retraction into a premolar extraction space that was generated clinically from a study on 15 patients. However, their approach falls short of direct clinical interpretation, albeit the method offers a component of research methodology that may be used in more encompassing research, along with the inclusion of individual variation such as we proceeded.

Our study indicated that dental reactions to a similar load did not vary significantly across subjects. In another FEA study where individual variation was introduced to gauge the initial stress on palatally impacted canines to forces from different directions, the responses varied significantly between the different force directions (Zeno et al., 2016). Distalization forces are mono-directional in nature and would not be expected to yield such variation. However, longer-term differences between patients may be gauged in the time-dependent FEA model.

5.9. Future research

- In the initial tooth movement, thickness was not shown to be a factor affecting the stresses because of the interposition of a layer of trabecular bone separating the PDL and the tooth from the cortical bone. However, a time dependent FEA study should help disclose the importance of this thickness when the tooth displaces closer to the cortex. At this stage, a thick cortical bone may be in contact with the tooth and impact its movement.

- In this context, other factors influencing the distance between the tooth and the stiff cortical bone should also be investigated: the width of the alveolus, height of the coronal cortical bone in contact with the PDL and the bucco-lingual width of the molar.

A critical factor in defining successful distalization may be the relationship between tooth displacement and the distance between the roots of the teeth and the corresponding cortical bone (Fig. 5.13).

- Because all these anatomical factors can be evaluated using 3D radiographic imaging, future research should also focus on establishing a “severity index of cortical bone” that helps in determining when it would be appropriate to use a direct or indirect distalization.

- Bone stiffness is not readily measurable; however it may be gathered from a measure of bone density directly on 3D scans, along with the measure of bone thickness.

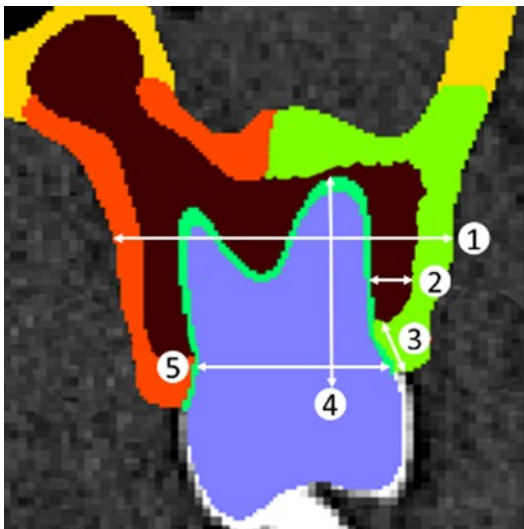


Fig 5.13: Anatomical factors that can affect the dental displacement:

- 1: Width of the alveolus
- 2: Distance from molar root to cortical bone
- 3: Height of the cortical bone
- 4: Height of the molar root
- 5: Width of the molar.

CHAPTER 6

CONCLUSION

1. This study was the first to contribute FE analysis and findings based on the consideration of genuine variation among human subjects. Accordingly, central tendencies of the stress values and displacements were compared between the two distalization approaches investigated.
2. Thickness of the cortical bone seemingly did not carry as much weight as stiffness on the initial displacement. As long as the tooth encounters the stiffer area of the cortical bone, tooth movement is affected, apparently regardless of the thickness of this bone.
3. The results on initial tooth movement suggest that indirect distalization of molars may be more advantageous or possibly efficient than the direct approach. However, long term application of this modality may result in more side effects, causing treatment delay thus ending up with similar treatment duration as the direct method.
4. Generic preferences for direct or indirect distalization are not appropriate, as morphologic and biologic individual characteristics may dictate one or the other in personalized treatment. Most morphologic documentation may be obtained from 3D radiographic imaging. Research should sort out the anatomical conditions under which one approach is better than the other.
5. This study has shown that not only force magnitude and vectors may cause side effects, but also individual anatomy. Moving teeth away from the stiff outer cortex might improve tooth displacement.

Our study showed that bone stiffness significantly affected the stress values obtained at the level of the molar PDL. Besides these positional and anatomical factors, researchers must consider the potential influence of the occlusion, musculature, metabolism and other biologic factors.

Accordingly, long term orthodontic tooth movement cannot be accurately simulated only mathematically and a single formulation for all types of movements and in all patients may not provide the ultimate formula for total mechanotherapy planning. Yet, the ability for FEA in conjunction with clinical data input in the analysis should help in the determination of “movement-specific” and “patient-specific” outcome planning and prediction.

REFERENCES

- Ackerman, J. L., & Proffit, W. R. (1969). The characteristics of malocclusion: a modern approach to classification and diagnosis. *Am J Orthod*, 56(5), 443-454.
- Ammar, H. H., Ngan, P., Crout, R. J., Mucino, V. H., & Mukdadi, O. M. (2011). Three-dimensional modeling and finite element analysis in treatment planning for orthodontic tooth movement. *American Journal of Orthodontics and Dentofacial Orthopedics*, 139(1), e59-e71.
- An, Y. H., & Draughn, R. A. (1999). *Mechanical testing of bone and the bone-implant interface*: CRC press.
- Angle, E. H. (1899). Classification of malocclusion.
- Arcuri, C., Muzzi, F., Santini, F., Barlattani, A., & Giancotti, A. (2007). Five years of experience using palatal mini-implants for orthodontic anchorage. *Journal of Oral And Maxillofacial Surgery*, 65(12), 2492-2497.
- Armstrong, R. T. (2006). Acceptability of cone beam CT vs. multi-detector CT for 3D anatomic model construction. *Journal Of Oral And Maxillofacial Surgery*, 64(9), 37.
- Baumrind, S., Korn, E. L., Boyd, R. L., & Maxwell, R. (1996). The decision to extract: part II. Analysis of clinicians' stated reasons for extraction. *American Journal of Orthodontics And Dentofacial Orthopedics*, 109(4), 393-402.
- Bechtold, T. E., Kim, J.-W., Choi, T.-H., Park, Y.-C., & Lee, K.-J. (2012). Distalization pattern of the maxillary arch depending on the number of orthodontic miniscrews. *Angle Orthod*, 83(2), 266-273.
- Bell, W. (1975). Le Forte I osteotomy for correction of maxillary deformities. *Journal of Oral Surgery (American Dental Association: 1965)*, 33(6), 412-426.
- Bjork, A., Krebs, A., & Solow, B. (1964). A Method For Epidemiological Registration of Malocclusion. *Acta Odontol Scand*, 22, 27-41.
- Bondemark, L., Kurol, J., & Bernhold, M. (1994). Repelling magnets versus superelastic nickel-titanium coils in simultaneous distal movement of maxillary first and second molars. *Angle Orthod*, 64(3), 189-198.
- Bowers, G. M. (1963). A study of the width of attached gingiva. *Journal of Periodontology*, 34(3), 201-209.
- Brachvogel, P., Berten, J., Hessling, K., & Tränkmann, J. (1991). The possibilities for surgical correction of dentoalveolar adaptations within skeletal repositioning osteotomy. *Fortschritte der Kieferorthopädie*, 52(1), 21.
- Cai, Y., Yang, X., He, B., & Yao, J. (2015). Finite element method analysis of the periodontal ligament in mandibular canine movement with transparent tooth correction treatment. *BMC Oral Health*, 15(1), 106.
- Carano, A., & Testa, M. (2001). Distal jet designed to be used alone. *American Journal of Orthodontics and Dentofacial Orthopedics*, 120(6), 13A-14A.
- Carano, A., Velo, S., Leone, P., & Siciliani, G. (2005). Clinical applications of the miniscrew anchorage system. *J Clin Orthod*, 39(1), 9-24.
- Chen, Y. J., Chang, H. H., Lin, H. Y., Lai, E. H. H., Hung, H. C., & Yao, C. C. J. (2008). Stability of miniplates and miniscrews used for orthodontic anchorage: experience with 492 temporary anchorage devices. *Clinical Oral Implants Research*, 19(11), 1188-1196.
- Cheng, S.-J., Tseng, I.-Y., Lee, J.-J., & Kok, S.-H. (2004). A prospective study of the risk factors associated with failure of mini-implants used for orthodontic anchorage. *International Journal of Oral & Maxillofacial Implants*, 19(1).

- Chugh, T., Ganeshkar, S. V., Revankar, A. V., & Jain, A. K. (2013). Quantitative assessment of interradicular bone density in the maxilla and mandible: implications in clinical orthodontics. *Prog Orthod*, *14*(1), 1.
- Çifter, M., & Saraç, M. (2011). Maxillary posterior intrusion mechanics with mini-implant anchorage evaluated with the finite element method. *American Journal of Orthodontics and Dentofacial Orthopedics*, *140*(5), e233-e241.
- Cobo, J., Sicilia, A., Argüelles, J., Suárez, D., & Vijande, M. (1993). Initial stress induced in periodontal tissue with diverse degrees of bone loss by an orthodontic force: tridimensional analysis by means of the finite element method. *American Journal of Orthodontics and Dentofacial Orthopedics*, *104*(5), 448-454.
- Cope, J. B., Buschang, P. H., Cope, D. D., Parker, J., & Blackwood III, H. (1994). Quantitative evaluation of craniofacial changes with Jasper Jumper therapy. *Angle Orthod*, *64*(2), 113-122.
- Cowin, S. C., & Hart, R. T. (1990). Errors in the orientation of the principal stress axes if bone tissue is modeled as isotropic. *Journal of Biomechanics*, *23*(4), 349-352.
- Creekmore, T. D., & Eklund, M. K. (1983). The possibility of skeletal anchorage. *J Clin Orthod*, *17*(4), 266-269.
- Crismani, A. G., Bertl, M. H., Čelar, A. G., Bantleon, H.-P., & Burstone, C. J. (2010). Miniscrews in orthodontic treatment: review and analysis of published clinical trials. *American Journal of Orthodontics and Dentofacial Orthopedics*, *137*(1), 108-113.
- Cura, N., & Saraç, M. (1997). The effect of treatment with the Bass appliance on skeletal Class II malocclusions: a cephalometric investigation. *The European Journal of Orthodontics*, *19*(6), 691-702.
- De Vos, W., Casselman, J., & Swennen, G. (2009). Cone-beam computerized tomography (CBCT) imaging of the oral and maxillofacial region: a systematic review of the literature. *International Journal of Oral and Maxillofacial Surgery*, *38*(6), 609-625.
- Deguchi, T., Nasu, M., Murakami, K., Yabuuchi, T., Kamioka, H., & Takano-Yamamoto, T. (2006). Quantitative evaluation of cortical bone thickness with computed tomographic scanning for orthodontic implants. *American Journal of Orthodontics and Dentofacial Orthopedics*, *129*(6), 721. e727-721. e712.
- Efstratiadis, S., Baumrind, S., Shofer, F., Jacobsson-Hunt, U., Laster, L., & Ghafari, J. (2005). Evaluation of Class II treatment by cephalometric regional superpositions versus conventional measurements. *American Journal of Orthodontics and Dentofacial Orthopedics*, *128*(5), 607-618.
- Field, C., Ichim, I., Swain, M. V., Chan, E., Darendeliler, M. A., Li, W., & Li, Q. (2009). Mechanical responses to orthodontic loading: a 3-dimensional finite element multi-tooth model. *American Journal of Orthodontics and Dentofacial Orthopedics*, *135*(2), 174-181.
- Fill, T. S., Toogood, R. W., Major, P. W., & Carey, J. P. (2012). Analytically determined mechanical properties of, and models for the periodontal ligament: critical review of literature. *Journal of Biomechanics*, *45*(1), 9-16.
- Fischer, K., Stenberg, T., Hedin, M., & Sennerby, L. (2008). Five-year results from a randomized, controlled trial on early and delayed loading of implants supporting full-arch prosthesis in the edentulous maxilla. *Clinical Oral Implants Research*, *19*(5), 433-441.
- Gačnik, F., Ren, Z., & Hren, N. I. (2014). Modified bone density-dependent orthotropic material model of human mandibular bone. *Medical engineering & physics*, *36*(12), 1684-1692.
- Ghafari, J., Shofer, F., Jacobsson-Hunta, U., Markowitz, D., & Laster, L. (1998). Headgear versus function regulator in the early treatment of Class II, division 1 malocclusion: a randomized clinical trial. *American Journal of Orthodontics and Dentofacial Orthopedics*, *113*(1), 51-61.

- Giancotti, A., Arcuri, C., & Barlattani, A. (2004). Treatment of ectopic mandibular second molar with titanium miniscrews. *American Journal of Orthodontics and Dentofacial Orthopedics*, *126*(1), 113-117.
- Gianelly, A. A. (1998). Distal movement of the maxillary molars. *American Journal of Orthodontics and Dentofacial Orthopedics*, *114*(1), 66-72.
- Gomez, J. P., Peña, F. M., Martínez, V., Giraldo, D. C., & Cardona, C. I. (2014). Initial force systems during bodily tooth movement with plastic aligners and composite attachments: A three-dimensional finite element analysis. *Angle Orthod*, *85*(3), 454-460.
- González Carcedo, M. (2010). Anthropometric Characterization of Human Subjects.
- Graber, L. W., Vanarsdall Jr, R. L., & Vig, K. W. (2011). *Orthodontics: Current principles and techniques*: Elsevier Health Sciences.
- Graber, T. (1972). *Orthodontics: Principles and Practice* (2nd ed.). Philadelphia: WB Saunders Company.
- Graber, T. M., Vanarsdall Jr, R. L., & Vig, K. W. (2006). Orthodontics. Current principles & techniques, (2005). *European Journal of Orthodontics*, *28*, 197.
- Gultekin, B. A., Gultekin, P., & Yalcin, S. (2012). *Application of Finite Element Analysis in Implant Dentistry*: INTECH Open Access Publisher.
- Han, U. A., Kim, Y., & Park, J. U. (2009). Three-dimensional finite element analysis of stress distribution and displacement of the maxilla following surgically assisted rapid maxillary expansion. *Journal of Cranio-Maxillofacial Surgery*, *37*(3), 145-154.
- Harrison, J. E., O'Brien, K. D., & Worthington, H. V. (2007). Orthodontic treatment for prominent upper front teeth in children. *Cochrane Database Syst Rev*, *3*.
- Haydar, S., & Üner, O. (2000). Comparison of Jones jig molar distalization appliance with extraoral traction. *American Journal of Orthodontics and Dentofacial Orthopedics*, *117*(1), 49-53.
- Hegtvædt, A., Ollins, M., White, R. P., & Turvey, T. A. (1987). Minimizing the risk of transfusions in orthognathic surgery. *The International Journal of Adult Orthodontics and Orthognathic Surgery*, *2*(4), 185-192.
- Heymann, G. C., & Tulloch, J. (2006). Implantable devices as orthodontic anchorage: a review of current treatment modalities. *Journal of Esthetic and Restorative Dentistry*, *18*(2), 68-79.
- Hilgers, J. J. (1992). The pendulum appliance for Class II non-compliance therapy. *Journal of Clinical Orthodontics: JCO*, *26*(11), 706-714.
- Hohmann, A., Kober, C., Young, P., Dorow, C., Geiger, M., Boryor, A., . . . Sander, F. G. (2011). Influence of different modeling strategies for the periodontal ligament on finite element simulation results. *American Journal of Orthodontics and Dentofacial Orthopedics*, *139*(6), 775-783.
- Holberg, C., Winterhalder, P., Rudzki-Janson, I., & Wichelhaus, A. (2014). Finite element analysis of mono-and bicortical mini-implant stability. *The European Journal of Orthodontics*, *36*(5), 550-556.
- Holberg, P. D. D. C., Winterhalder, P., Holberg, N., Wichelhaus, A., & Rudzki-Janson, I. (2014). Indirect miniscrew anchorage: biomechanical loading of the dental anchorage during mandibular molar protraction—an FEM analysis. *Journal of Orofacial Orthopedics/Fortschritte der Kieferorthopädie*, *75*(1), 16-24.
- Illing, H. M., Morris, D. O., & Lee, R. T. (1998). A prospective evaluation of bass, bionator and twin block appliances. Part I-the hard tissues. *The European Journal of Orthodontics*, *20*(5), 501-516.

- Janson, G., Barros, S. E. C., Simão, T. M., & Freitas, M. R. d. (2009). Relevant variables of Class II malocclusion treatment. *Revista Dental Press de Ortodontia e Ortopedia Facial*, 14(4), 149-157.
- Jung, R. E., Pjetursson, B. E., Glauser, R., Zembic, A., Zwahlen, M., & Lang, N. P. (2008). A systematic review of the 5-year survival and complication rates of implant-supported single crowns. *Clin Oral Implants Res*, 19(2), 119-130.
- Kaipatur, N., Wu, Y., Adeeb, S., Stevenson, T., Major, P., & Doschak, M. (2014). A novel rat model of orthodontic tooth movement using temporary skeletal anchorage devices: 3D finite element analysis and in vivo validation. *Intern J Dent*, 2014.
- Kamble, R. H., Lohkare, S., Hararey, P. V., & Mundada, R. D. (2012). Stress distribution pattern in a root of maxillary central incisor having various root morphologies: a finite element study. *Angle Orthod*, 82(5), 799-805.
- Kang, J.-M., Park, J. H., Bayome, M., Oh, M., Park, C. O., Kook, Y.-A., & Mo, S.-S. (2016). A three-dimensional finite element analysis of molar distalization with a palatal plate, pendulum, and headgear according to molar eruption stage. *The Korean Journal of Orthodontics*, 46(5), 290-300.
- Keles, A., & Sayinsu, K. (2000). A new approach in maxillary molar distalization: intraoral bodily molar distalizer. *American Journal of Orthodontics and Dentofacial Orthopedics*, 117(1), 39-48.
- Kim, D.-G. (2014). Can dental cone beam computed tomography assess bone mineral density? *Journal of Bone Metabolism*, 21(2), 117-126.
- Kim, K. Y., Bayome, M., Park, J. H., Kim, K. B., Mo, S.-S., & Kook, Y.-A. (2015). Displacement and stress distribution of the maxillofacial complex during maxillary protraction with buccal versus palatal plates: finite element analysis. *The European Journal of Orthodontics*, 37(3), 275-283.
- Ko, C.-C., Rocha, E. P., & Larson, M. (2012). *Past, Present and Future of Finite Element Analysis in Dentistry*: INTECH Open Access Publisher.
- Kojima, Y., & Fukui, H. (2008). Effects of transpalatal arch on molar movement produced by mesial force: a finite element simulation. *American Journal of Orthodontics and Dentofacial Orthopedics*, 134(3), 335. e331-335. e337.
- Kojima, Y., Kawamura, J., & Fukui, H. (2012). Finite element analysis of the effect of force directions on tooth movement in extraction space closure with miniscrew sliding mechanics. *American Journal of Orthodontics and Dentofacial Orthopedics*, 142(4), 501-508.
- Kokich, V. G. (1996). *Managing complex orthodontic problems: the use of implants for anchorage*. Paper presented at the Seminars in Orthodontics.
- Kravitz, N. D., & Kusnoto, B. (2007). Risks and complications of orthodontic miniscrews. *American journal of orthodontics and dentofacial orthopedics*, 131(4), S43-S51.
- Kuroda, S., Sugawara, Y., Deguchi, T., Kyung, H.-M., & Takano-Yamamoto, T. (2007). Clinical use of miniscrew implants as orthodontic anchorage: success rates and postoperative discomfort. *American Journal of Orthodontics and Dentofacial Orthopedics*, 131(1), 9-15.
- Lagravère, M. O., Carey, J., Heo, G., Toogood, R. W., & Major, P. W. (2010). Transverse, vertical, and anteroposterior changes from bone-anchored maxillary expansion vs traditional rapid maxillary expansion: a randomized clinical trial. *American Journal of Orthodontics and Dentofacial Orthopedics*, 137(3), 304. e301-304. e312.
- Ledley, R. S., & Huang, H. K. (1968). Linear model of tooth displacement by applied forces. *Journal of Dental Research*, 47(3), 427-432.
- Lee, H. K., Bayome, M., Ahn, C. S., Kim, S.-H., Kim, K. B., Mo, S.-S., & Kook, Y.-A. (2012). Stress distribution and displacement by different bone-borne palatal expanders with micro-

- implants: a three-dimensional finite-element analysis. *The European Journal of Orthodontics*, cjs063.
- Lee, T. C.-K., Leung, M. T.-C., Wong, R. W.-K., & Rabie, A. B. M. (2008). Versatility of skeletal anchorage in orthodontics. *World Journal of Orthodontics*, 9(3).
- Li, K. K., Guilleminault, C., Riley, R. W., & Powell, N. B. (2002). Obstructive sleep apnea and maxillomandibular advancement: an assessment of airway changes using radiographic and nasopharyngoscopic examinations. *Journal of Oral and Maxillofacial Surgery*, 60(5), 526-530.
- Liang, W., Rong, Q., Lin, J., & Xu, B. (2009). Torque control of the maxillary incisors in lingual and labial orthodontics: a 3-dimensional finite element analysis. *American Journal of Orthodontics and Dentofacial Orthopedics*, 135(3), 316-322.
- Lim, J. W., Kim, W. S., Kim, I. K., Son, C. Y., & Byun, H. I. (2003). Three dimensional finite element method for stress distribution on the length and diameter of orthodontic miniscrew and cortical bone thickness. *Korean Journal of Orthodontics*, 33(1), 11-20.
- Lindh, C., Obrant, K., & Petersson, A. (2004). Maxillary bone mineral density and its relationship to the bone mineral density of the lumbar spine and hip. *Oral Surgery, Oral Medicine, Oral Pathology, Oral Radiology, and Endodontology*, 98(1), 102-109.
- Liu, C., Zhu, X., & Zhang, X. (2015). Three-dimensional finite element analysis of maxillary protraction with labiolingual arches and implants. *American Journal of Orthodontics and Dentofacial Orthopedics*, 148(3), 466-478.
- Locatelli, R. (1992). Molar distalization with superelastic NiTi wire. *J Clin Orthod*, 26, 277-279.
- Lombardo, L., Scuzzo, G., Arreghini, A., Gorgun, Ö., Ortan, Y. Ö., & Siciliani, G. (2014). 3D FEM comparison of lingual and labial orthodontics in en masse retraction. *Prog Orthod*, 15(1), 1-12.
- Melsen, B. (1978). Effects of cervical anchorage during and after treatment: an implant study. *American Journal of Orthodontics*, 73(5), 526-540.
- Middleton, J., Jones, M., & Wilson, A. (1996). The role of the periodontal ligament in bone modeling: the initial development of a time-dependent finite element model. *American Journal of Orthodontics and Dentofacial Orthopedics*, 109(2), 155-162.
- Miyawaki, S., Koyama, I., Inoue, M., Mishima, K., Sugahara, T., & Takano-Yamamoto, T. (2003). Factors associated with the stability of titanium screws placed in the posterior region for orthodontic anchorage. *American Journal of Orthodontics and Dentofacial Orthopedics*, 124(4), 373-378.
- Mizrahi, E., & Mizrahi, B. (2007). Mini-screw implants (temporary anchorage devices): orthodontic and pre-prosthetic applications. *Journal of Orthodontics*, 34(2), 80-94.
- Morris, D. O., Illing, H. M., & Lee, R. T. (1998). A prospective evaluation of Bass, Bionator and Twin Block appliances. *The European Journal of Orthodontics*, 20(6), 663-684.
- Motoyoshi, M., Hirabayashi, M., Uemura, M., & Shimizu, N. (2006). Recommended placement torque when tightening an orthodontic mini-implant. *Clinical Oral Implants Research*, 17(1), 109-114.
- Nanda, R. (2005). *Biomechanics and esthetic strategies in clinical orthodontics*: Elsevier Health Sciences.
- Nihara, J., Gielo-Perczak, K., Cardinal, L., Saito, I., Nanda, R., & Uribe, F. (2015). Finite element analysis of mandibular molar protraction mechanics using miniscrews. *The European Journal of Orthodontics*, 37(1), 95-100.
- Norton, M. R., & Gamble, C. (2001). Bone classification: an objective scale of bone density using the computerized tomography scan. *Clinical oral implants research*, 12(1), 79-84.
- O'Brien, K., Wright, J., Conboy, F., Sanjie, Y., Mandall, N., Chadwick, S., Hammond, M. (2003). Effectiveness of early orthodontic treatment with the Twin-block appliance: a

- multicenter, randomized, controlled trial. Part 1: dental and skeletal effects. *American Journal of Orthodontics and Dentofacial Orthopedics*, 124(3), 234-243.
- Ohashi, E., Pecho, O. E., Moron, M., & Lagravere, M. O. (2006). Implant vs screw loading protocols in orthodontics: a systematic review. *Angle Orthod*, 76(4), 721-727.
- Ortial, J. P. (1987). [The Tweed technic. Choice of extraction and treatment strategy. 1]. *Actual Dent*, 3(16), 10-11, 13-15, 17-21 passim.
- Papadopoulos, M. A., & Tarawneh, F. (2007). The use of miniscrew implants for temporary skeletal anchorage in orthodontics: a comprehensive review. *Oral Surgery, Oral Medicine, Oral Pathology, Oral Radiology, and Endodontology*, 103(5), e6-e15.
- Park, H.-S., Bae, S.-M., Kyung, H.-M., & Sung, J.-H. (2001). Micro-implant anchorage for treatment of skeletal Class I bialveolar protrusion. *Journal of Clinical Orthodontics: JCO*, 35(7), 417.
- Park, H.-S., Bae, S.-M., Kyung, H.-M., & Sung, J.-H. (2004). Simultaneous incisor retraction and distal molar movement with microimplant anchorage. *World Journal of Orthodontics*, 5(2).
- Park, H.-S., Jeong, S.-H., & Kwon, O.-W. (2006). Factors affecting the clinical success of screw implants used as orthodontic anchorage. *American Journal of Orthodontics and Dentofacial Orthopedics*, 130(1), 18-25.
- Park, H.-S., Kwon, O.-W., & Sung, J.-H. (2004a). Micro-implant anchorage for forced eruption of impacted canines. *Journal of Clinical Orthodontics*, 38, 297-302.
- Park, H.-S., Kwon, O.-W., & Sung, J.-H. (2004b). Uprighting second molars with micro-implant anchorage. *Journal of Clinical Orthodontics: JCO*, 38(2), 100-103; quiz 192.
- Park, H.-S., Kwon, O.-W., & Sung, J.-H. (2005). Microscrew implant anchorage sliding mechanics. *World Journal of Orthodontics*, 6(3).
- Park, H. S. (2002). An anatomical study using CT images for the implantation of micro-implants. *Korean Journal of Orthodontics*, 32(6), 435-441.
- Park, Y.-C., Chu, J.-H., Choi, Y.-J., & Choi, N.-C. (2005). Extraction space closure with vacuum-formed splints and miniscrew anchorage. *Journal of Clinical Orthodontics: JCO*, 39, 76.
- Park, Y.-C., Lee, S.-Y., Kim, D.-H., & Jee, S.-H. (2003). Intrusion of posterior teeth using mini-screw implants. *American Journal of Orthodontics and Dentofacial Orthopedics*, 123(6), 690-694.
- Peterson, J., Wang, Q., & Dechow, P. C. (2006). Material properties of the dentate maxilla. *The Anatomical Record Part A: Discoveries in Molecular, Cellular, and Evolutionary Biology*, 288(9), 962-972.
- Pollei, J. K. (2009). *Finite element analysis of miniscrew placement in maxillary alveolar bone with varied angulation and material type*: THE UNIVERSITY OF NORTH CAROLINA AT CHAPEL HILL.
- Proffit, W. R., Fields Jr, H. W., & Sarver, D. M. (2012). *Contemporary Orthodontics* (5th Ed.). St. Louis: Mosby.
- Proffit, W. R., Turvey, T. A., & Phillips, C. (2007). The hierarchy of stability and predictability in orthognathic surgery with rigid fixation: an update and extension. *Head & Face Medicine*, 3(1), 1.
- Qian, H., Chen, J., & Katona, T. R. (2001). The influence of PDL principal fibers in a 3-dimensional analysis of orthodontic tooth movement. *American Journal of Orthodontics and Dentofacial Orthopedics*, 120(3), 272-279.
- Rees, J., & Jacobsen, P. (1997). Elastic modulus of the periodontal ligament. *Biomaterials*, 18(14), 995-999.
- Rho, J., Hobatho, M., & Ashman, R. (1995). Relations of mechanical properties to density and CT numbers in human bone. *Medical Engineering & Physics*, 17(5), 347-355.

- Rinchuse, D. J., & Rinchuse, D. J. (1989). Ambiguities of Angle's classification. *Angle Orthod*, 59(4), 295-298.
- Roberts, W. E., Arbuckle, G. R., & Analoui, M. (1996). Rate of mesial translation of mandibular molars using implant-anchored mechanics. *Angle Orthod*, 66(5), 331-338.
- Roberts, W. E., Marshall, K. J., & Mozsary, P. G. (1990). Rigid endosseous implant utilized as anchorage to protract molars and close an atrophic extraction site. *Angle Orthod*, 60(2), 135-152.
- Roth, A., Yildirim, M., & Diedrich, P. (2004). Forced eruption with microscrew anchorage for preprosthetic leveling of the gingival margin. *Journal of Orofacial Orthopedics/Fortschritte der Kieferorthopädie*, 65(6), 513-519.
- Scarfe, W. C. (2012). A comparison of maxillofacial CBCT and medical CT. *Atlas of the Oral and Maxillofacial Surgery Clinics of North America: Digital Technologies in Oral and Maxillofacial Surgery*, 20(1), 1.
- Schnelle, M. A., Beck, F. M., Jaynes, R. M., & Huja, S. S. (2004). A radiographic evaluation of the availability of bone for placement of miniscrews. *Angle Orthod*, 74(6), 832-837.
- Sicher, H., & Du Brul, E. (1970). The blood vessels of head and neck: maxillary artery. *Oral Anatomy*, 5th ed. Saint Louis, MO: CV Mosby Co, 315-320.
- Sicher, H., & DuBrul, E. L. (1970). Temporomandibular articulation. *Oral anatomy*. 5th edition. St. Louis (MO): CV Mosby.
- Sung, E.-H., Kim, S.-J., Chun, Y.-S., Park, Y.-C., Yu, H.-S., & Lee, K.-J. (2015). Distalization pattern of whole maxillary dentition according to force application points. *The Korean Journal of Orthodontics*, 45(1), 20-28.
- Sung, S.-J., Jang, G.-W., Chun, Y.-S., & Moon, Y.-S. (2010). Effective en-masse retraction design with orthodontic mini-implant anchorage: a finite element analysis. *American Journal of Orthodontics and Dentofacial Orthopedics*, 137(5), 648-657.
- Suzuki, A., Masuda, T., Takahashi, I., Deguchi, T., Suzuki, O., & Takano-Yamamoto, T. (2011). Changes in stress distribution of orthodontic miniscrews and surrounding bone evaluated by 3-dimensional finite element analysis. *American Journal of Orthodontics and Dentofacial Orthopedics*, 140(6), e273-e280.
- Taddei, F., Cristofolini, L., Martelli, S., Gill, H., & Viceconti, M. (2006). Subject-specific finite element models of long bones: an in vitro evaluation of the overall accuracy. *Journal of Biomechanics*, 39(13), 2457-2467.
- Tanne, K., Koenig, H. A., & Burstone, C. J. (1988). Moment to force ratios and the center of rotation. *American Journal of Orthodontics and Dentofacial Orthopedics*, 94, 426-431.
- Tanne, K., Sakuda, M., & Burstone, C. J. (1987). Three-dimensional finite element analysis for stress in the periodontal tissue by orthodontic forces. *American Journal of Orthodontics and Dentofacial Orthopedics*, 92(6), 499-505.
- Techalertpaisarn, P., & Versluis, A. (2013). Mechanical properties of Opus closing loops, L-loops, and T-loops investigated with finite element analysis. *American Journal of Orthodontics and Dentofacial Orthopedics*, 143(5), 675-683.
- Ten Hoeve, A., Mulie, R. M., & Brandt, S. (1977). Technique modifications to achieve intrusion of the maxillary anterior segment. *Journal of clinical orthodontics: JCO*, 11(3), 174.
- Trabelsi, N., Yosibash, Z., Wutte, C., Augat, P., & Eberle, S. (2011). Patient-specific finite element analysis of the human femur—a double-blinded biomechanical validation. *Journal of Biomechanics*, 44(9), 1666-1672.
- Trauner, R., & Obwegeser, H. (1957). The surgical correction of mandibular prognathism and retrognathia with consideration of genioplasty: Part I. Surgical procedures to correct mandibular prognathism and reshaping of the chin. *Oral Surgery, Oral Medicine, Oral Pathology*, 10(7), 677-689.

- Tseng, Y.-C., Hsieh, C.-H., Chen, C.-H., Shen, Y.-S., Huang, I.-Y., & Chen, C.-M. (2006). The application of mini-implants for orthodontic anchorage. *International Journal Of Oral And Maxillofacial Surgery*, 35(8), 704-707.
- Vasudeva, G. (2009). Finite element analysis: a boon to dental research. *The Internet Journal of Dental Science*, 6(2).
- Viceconti, M., Davinelli, M., Taddei, F., & Cappello, A. (2004). Automatic generation of accurate subject-specific bone finite element models to be used in clinical studies. *Journal of Biomechanics*, 37(10), 1597-1605.
- Wachter, N., Krischak, G., Mentzel, M., Sarkar, M., Ebinger, T., Kinzl, L., Augat, P. (2002). Correlation of bone mineral density with strength and microstructural parameters of cortical bone in vitro. *Bone*, 31(1), 90-95.
- Wang, X.-x., Li, N., Xu, J.-g., Ren, X.-s., Ma, S.-l., & Zhang, J. (2014). 3-Dimensional Finite Element Analysis on Periodontal Stress Distribution of Impacted Teeth During Orthodontic Treatment *Frontier and Future Development of Information Technology in Medicine and Education* (pp. 1247-1252): Springer.
- Wiechmann, D., Meyer, U., & Büchter, A. (2007). Success rate of mini-and micro-implants used for orthodontic anchorage: a prospective clinical study. *Clinical Oral Implants Research*, 18(2), 263-267.
- Williams, A. C., & Stephens, C. D. (1992). A modification to the incisor classification of malocclusion. *Br J Orthod*, 19(2), 127-130.
- Wolford, L. M., & Epker, B. N. (1975). The combined anterior and posterior maxillary ostectomy: a new technique. *J Oral Surg*, 33(11), 842-851.
- Yan, X., He, W., Lin, T., Liu, J., Bai, X., Yan, G., & Lu, L. (2013). Three-dimensional finite element analysis of the craniomaxillary complex during maxillary protraction with bone anchorage vs conventional dental anchorage. *American Journal of Orthodontics and Dentofacial Orthopedics*, 143(2), 197-205.
- Yu, I.-J., Kook, Y.-A., Sung, S.-J., Lee, K.-J., Chun, Y.-S., & Mo, S.-S. (2014). Comparison of tooth displacement between buccal mini-implants and palatal plate anchorage for molar distalization: a finite element study. *The European Journal of Orthodontics*, 36(4), 394-402.